FAST Facility for Accelerated Service Testing

An international, cooperative government-industry research program

FRA/ORD-86/05

Characterization of Locomotive Tractive Effort from the Electrical Power to the Traction Motors

FEBRUARY, 1987

U.S. Department of Transportation
Federal Railroad Administration
Washington, DC 20590

ASSOCIATION OF AMERICAN RAILROADS
50 F Street N.W.
Washington, DC 20001

RPI RAILWAY PROGRESS INSTITUTE
801 North Fairfax Street
Alexandria, VA 22314

NOTICE

This document reflects events relating to testing at the Facility for Accelerated Service Testing (FAST) at the Transportation Test Center, which may have resulted from conditions, procedures, or the test environment peculiar to that facility. This document is disseminated for the FAST Program under the sponsorship of the U.S. Department of Transportation, the Association of American Railroads, and the Railway Progress Institute in the interest of information exchange. The sponsors assume no liability for its contents or use thereof.

The FAST Program does not endorse products or manufacturers. Trade or manufacturers' names appear herein solely because they are considered essential to the object of this report.

Technical Report Documentation Page

1. Report No.	2. Government Accession No.	3. Recipient's Catalog No.
FRA/ORD-86/05		PB88 151030/AS

4. Title and Subtitle	5. Report Date
Characterization of Locomotive Tractive Effort from Electrical Power to the Traction Motors	March, 1986
	6. Performing Organization Code
7. Author(s)	8. Performing Organization Report No.
N. Wilson, K. Rownd, M. Dembosky, R. Washburn	TTC-042(FAST-FR86)
9. Performing Organization Name and Address	10. Work Unit No. (TRAIS)
Association of American Railroads Transportation Test Center Pueblo, Colorado 81001	11. Contract or Grant No. DTFR-53-82-C-00282
	13. Type of Report and Period Covered
12. Sponsoring Agency Name and Address	Final, May-December 1983
U.S. Department of Transportation Federal Railroad Administration Washington, D.C. 20590	14. Sponsoring Agency Code

15. Supplementary Notes

16. Abstract

Experiments to be performed on the FAST track at the Transportation Test Center (TTC) required a method of measuring train resistance and related fuel consumption in moving the train. Previous experiments had shown that the Roll Dynamics Unit (RDU) in the Rail Dynamics Laboratory (RDL) might be used as a dynamometer to measure the performance of a locomotive.

A GP40-2 locomotive was already being used on the RDU as a test bed for fuel flowmeters; this locomotive was contributed by Burlington Northern Railroad to the project. The locomotive, BN 3054, was instrumented so that input power to the traction motor armatures was calibrated to measure train resistance by developing accurate performance curves that related traction-motor armature input to tractive power.

Results showed that tractive power could be measured under steady conditions to within 3% accuracy. Subsequent analysis showed that improved instrumentation could further decrease error, providing measurements at better than 1% accuracy.

Field trials with this locomotive hauling test consists of cars with ordinary three-piece trucks and two types of radial trucks were performed to test the instrumentation package. Results showed the system to be reliable, durable, and accurate. In addition, the use of radial trucks, or truck lubrication, was shown to be beneficial in reducing train resistance.

17. Key Words		18. Distribution Statement
Locomotive Calibration Radial Trucks Track Lubrication Traction Motor Tractive Effort	Train Energy Savings Train Resistance	Available from: The National Technical Information Service 5285 Port Royal Road Springfield, VA 22161

19. Security Classif. (of this report)	20. Security Classif. (of this page)	21. No. of Pages	22. Price
Unclassified	Unclassified	126	

Form DOT F 1700.7 (8-72) Reproduction of completed page authorized

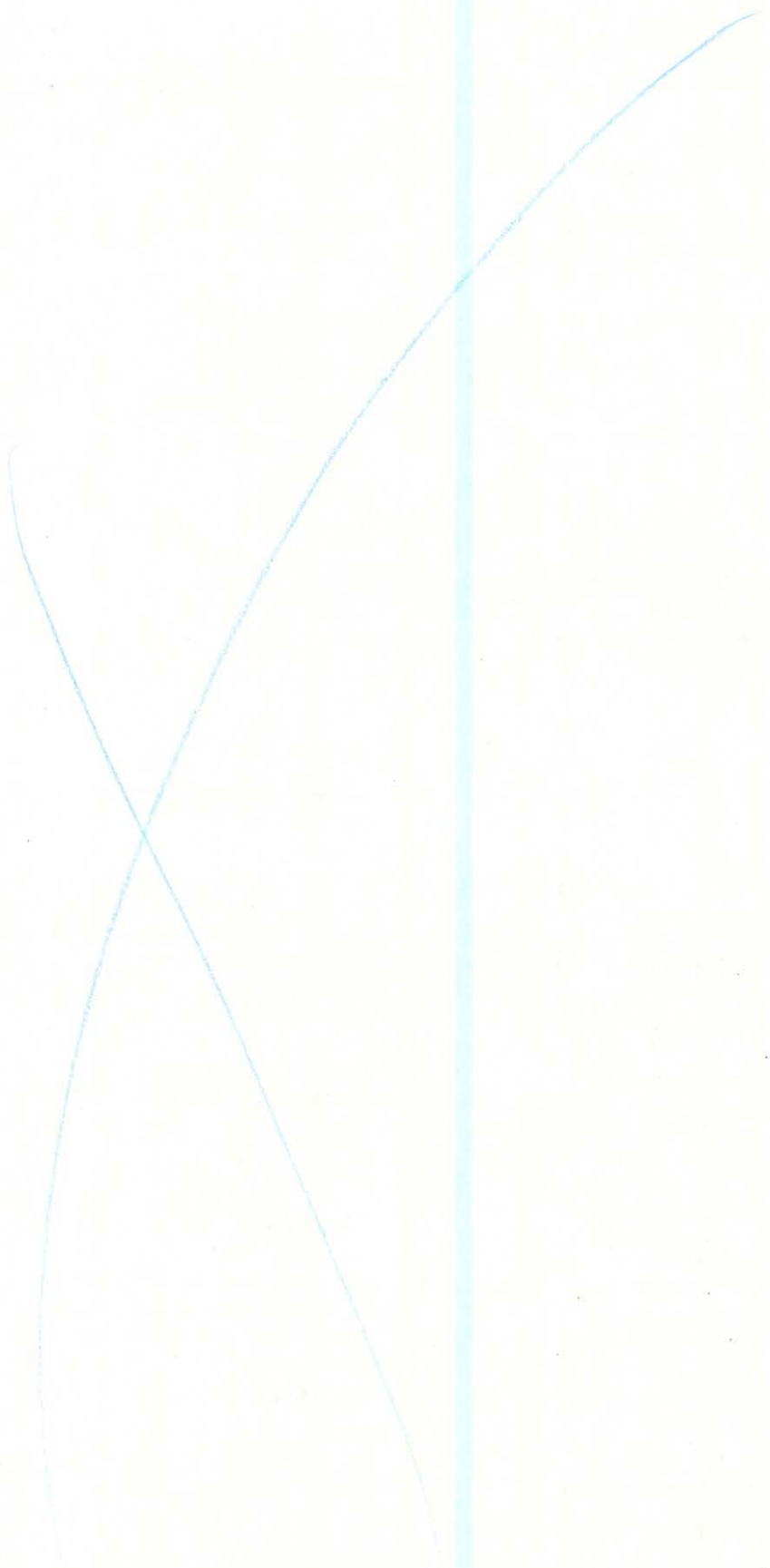

TABLE OF CONTENTS

TABLE OF CONTENTS (CONTINUED)

LIST OF FIGURES

LIST OF FIGURES (CONTINUED)

LIST OF FIGURES (CONTINUED)

LIST OF TABLES

EXECUTIVE SUMMARY

INTRODUCTION

Large increases in fuel costs and the cost of locomotive ownership over the past several years have greatly increased the incentives to reduce train energy requirements. In 1981 railroad diesel fuel purchases amounted to 3.4 billion dollars. Another 1.4 billion dollars was expended on locomotive maintenance. Given a service life of 27 years per locomotive, an annual expenditure of approximately 1 billion dollars would be required to renew the existing fleet of 27,000 locomotives. Due to the extreme leverage available for potential savings from small reductions in train resistance, it was decided that the Transportation Test Center should develop a one-percent accurate system for measuring train resistance. With this tool even small percentage savings in train resistance could be accurately documented.

Many past efforts to measure train resistance have concentrated on the use of load-measuring couplers. These have the inherent disadvantage that forces due to train handling and slack action become superimposed on the measured train resistance forces. This prevents accurate measurement of small changes in train resistance. In addition, load measuring couplers are somewhat susceptible to damage, being fully exposed to the operating environment.

During the Spring of 1983, at the Transportation Test Center (TTC) in Pueblo, Colorado, a series of tests was performed wherein a GP40-2 locomotive was installed on the Roll Dynamics Unit (RDU), a major test fixture in the TTC's Rail Dynamics Laboratory (RDL). These tests were to evaluate the performance of the RDU as a dynamometer. Tests showed that the RDU could be successfully used in a dynamometer mode to evaluate locomotive performance. Subsequently, a proposal was made to instrument a locomotive's traction motor input power as a means of measuring its tractive effort capability. This locomotive would then be used to measure differences in energy demand posed by the use of radial trucks versus regular trucks and lubricated track versus dry track. These energy tests would be performed on the FAST track.

If this system proved successful, a locomotive instrumented in such a way could then be used to measure the differences in energy required by conventional rail equipment versus the energy required by various proposed energy-saving devices such as radial trucks, track lubrication, and train aerodynamic aids.

The ultimate goal would be to develop an instrumentation package that could be fitted to any locomotive in the field. In order to measure the small changes of resistance expected, an accuracy of one percent would be necessary.

OBJECTIVES

The overall test objectives were as follows:

1. Develop an instrumentation package that could be easily installed on a locomotive to measure its tractive power. This package would be portable and accurate to within one percent.

2. Utilize the instrumented locomotive in a controlled experiment on the FAST track to demonstrate the use of the instrument package by identi-

fying any possible energy savings from the use of radial trucks and rail lubrication.

TEST SEQUENCES

To meet the above objectives, testing was performed in three phases.

First, to calibrate the instrumented locomotive, it was placed on the RDU and its tractive performance evaluated using the RDU as a dynamometer. Tests were performed that would identify the conversion efficiencies of traction motor input electrical power to tractive power at the wheels.

Initial test results indicated linear relationships between input electrical power to the traction motor armatures and resultant tractive power in both driving and dynamic braking conditions. Based on these results, the locomotive was released from the RDU and a locomotive-based data acquisition system was installed.

Next, the locomotive was used in some preliminary tractive effort studies on the FAST track, wherein the use of radial trucks and rail lubrication for energy savings was investigated.

In addition, since the initial RDU results showed that there were some calibration errors in the RDU torquemeters, an RDU system check was performed and the RDU torquemeters were recalibrated.

Finally, upon the completion of the FAST track tests, the locomotive was remounted on the RDU and certain tests were repeated. In addition, new tests were performed in order to recalibrate the locomotive for a larger range of operating conditions.

Reports of these test programs are fully detailed in the following sections. Part 1 details the calibration procedures performed in the RDU. Part 2 covers the field testing of the successfully calibrated locomotive on the FAST track.

CONCLUSIONS

This experimental program has proved to be quite successful. The calibrated, instrumented locomotive has been used in several successful AAR and proprietary train resistance test programs, both at the TTC and in the field. In addition, several proprietary tests of train resistance have been performed using similar portable instrumentation systems on other locomotives.

When compared with dry track results, resistance savings of greater than 30 percent were measured for both track lubrication and for radial design trucks, as operated on the FAST track at 40 mph. Savings for individual track segments are the subject of Part 2 of this report.

The measured savings due to track lubrication have been validated by fuel top-off readings on the FAST locomotive power over several months of alternating dry and lubrication operation.

These top-off readings are for four locomotives pulling a seventy-car (loaded 100-ton hoppers) train on the FAST loop.

The microcomputer-based portable data acquisition system gained broader acceptance during this test and more advanced systems are now widely used throughout AAR research programs, both at the TTC and in the field.

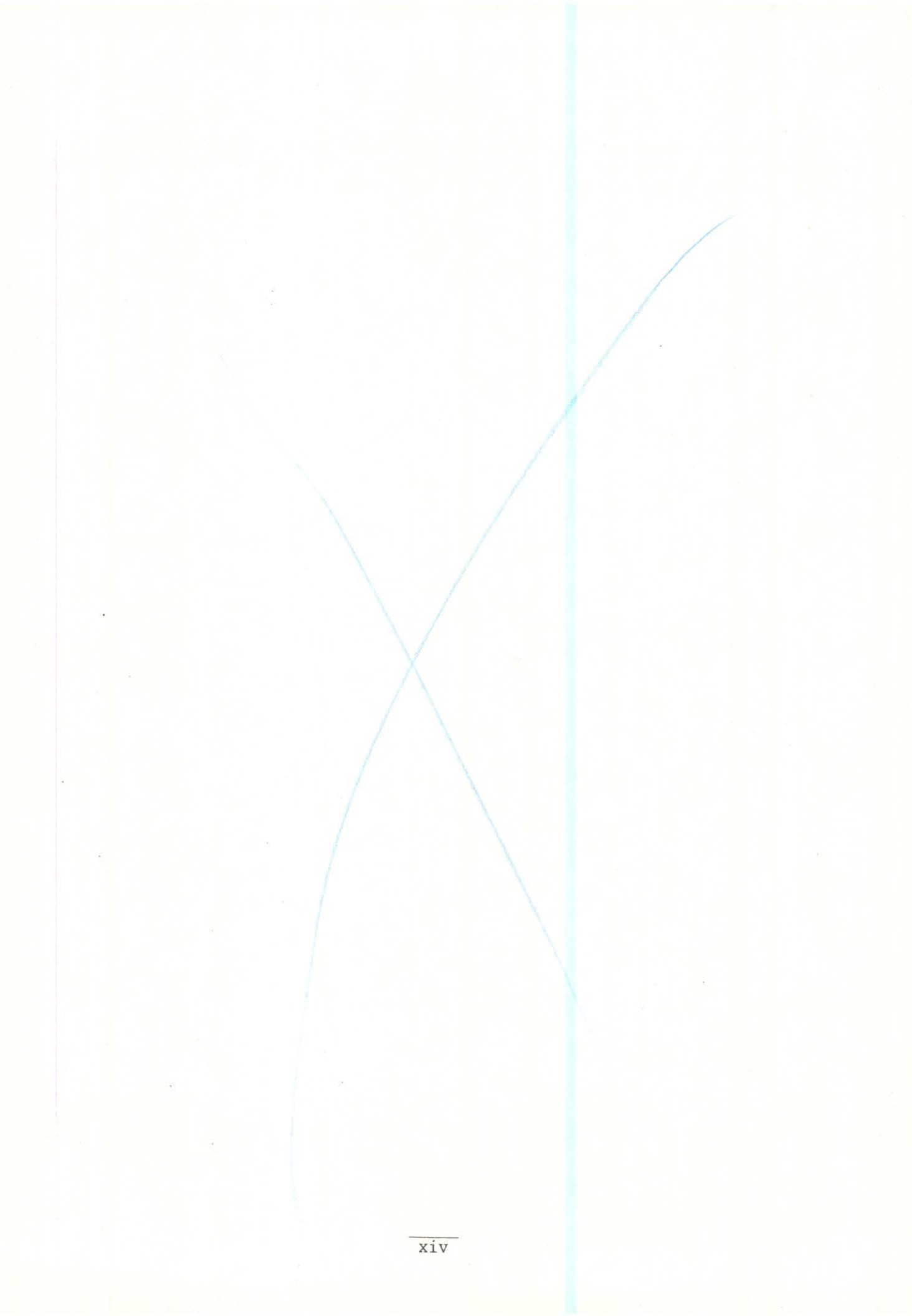

PART 1: INSTRUMENTATION SYSTEM DEVELOPMENT AND CALIBRATION ON THE RDU

1.0 INTRODUCTION

The general methodologies for the calibration tests on the RDU were based on the successful previous tests demonstrating the Dynamometer capability of the RDU and using a locomotive on the RDU to evaluate fuel flowmeters [1,2]*. In order to achieve the desired accuracy of one percent, a wide range of tests would be required to evaluate several instrumentation schemes and locomotive performance ranges.

2.0 TEST OBJECTIVES

In order to calibrate the required instrumented locomotive, the following major test objectives were identified:

a. Provide conversion efficiencies for each traction motor and wheelset from input electrical power to tractive power at the rails. Efficiencies were to be calculated in both driving and dynamic braking conditions, at different speeds and throttle settings.

b. Compare individual traction motor and wheelset assemblies with each other to determine whether their performances were similar.

c. Identify the accuracy with which the final calibrated locomotive could measure tractive power.

3.0 TEST DESCRIPTIONS

Calibration testing on the RDU was performed in two phases. The first sequence immediately followed the fuel flowmeter evaluations [2]. Because of initial good results, the locomotive was released for use at FAST during the Summer of 1984 for the track tests reported in Part 2.

Upon completion of the track tests, a more thorough recalibration was performed on the RDU during October and November of 1984. These were prompted by findings at the FAST and the discovery of a calibration error in some of the RDU torquemeters.

The individual tests performed were as follows:

3.1 PHASE 1

a. Investigate the waveforms of voltages and currents at the traction motors. This was to ascertain the degree of error in using filtered voltages and currents to calculate the input power.

---

*References are listed following the text of Part 2.

b. Measure the input electrical power to the locomotive traction motor armatures under constant speed in various control notches to calculate drive mode conversion efficiency.

c. Measure the output power of the traction motors to the dynamic brake grids while stopping the rollers in various dynamic brake ranges to calculate brake mode conversion efficiency.

3.2 PHASE 2

a. Perform constant torque acceleration tests to recalculate RDU and locomotive rotational inertias.

b. Perform free roll deceleration tests with RDU in coast mode to recalculate locomotive and RDU gear train losses.

c. Investigate waveforms of traction motor voltages and currents to measure the effects of high current draw under low speed acceleration.

d. Measure locomotive input power under high acceleration with RDU in constant torque mode to measure high tractive effort conversion efficiency.

e. Repeat b. and c. of Phase 1 to recheck earlier data after the RDU recalibration.

4.0 TEST EQUIPMENT AND INSTRUMENTATION

4.1 TEST EQUIPMENT

4.1.1 Roll Dynamics Unit

The RDU, described in [1], consists of four identical modules, each designed to support one wheelset of a test vehicle. The wheels are supported on 60-inch diameter rollers that simulate the heads of rails.

Each pair of rollers is coupled through flywheels, gearboxes, and a torquemeter to a 600 hp electric motor/generator.

The RDU is equipped to drive the test vehicle at either a constant speed or with a constant torque applied to the rollers.

When the test vehicle is being slowed down, or is applying power to the rollers, the energy being absorbed by the RDU motors is regenerated by the motor and resupplied to the electric power system.

4.1.2 Test Vehicle

The test vehicle for this project was a GP40-2 locomotive, Number 3054, provided by the Burlington Northern Railroad. Figure 1 shows this locomotive in place on the RDU during the Phase 2 testing.

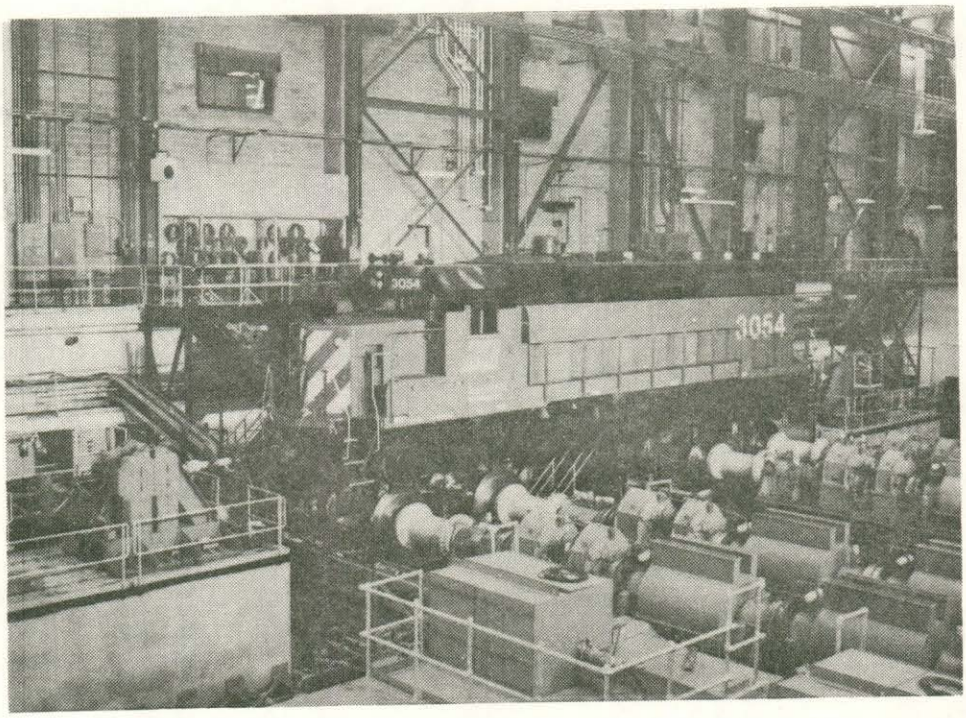

TTC N83-0165

FIGURE 1. LOCOMOTIVE ON THE RDU.

This is a 3000-hp diesel-electric locomotive built by General Motors' Electro-Motive Division (EMD). It is equipped with four EMD type D77 direct current traction motors permanently connected in parallel. The main generator was a model AR-10 alternator, providing a nominal rectified 1200 volts dc with 4000-ampere direct current rating. The engine was a 16-cylinder GM 2-cycle diesel, model 16-645E3. The traction motors were geared with a 62:15 ratio to 40" diameter wheels.

This was the same unit as that used for the dynamometer tests [1]. (The vehicle had undergone no technical alterations except for repair of the dynamic brake controller, which had failed during the dynamometer tests.)

4.2 INSTRUMENTATION

Instrumentation for this test involved many devices connected in parallel in order to determine, by comparison, which would be most appropriate for our use in terms of accuracy, durability, and simplicity. Most of these determinations had been made by the end of Phase 1. Consequently, Phase 2 instrumentation requirements were reduced.

4.2.1 RDU Instrumentation

The RDU is extensively instrumented; therefore, no additional instrumentation was required. The instrumentation used was as follows:

4.2.1.1 RDU Torque and Speed

Each RDU drive train has one Himmelstein torquemeter located between the RDU motor output and the inertia modules (flywheels). These are patched to the control room for recording. The torquemeters were recalibrated between Phase 1 and 2 as described in Appendix A.

A speed-calibrated tachometer is also mounted on each RDU motor outboard shaft. The digital pulses generated by the tachometers are converted to analog voltages, which are available at the control room patch panel. Speed (mph) and torque data (ft-lbs) were both recorded digitally.

4.2.1.2 RDU Motor Voltage and Current

Each motor's armature voltage and current are measured and displayed on analog meters in the RDL control room and on each power control room operator's panel. In addition, analog voltages representing these signals are available on the patch panel. Proper calibration of these signals was not performed but the data were recorded digitally for reference purposes.

All instrumentation was patched into the RDL control room patch panel for recording by the RDL Data Acquisition System (DAS) computer.

Data were analog filtered at 2 Hz during all tests except those described in Section 5.1 during high speed data collection.

A general schematic of the instrumentation data collection scheme is shown in Figure 2.

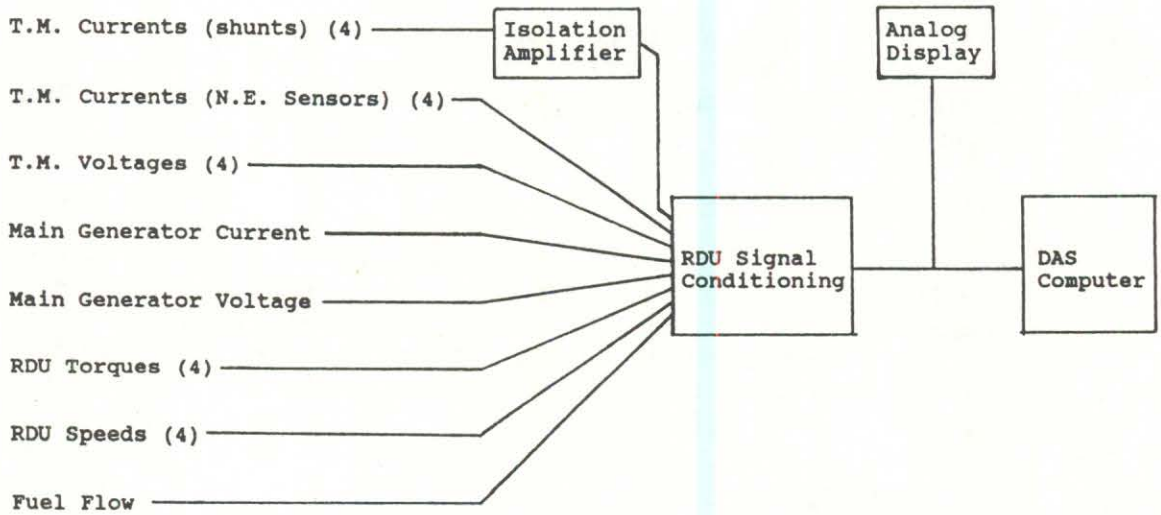

FIGURE 2. GENERAL SCHEMATIC, INSTRUMENTATION DATA COLLECTION SCHEME.

4.2.2 Locomotive Instrumentation

To determine the input and output power of the traction motors, the current and armature voltage were measured and their product taken to calculate power.

4.2.2.1 Traction Motor Armature Voltage

During Phase 1 the armature voltage was measured using voltage dividers placed across the traction motor cable connections in the high voltage cabinet of the locomotive cab. A schematic of the divider installation is shown in Figure 3.

Since the locomotive had a floating ground, it remained possible that an inadvertent ground fault could result in high voltage being applied to the data lines. Therefore, a two-leg voltage divider was used, which effectively isolated the data collection system from the locomotive.

During Phase 2, the voltage dividers were replaced with Ohio Semitronics, Inc., (OSI) VT7 voltage transducers, shown installed under an equipment table in the locomotive cab (Figure 4). In addition to being more accurate and reliable than the voltage dividers, the transducers are also self-isolating.

4.2.2.2 Traction Motor Current

Two methods were used to measure the motor current. The first was to use current shunts in series with the input cable connections in the high voltage cabinet. In Figure 5, the shunt for traction motor 3 is shown as it was installed on the P3 power contactor. The current signal was isolated from the data collection system by means of Analog Devices 273 K isolation amplifiers, which provided over 1000 volts isolation.

The second method for measuring the current was by means of AAC #909M4C inductive current probes placed around the traction motor leads. The design of these probes isolated them from the problems of the floating locomotive ground. However, the physical constraints in mounting prevented the installation of these devices according to their specifications. Because this prevented their readings from being as accurate as the current shunts, they were removed after Phase 1, before the FAST track tests.

4.2.2.3 Main Generator Voltage

The main generator voltage was measured using a voltage divider similar to those used for the traction motors. Its design provided isolation from the locomotive floating ground.

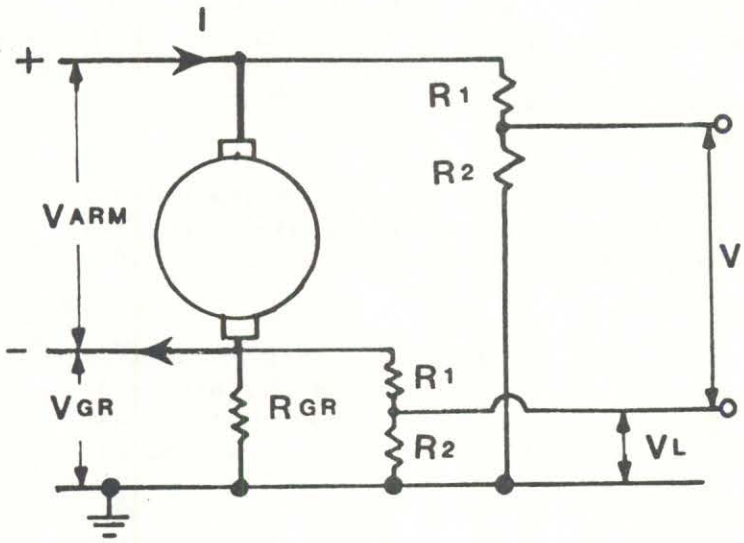

$$V_S + V_L = \frac{R_2}{R_2 + R_1} \times (V_{ARM} + V_{GR})$$

$$V_L = \frac{R_2}{R_2 + R_1} \times V_{GR}$$

$$\therefore V_S = \frac{R_2}{R_2 + R_1} \times V_{ARM}$$

FIGURE 3. VOLTAGE DIVIDER NETWORK.

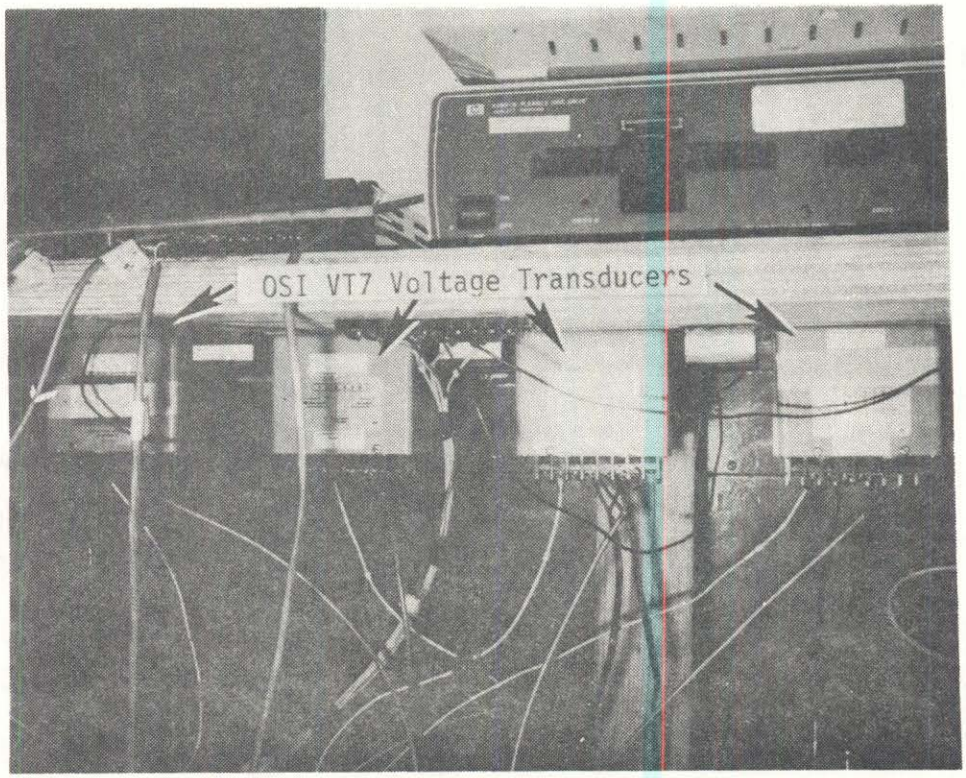

TTC N83-1916

FIGURE 4. OSI VT7 VOLTAGE TRANSDUCERS.

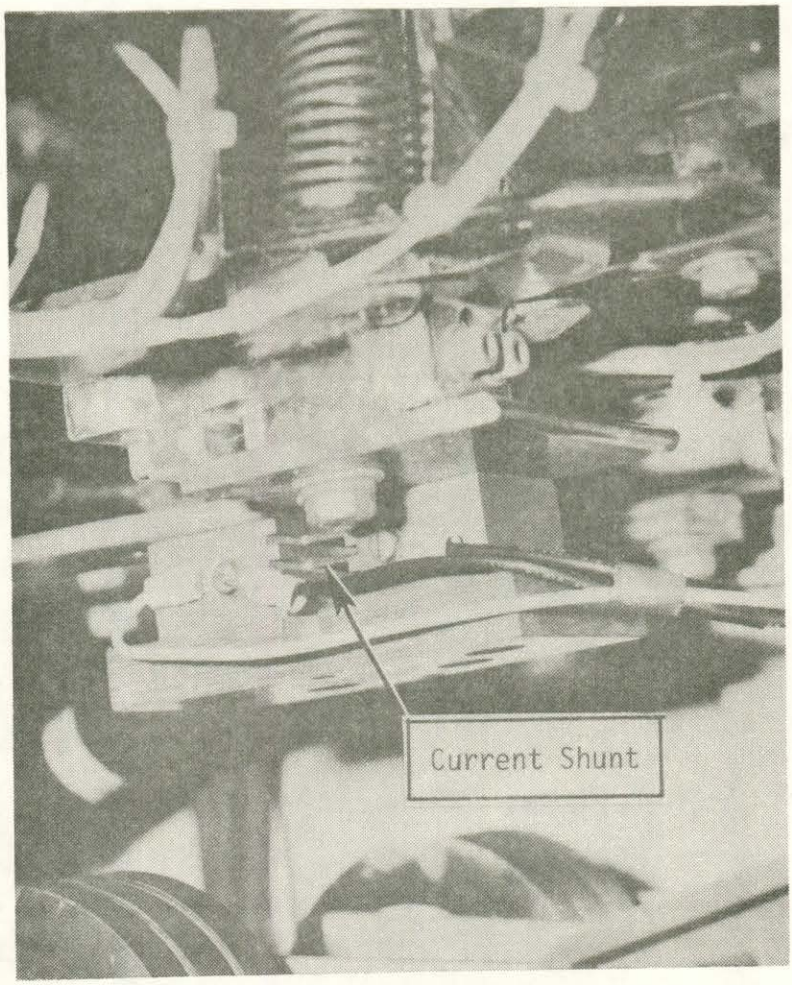

TTC N83-1914

FIGURE 5. CURRENT SHUNT ON P3 POWER CONTRACTOR.

4.2.2.4 Main Generator Current

Two methods were used to measure main generator current. The first used was the factory-installed current shunt. This signal was also passed through an isolation amplifier.

An inductive current probe (Ohio Semitronics CT8KLTS) was also used. This probe was installed around the main generator output bus bar, as shown in Figure 6. The design precluded the need for isolation amplifiers. This unit proved to be too sensitive as to its orientation to the bus bar and was also prone to being jiggled apart by vibrations. Therefore, it was not used for Phase 2. Otherwise, it proved to be quite accurate and was removed after the FAST track tests, for use in field testing on Seaboard Coast Lines (SCL) Railroad.

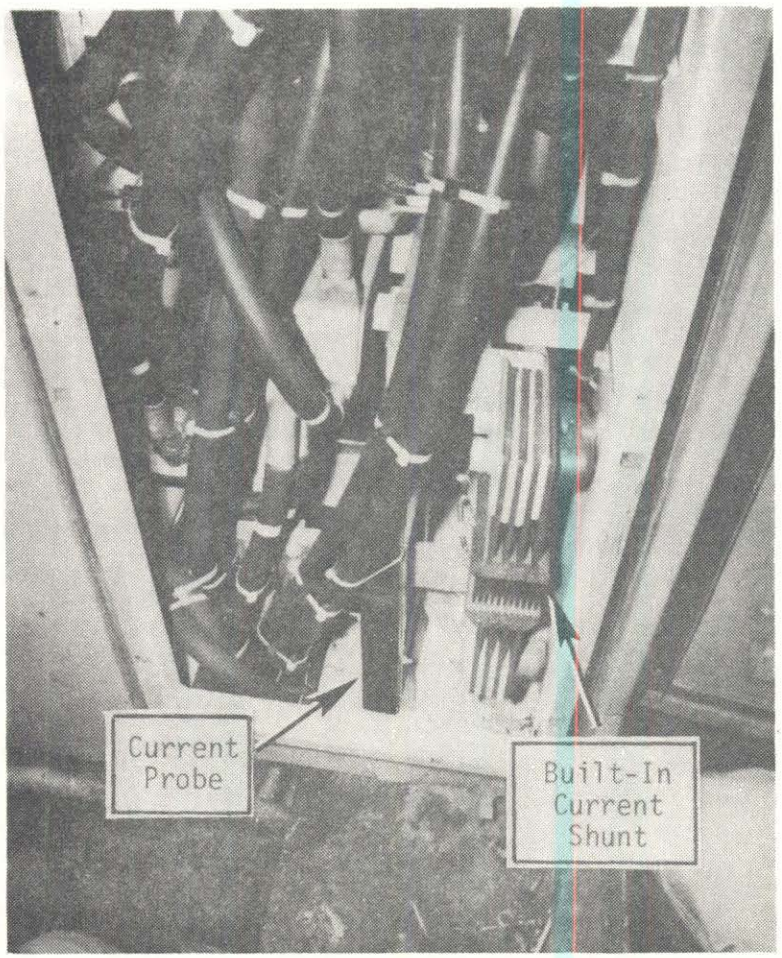

TTC N83-0951

FIGURE 6. CT8 KLTS MAIN GENERATOR CURRENT PROBE.

4.2.2.5 Locomotive Speed

A digital tachometer mounted on axle 1 provides the locomotive with a built-in speedometer for the engineer's use. A pulse counter and digital-to-analog speed converter were connected into this tachometer for reading locomotive speed. This was installed after Phase 1 for use during the FAST track tests. During Phase 2 it was patched into the RDL data collection system for comparison purposes.

4.2.2.6 Fuel Flowmeter

Previous to the locomotive tractive effort test, this same locomotive had been used on the RDU for comparison testing of fuel flowmeters.[2] All the fuel flowmeters remained installed during the tractive effort testing because followup flowmeter testing was to continue subsequent to the FAST track tests. One flowmeter, the MAX, with a range of 0-200 gallons per hour, was patched into the data collection system during Phases 1 and 2 of the testing. In addition, it was monitored during the FAST track testing.

5.0 TEST PROCEDURES AND ANALYSIS

The required tests were performed as outlined in Section 3. All tests were performed sequentially, with very little time in between for quick-look data analysis. Using the RDL's data acquisition system computer, data were recorded on digital tape for future analysis.

Data reduction was accomplished with the RDL's PDP 11/60 computer, using the TTC's Data Reduction System (DRS) analysis package. Some of the statistical analysis for calculating data accuracy was performed on the TTC's VAX 11/780 computer, using the Statistical Package for the Social Sciences (SPSS) analysis software.

5.1 WAVEFORM ANALYSIS

The proposed measuring system was to obtain input power to each traction motor by multiplying the digital voltage and current measurements together. The output power at the rail could be determined from the roller speed and torque measurements and, thus, performance curves for each traction motor could be developed.

Due to the varying waveforms of the voltages and currents (dc level with an ac ripple superimposed), the initial task was to determine whether the product of the voltage and current, when filtered and sampled at a low rate, would accurately represent the actual power input to the traction motor. Thus, the first test was to run the locomotive at various speeds and sample unfiltered voltage and current data at a very high rate (4096 samples per second) in order to determine the waveforms. The products of the voltage and current were then calculated in two ways, the first being an instantaneous product to give the actual power waveform. The second was to take the average of each voltage and current over a 1-second period and then multiply averages together to obtain the average power. This is essentially the same as applying a 1-Hz filter to the raw signals.

The tests were performed in Constant Speed Mode by running the rollers at 62.9 mph. The locomotive throttle was then placed in Notch 1 and all data channels were monitored until performance stabilized. Voltage and current data from traction motor armature number 1 were collected for 10 seconds.

This test was repeated for Notches 2-8 and again for Notch 8, but while the locomotive was accelerating from approximately 10-15 mph.

Typical resultant waveforms for current and voltage for Notch 8 at 62.9 mph are shown in Figures 7 and 8. As shown in Figure 9, the product of these two curves is power (kW).

The mean values of the voltage and current data were then calculated and multiplied together. This 'average power' was then compared to the RMS value of power from Figure 9.

A comparison for all 9 tests is shown in Table 1. As can be seen, the 'average power' is different from the RMS average power by less than -0.5% in most cases, except for the unusual case of Notch 1 at 62.9 mph.

A check of the frequency content of the voltage and current data was made. Typical PSD plots for Notch 8 62.9 mph are shown in Figures 10 and 11.

These results show that in all realistic operating ranges the error in using filtered voltage and current signals to calculate input power to the traction motors should not exceed -0.5% of the actual RMS power.

5.2 CONSTANT SPEED DRIVE MODE TESTS

During these tests the RDU was brought up to constant speed. The locomotive was then put into Notch 1 and all data channels monitored until locomotive performance stabilized (2-3 minutes). All data channels were then sampled, at 32 samples a second, for at least 128 seconds.

This was repeated for all control notches at the several speeds shown in Table 2. As can be seen, not all control notches were used at the lower speeds because the RDU is not capable of absorbing the high notch power at low rpm.

This test was repeated for the second test series, as shown. During the second test series the RDU motors had their maximum current limits set lower for greater reliability. Consequently, some of the lower speed high notch runs were not repeatable. In addition, due to the fact that only the three lowest notches were usable at 10 mph, the 10 mph runs were not repeated.

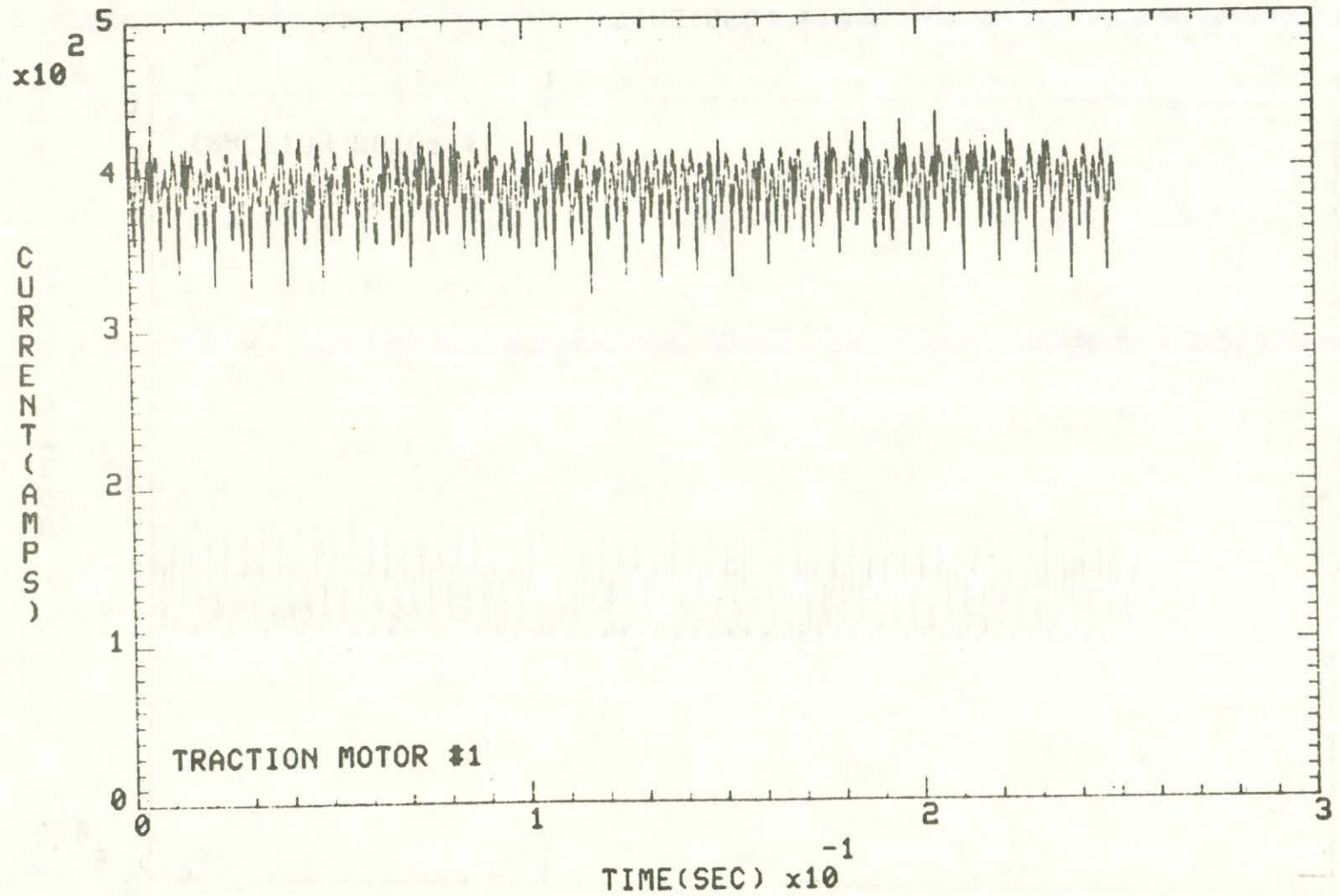
x10 2
5
4
3
2
1
0
CURRENT(AMPS)
TRACTION MOTOR #1
0
1
2
3
-1
TIME(SEC) x10

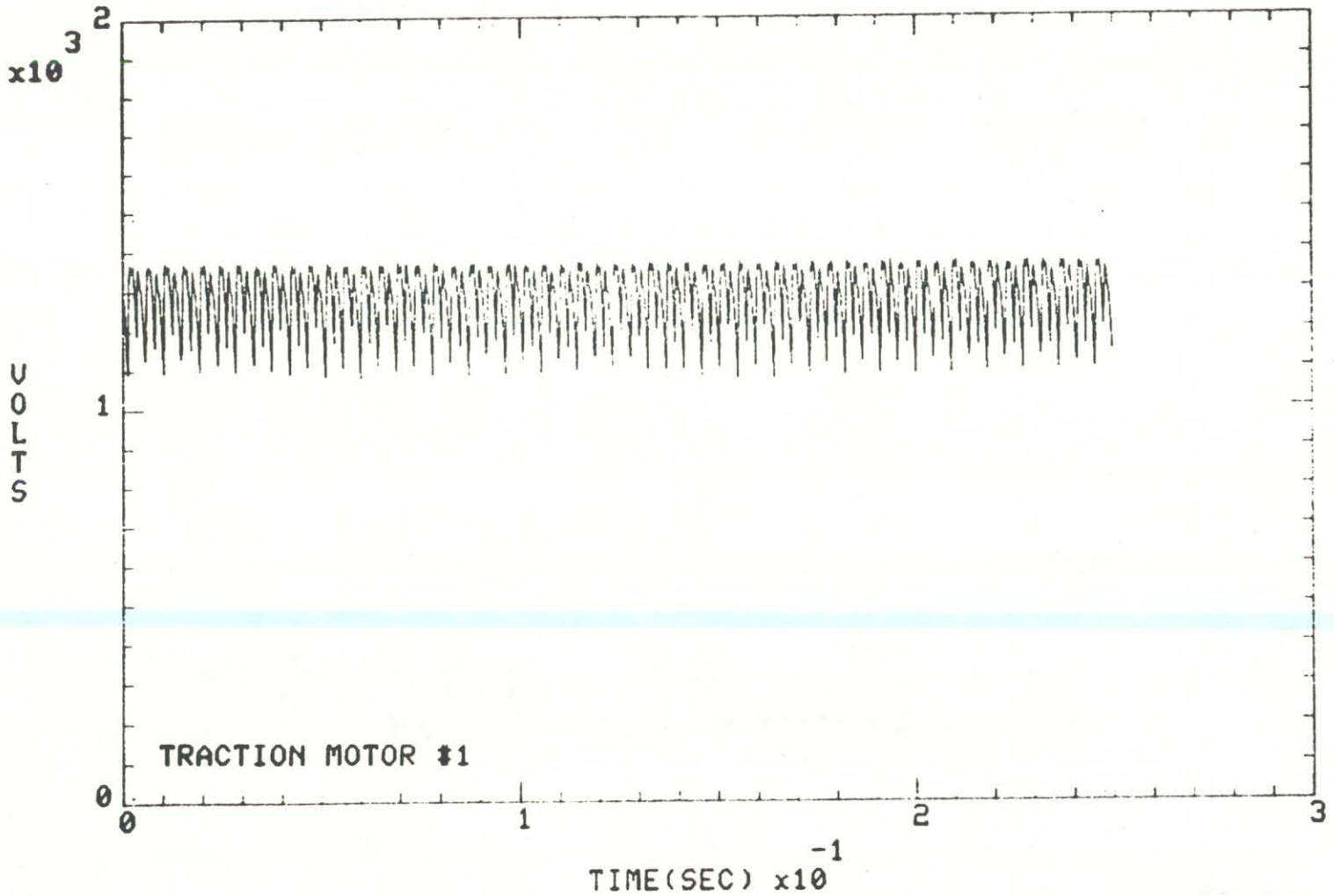

FIGURE 8. TRACTION MOTOR VOLTAGE, NOTCH 8.

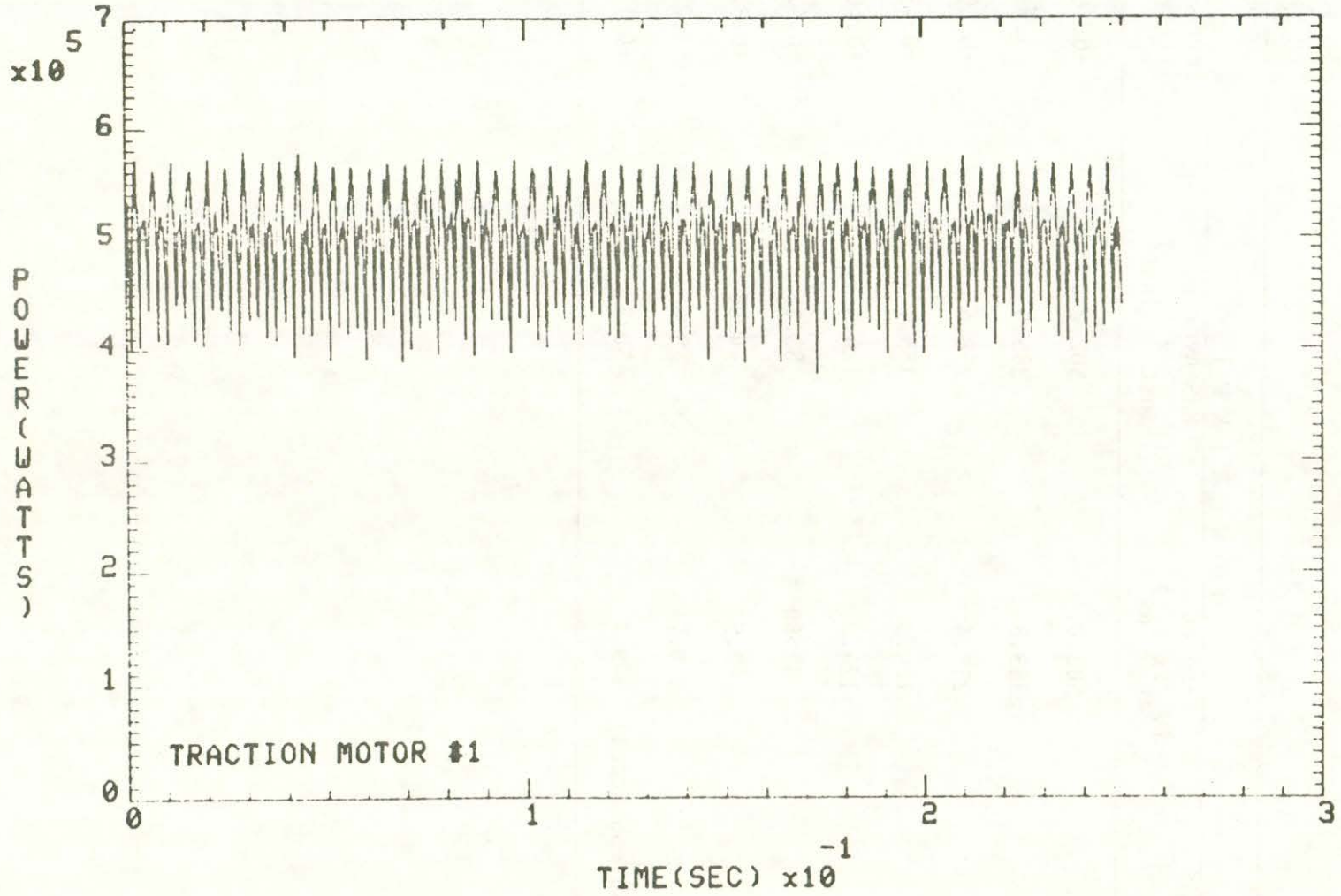

FIGURE 6 -- TRACTION MOTOR POWER - NOTCH 8

TABLE 1. COMPARISON OF PRODUCT OF MEAN CURRENT TIMES MEAN VOLTAGE WTH RMS AVERAGE POWER FOR 62.9 MPH.

Control Notch	POWER (KW)		Percent Difference
	Product ($V_{av} \times I_{av}$)	RMS Average ($V_{inst} \times I_{inst}$)	
8	503.0	502.2	+0.16%
7	383.8	385.0	+0.31%
6	257.4	258.4	+0.39%
5	184.3	185.1	+0.43%
4	124.0	124.5	+0.40%
3	82.80	83.15	+0.42%
2	43.92	44.06	+0.32%
1	9.74	9.86	+1.22%
8 (10-15 mph accel)	449.7	450.2	+0.11%

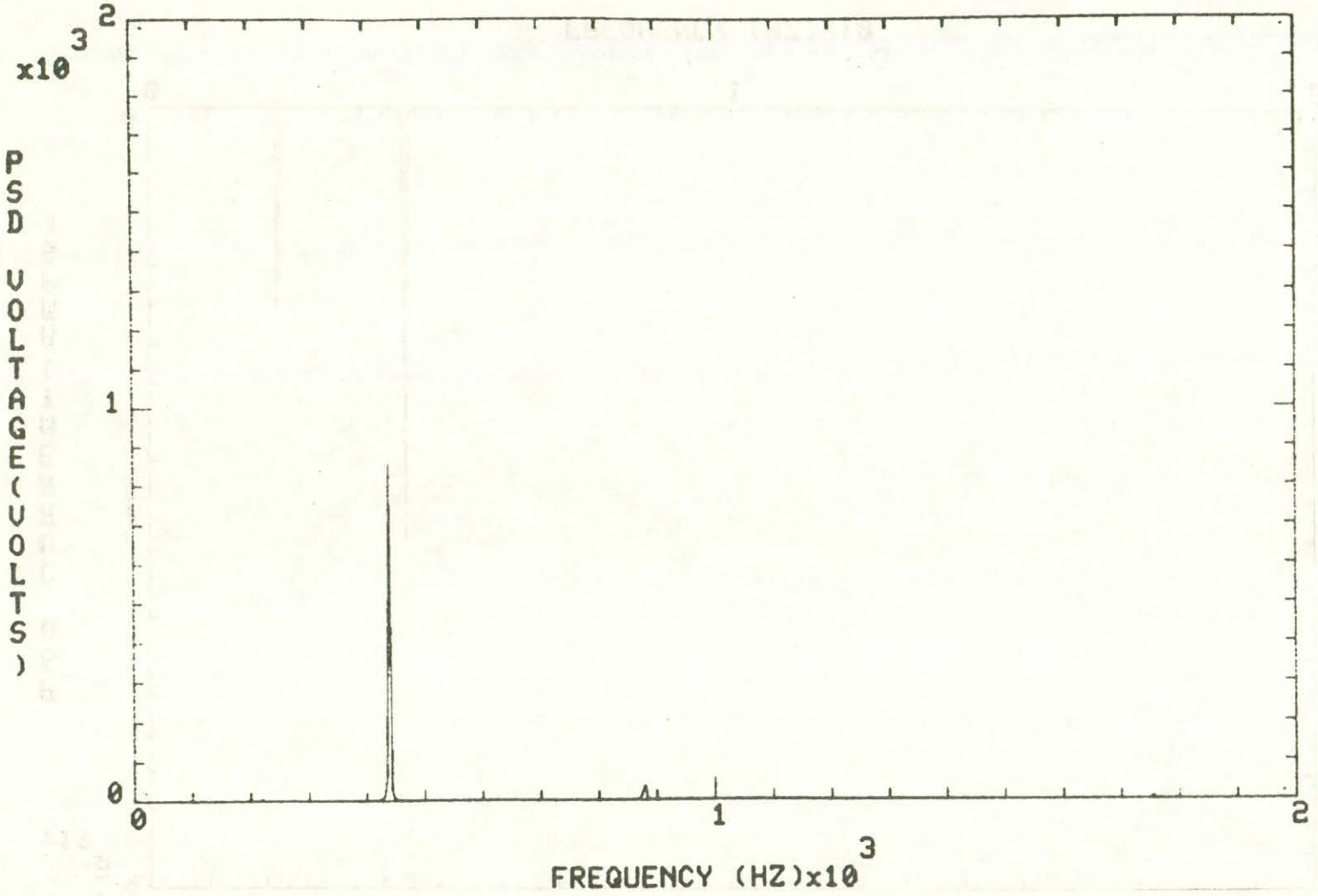

FIGURE 10 - TRACTION MOTOR #1 PSD - VOLTAGE

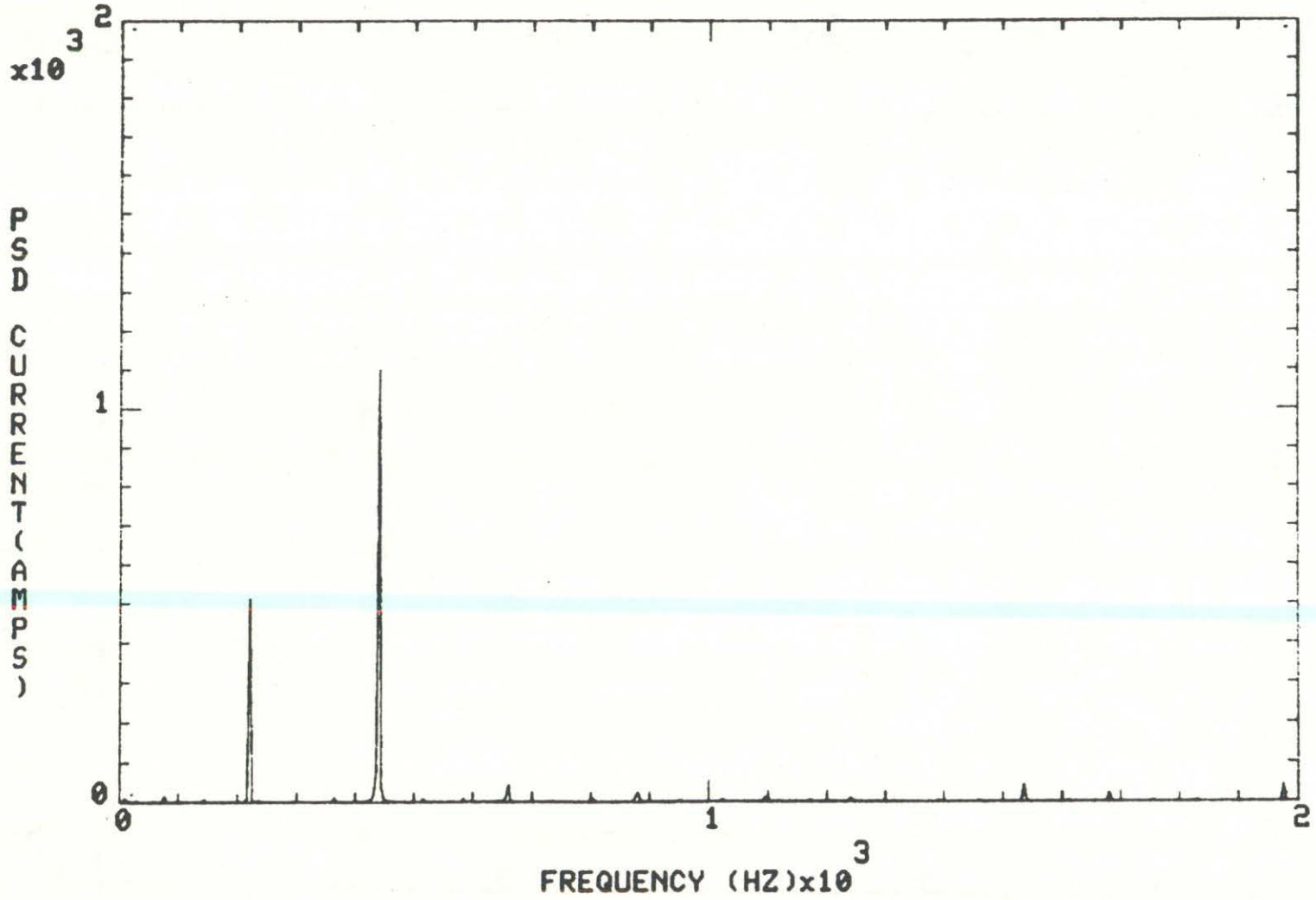

FIGURE 11. TRACTION MOTOR #1 PSD, CURRENT.

TABLE 2. TEST MATRIX FOR CONSTANT SPEED RUNS.

Speed	Notch							
	1	2	3	4	5	6	7	8
10	1	1	1					
20	1,2	1,2	1,2	1,2	1			
30	1,2	1,2	1,2	1,2	1,2	1,2		
40	1,2	1,2	1,2	1,2	1,2	1,2	1	
50	1,2	1,2	1,2	1,2	1,2	1,2	1,2	1
60	1,2	1,2	1,2	1,2	1,2	1,2	1,2	1,2
65	1,2	1,2	1,2	1,2	1,2	1,2	1,2	1,2

1 - Phase 1 Tests
2 - Phase 2 Tests

5.2.1 Data Analysis and Results

Analysis was performed by calculating the mean value for each data channel over the 128-second test period (4096 digital points). The mean values of current and voltage were multiplied to get input power and the mean values of speed and torque multiplied, using Equation 1, below, to get output mechanical power.

$$TP_M = \frac{(T + T_G) \times S}{1257} \qquad \text{(Equation 1)}$$

where

TP_M = Tractive power output at wheel roller interface (kW)

T = Torque from torquemeter at roller (ft-lbs)

T_G = Gear loss torque of RDU (ft-lbs)

S = Speed (mph)

These values for input and output power were plotted against each other for each locomotive axle, as shown in Figures 12 through 15 for series 2 tests. The results from series 1 were similar, showing very good linearity. Unfortunately, the series 1 data indicated that the torquemeter on at least one axle was in error by a large percentage. This threw into question the absolute values of all the output power data. Therefore, while the locomotive was undergoing track tests at FAST, the torquemeters were recalibrated as explained in Appendix A.

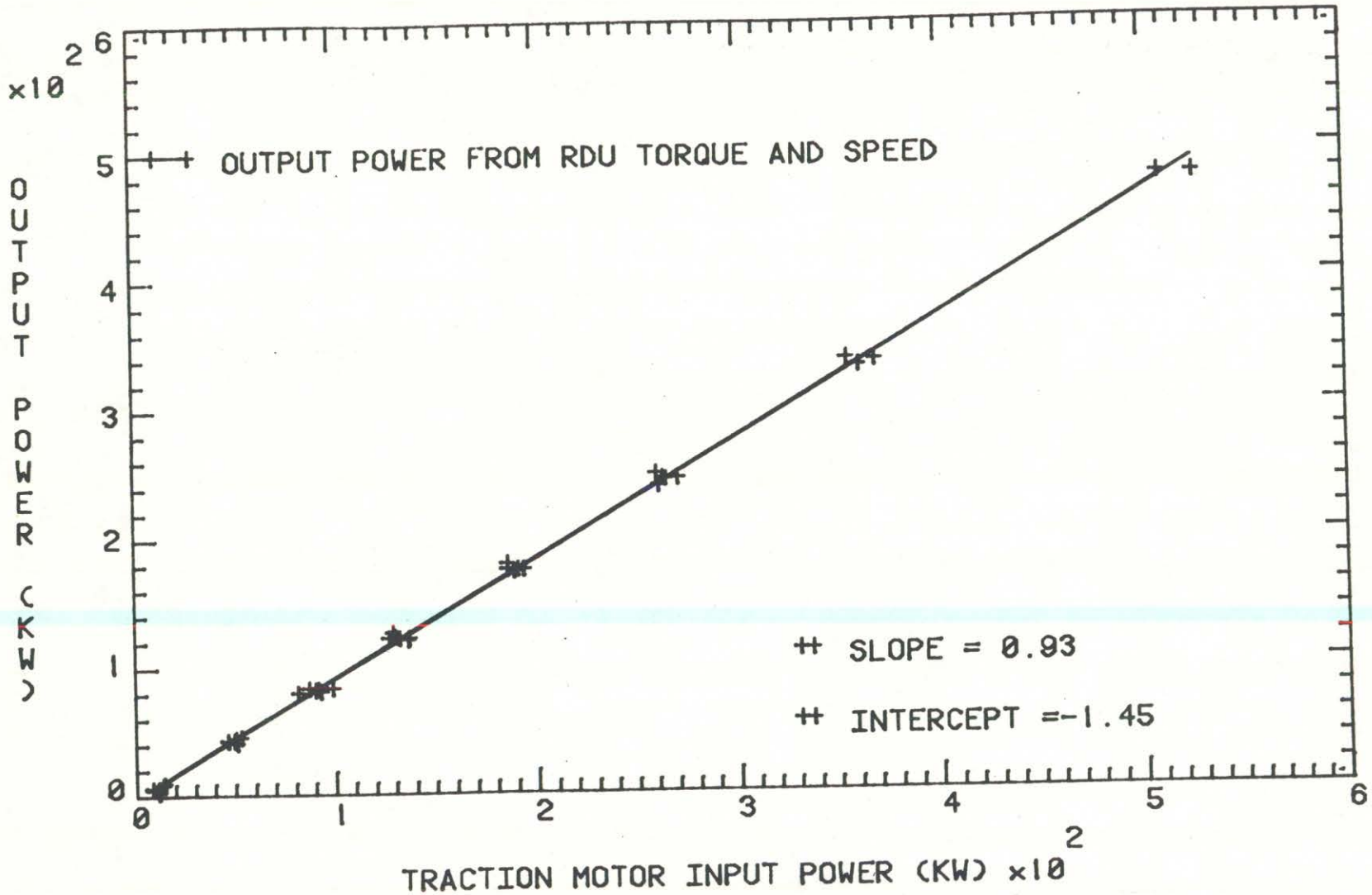

FIGURE 12. AXLE 1 OUTPUT POWER LESS RDU GEAR LOSS.

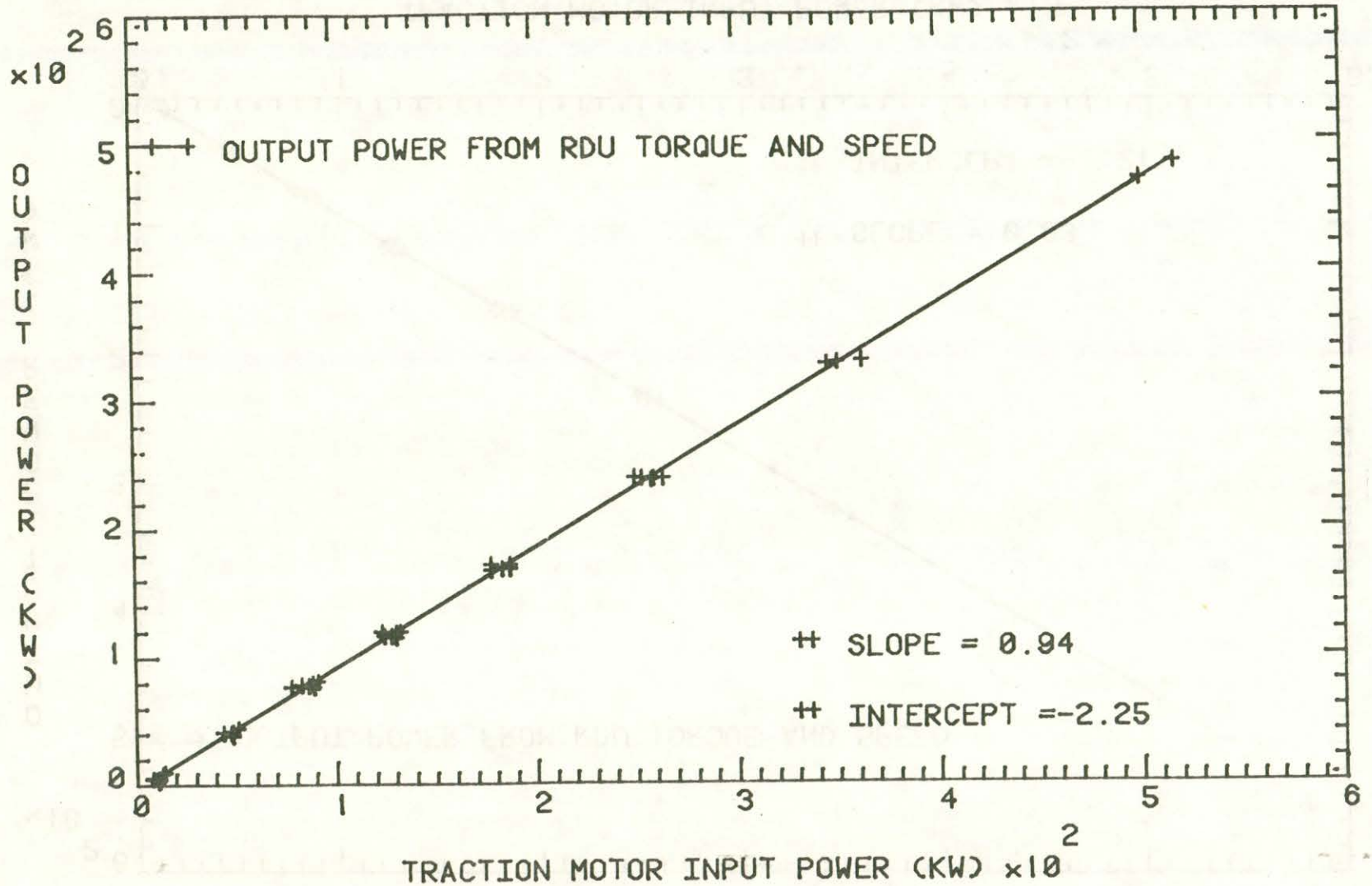

FIGURE 12. AXLE 2 OUTPUT POWER LESS RDU GEAR LOSS

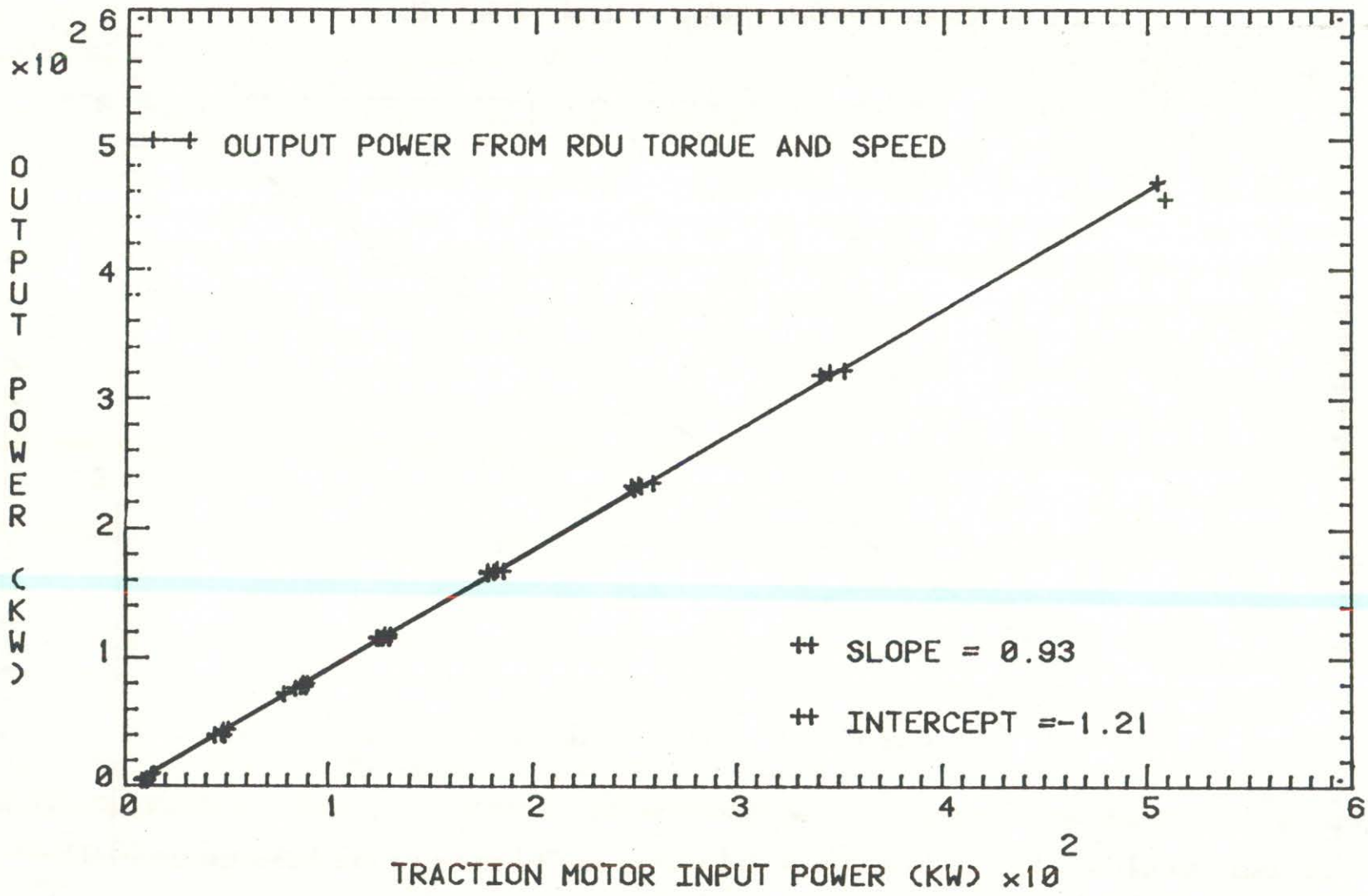

FIGURE 14. AXLE 3 OUTPUT POWER LESS RDU GEAR LOSS.

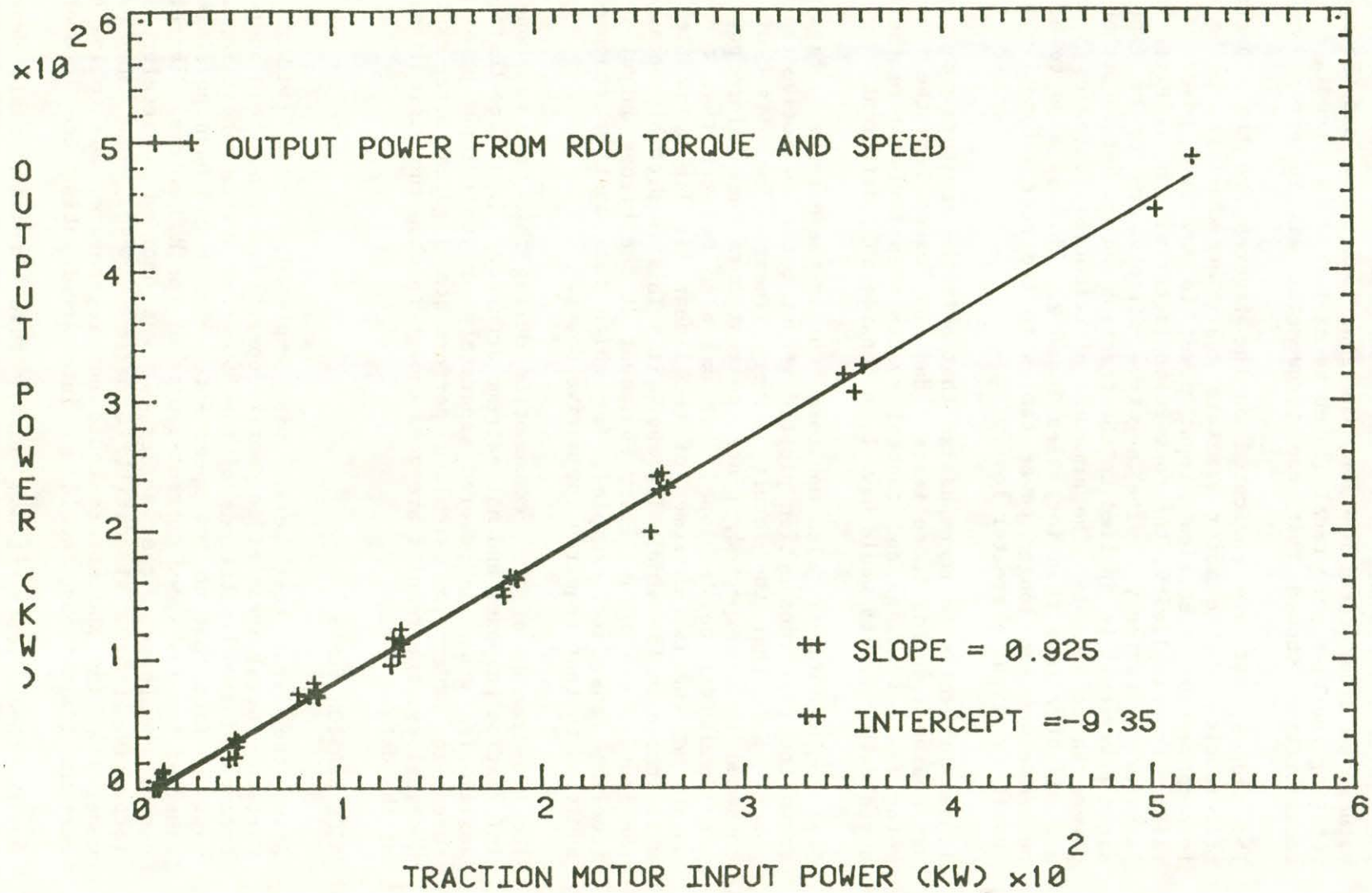

FIGURE 15. AXLE 4 OUTPUT POWER LESS RDU GEAR LOSS.

The faulty torque data threw into doubt the RDU gear loss torque values, so after recalibration, the gear loss torque and the system rotating inertias were recalculated as explained in Appendix B. The recalibration showed that one torquemeter was in error by 14%.

The slopes that are indicated on the figures are the conversion efficiencies of the motor armature gears and wheelset, to be used for converting electrical input power to tractive power at the rails. For simplicity, the conversion factor will be referred to as 'armature efficiency'. The negative offsets are to be expected since power must be applied to the traction motors before mechanical power can be output. The armature efficiencies for axles 3 and 4 are slightly less than for axles 1 and 2. This is also to be expected since the longer power cables to the rear locomotive truck result in slightly greater loss.

It is worthwhile to re-emphasize that only the armature power input was measured during these tests. Had the losses from the traction motor field windings and control system been included in the measured data, results would have been considerably different.

Fuel consumption was also monitored during these tests . Figure 16 shows the fuel consumption plotted versus total locomotive tractive power. Note that the result is very linear. The offset of fuel consumed is as expected, since one must burn fuel before power at the wheels can be developed. It can also be seen that the data points at the two extremes of the linear fit lie below the line while those in the middle lie above it. This is probably because of the heavier use of auxiliary equipment at the higher output levels (cooling fans, for example), for which fuel must be consumed in addition to that required for motive power.

The measurement of fuel consumption during this test was done for information purposes and not extreme accuracy. In future tests, all auxiliaries would be powered separately or their input power measured in order to calculate performance figures more exactly. Nonetheless, the results are good enough to show the basic linearity of the data.

5.3 ACCELERATION TESTS

After the first test series was completed, it was evident that certain crucial areas of locomotive operation had not been addressed because of the limitations of the RDU drive system. Most important was the fact that no low speed Notch 8 runs had been possible because of the low speed current limits of the RDU motors. Therefore, during the Phase 2 test series, it was decided to accelerate the locomotive from a standstill to maximum speed. Thus, any excess power that the RDU motors could not regenerate, due to low speed current limitations, would go into accelerating the locomotive.

During these tests it was likely that wheelslip could develop. Therefore, two test methods were tried. The first involved setting the RDU into Constant Torque control mode, with zero torque applied.

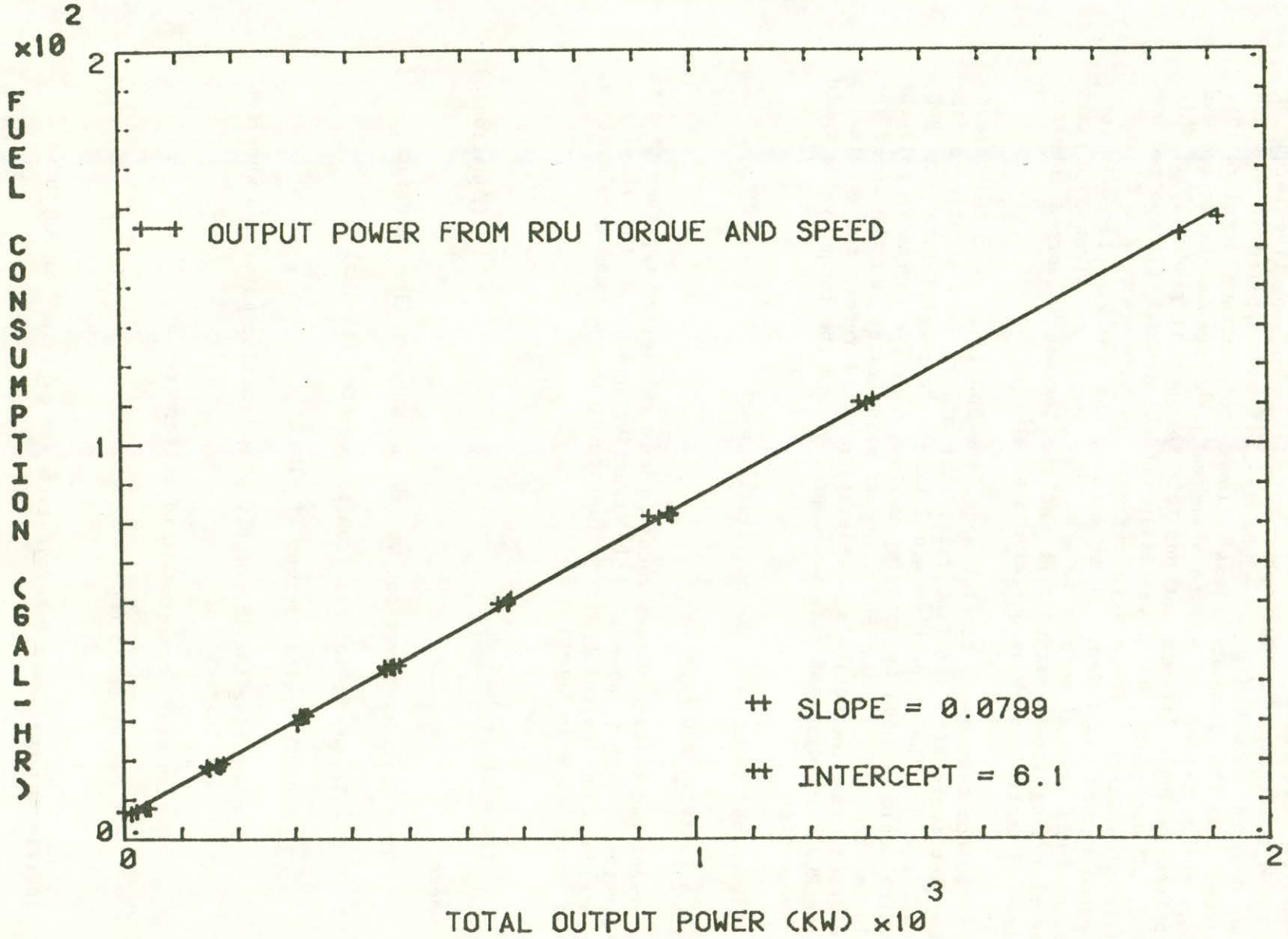

FIGURE 16. FUEL CONSUMPTION WHILE IN DRIVE MODE.

Then the locomotive was put into the desired control notch and allowed to accelerate to 5 mph. At that speed, negative torque of the desired amount (up to -3000 ft-lbs) was applied to the RDU system and the locomotive was allowed to continue accelerating. This method tended to lead to a sudden jerk because the torque was applied suddenly (it was not possible to apply it gradually). This led, at one point, to a wheelslip condition which flatspotted one pair of rollers. These were reground in situ (Appendix C) and a second method was tried. In this case, the RDU was placed in Constant Speed control mode at 65 mph. The system was allowed to start accelerating from a standstill and the locomotive worked into the desired control notch as quickly as possible.

In the Constant Speed control mode, the RDU tries to accelerate to the set speed at a constant rate, with all rollers rotating at the same speed. The locomotive would try to "out-accelerate" the RDU, which would respond by applying maximum negative torque to hold the locomotive back to the RDU's acceleration rate. As the speed increased, the locomotive's acceleration would reduce and eventually the RDU's acceleration rate would prevail and the torque value would change sign.

This second method was the one finally used.

5.3.1 Data Analysis and Results

Current and voltage values recorded were multiplied together to give electrical input power, while tractive power at the wheel/rail interface was calculated from the speed, torque, and acceleration, as shown below in Equation 2.

$$TP = \frac{(T + T_G + I\dot{\omega})S}{1257} \qquad \text{(Equation 2)}$$

where

TP = Tractive power output (kW) at wheel-roller interface

T = Torque at rollers from torquemeter (ft-lbs)

T_G = RDU gear loss torque (ft-lbs)

I = Rotating inertia of RDU plus traction motor and wheelset (ft-lbs-sec^2)

$\dot{\omega}$ = Angular acceleration of roller (rev/S^2)

S = Roller speed (mph)

Inertia and gear loss determination are explained in Appendix C.

Tractive power was then plotted versus input electrical power to the traction motor armature, as shown in Figures 17 through 20 for each axle in Notch 8. Similar results occur for the other notches. By including the traction motor and wheelset rotating inertia in the tractive power calculations, these figures show the tractive power as if the vehicle were not accelerating. The tractive power while accelerating is easily obtained by using Equation 2 with the variable (I) = the inertia of the RDU only. The result would be slightly less tractive power for axle 2, as shown in Figure 21.

By dividing the tractive power by the speed, the tractive effort may be calculated, as in Equation 3 below.

$$TE = \frac{TP \times 502.8}{S} \qquad \text{(Equation 3)}$$

where

TE = Tractive effort (lbs)

TP = Tractive power (kW)

S = Speed (mph)

The tractive effort was plotted versus speed for each axle as shown in Figures 22 through 25 for all eight control notches. Again, as with the tractive power plots, these data are representative of the tractive effort at constant speeds. Deletion of the inertia of the rotating wheelset and traction motor would decrease tractive effort as shown in Figure 26.

Once the RDU is accelerating at its own rate, the extreme 'noisiness' seen in the tractive effort (plots in Figures 22-25, especially for Traction Motor 4) is attributable entirely to the data obtained from the torquemeter signals. While accelerating to the preset speed, the RDU tries to keep all four axles rotating at the same instantaneous speed. This is accomplished by a feedback control system, which varies the torque applied to the drive train by the RDU motors. Because of the low sensitivity of the control system, the torque corrections applied to the drive train are non-gradual; i.e., they tend to be sudden and severe. This causes rapid, pronounced variations in the applied torque, and torsional vibrations in the drive train--all of which are evidenced as 'fighting' and noise in the data signals.

The data were fitted to a line by means of the least squares method. The linear coefficients are all somewhat different than those calculated for the constant speed runs. This is not entirely surprising because the data that comprise the main slope are all from the first few seconds of data, when the locomotive was quickly accelerating to about 18 mph. At that speed, the power input to the traction motors became stabilized at a relatively constant level. This is represented, on the power plots, by the smudge of data points; and, on the tractive effort plots, by the gentle downward slope (with noise) from 15-18 mph on up.

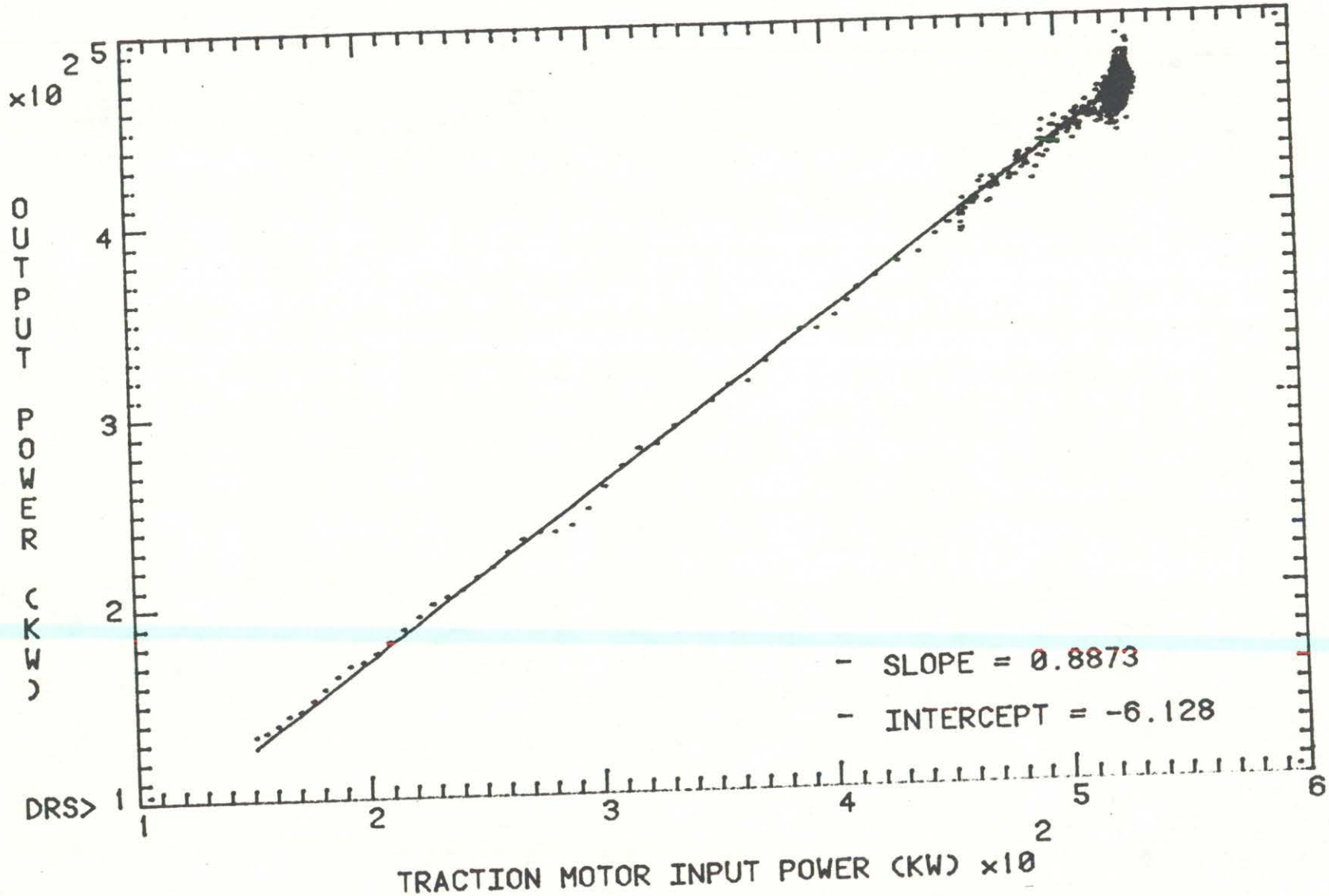

FIGURE 17. AXLE 1 OUTPUT POWER WHILE IN NOTCH 8.

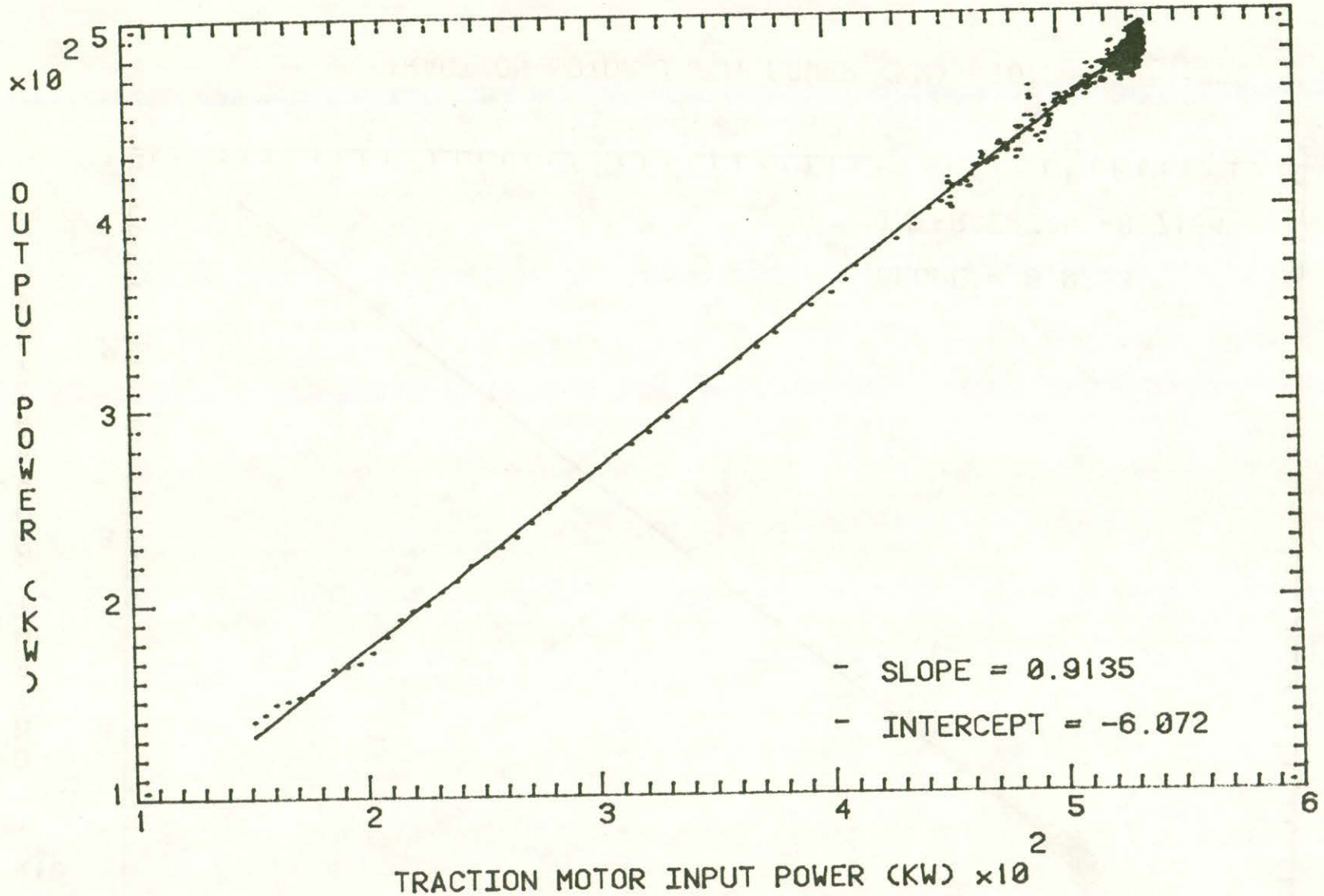

FIGURE 18. AXLE 2 OUTPUT POWER WHILE IN NOTCH 8.

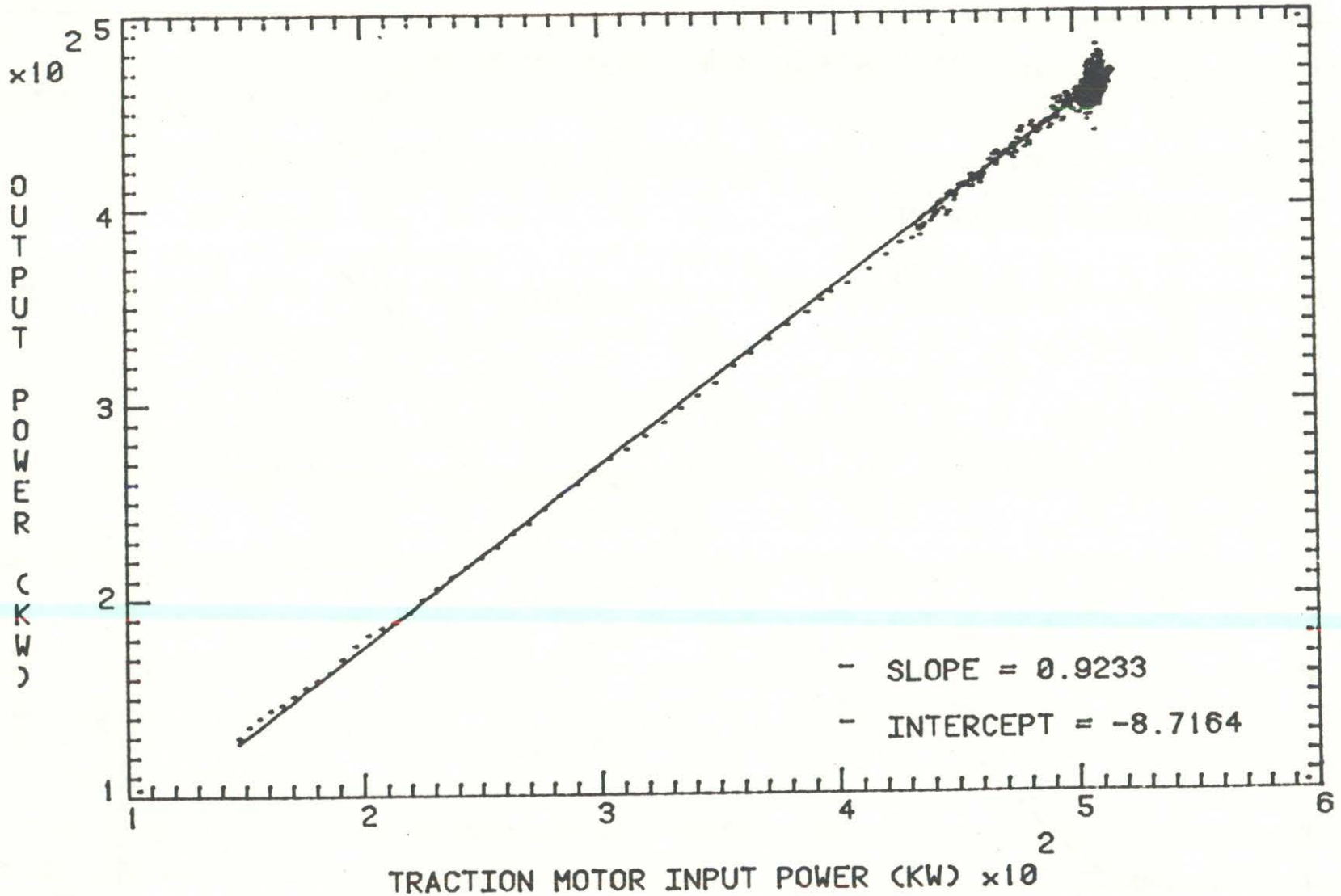

FIGURE 19. AXLE 3 OUTPUT POWER WHILE IN NOTCH 8.

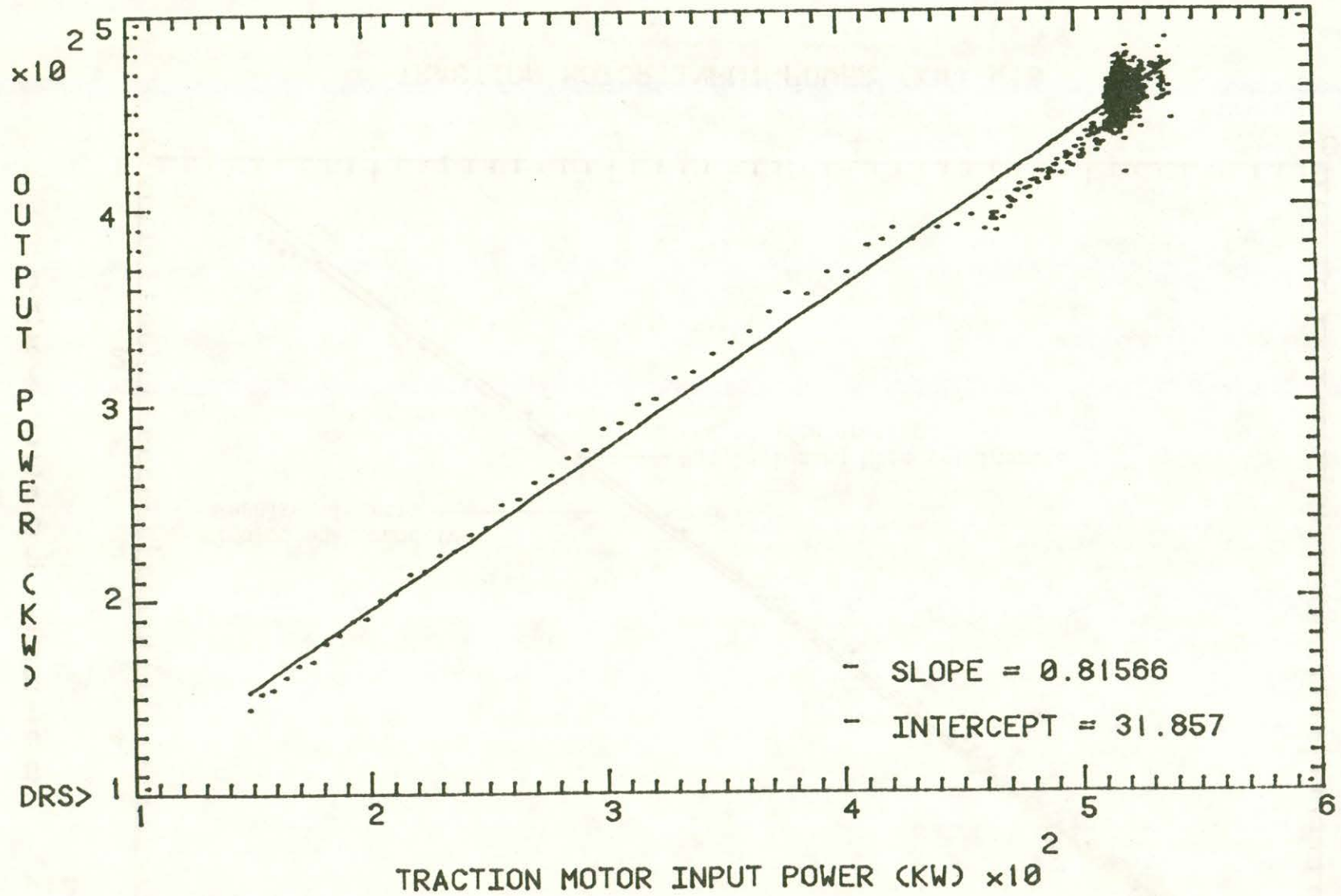

FIGURE 20. AXLE 4 OUTPUT POWER WHILE IN NOTCH 8.

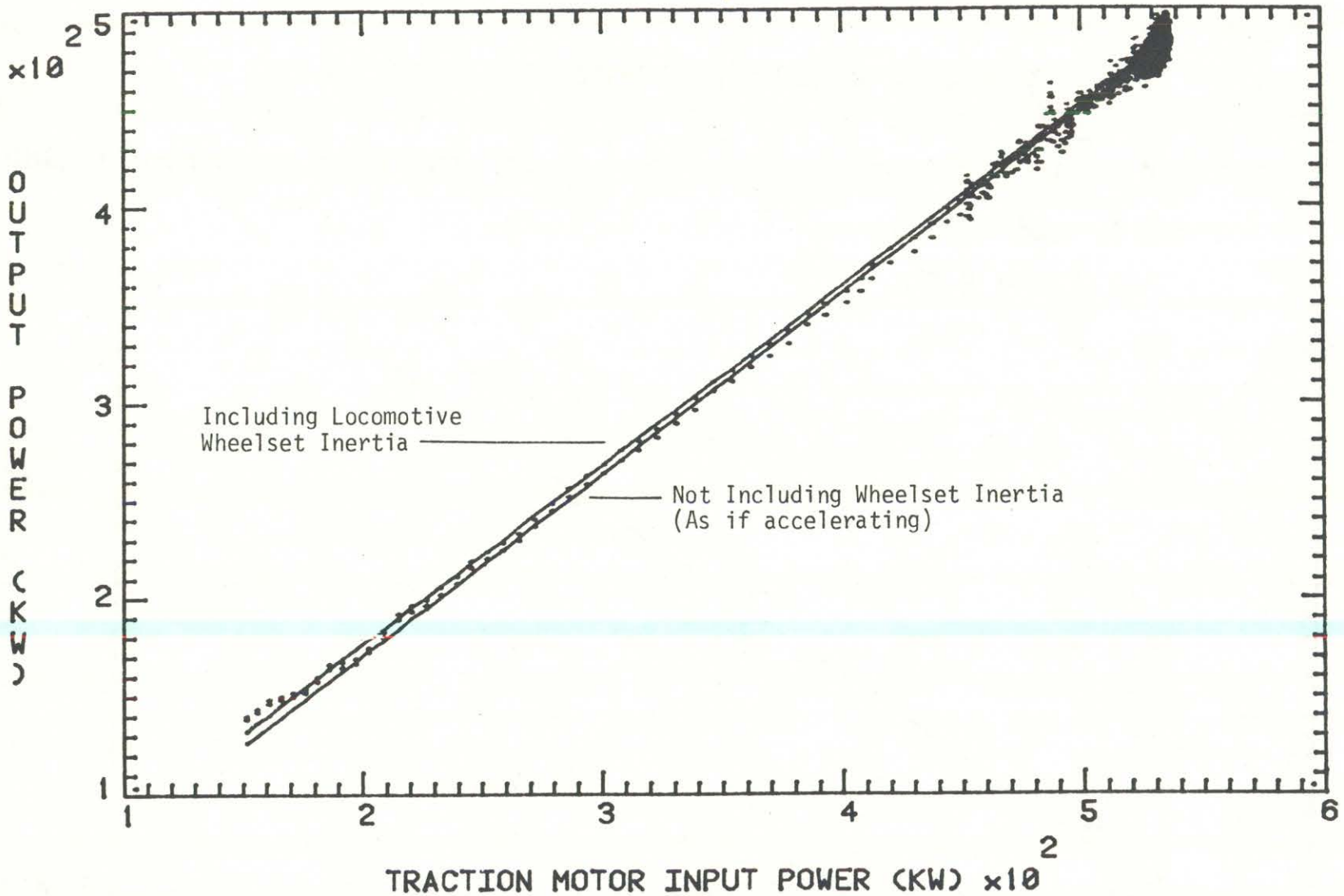

FIGURE 21. AXLE 2 OUTPUT POWER WHILE IN NOTCH 8, WITH AND WITHOUT LOCOMOTIVE.

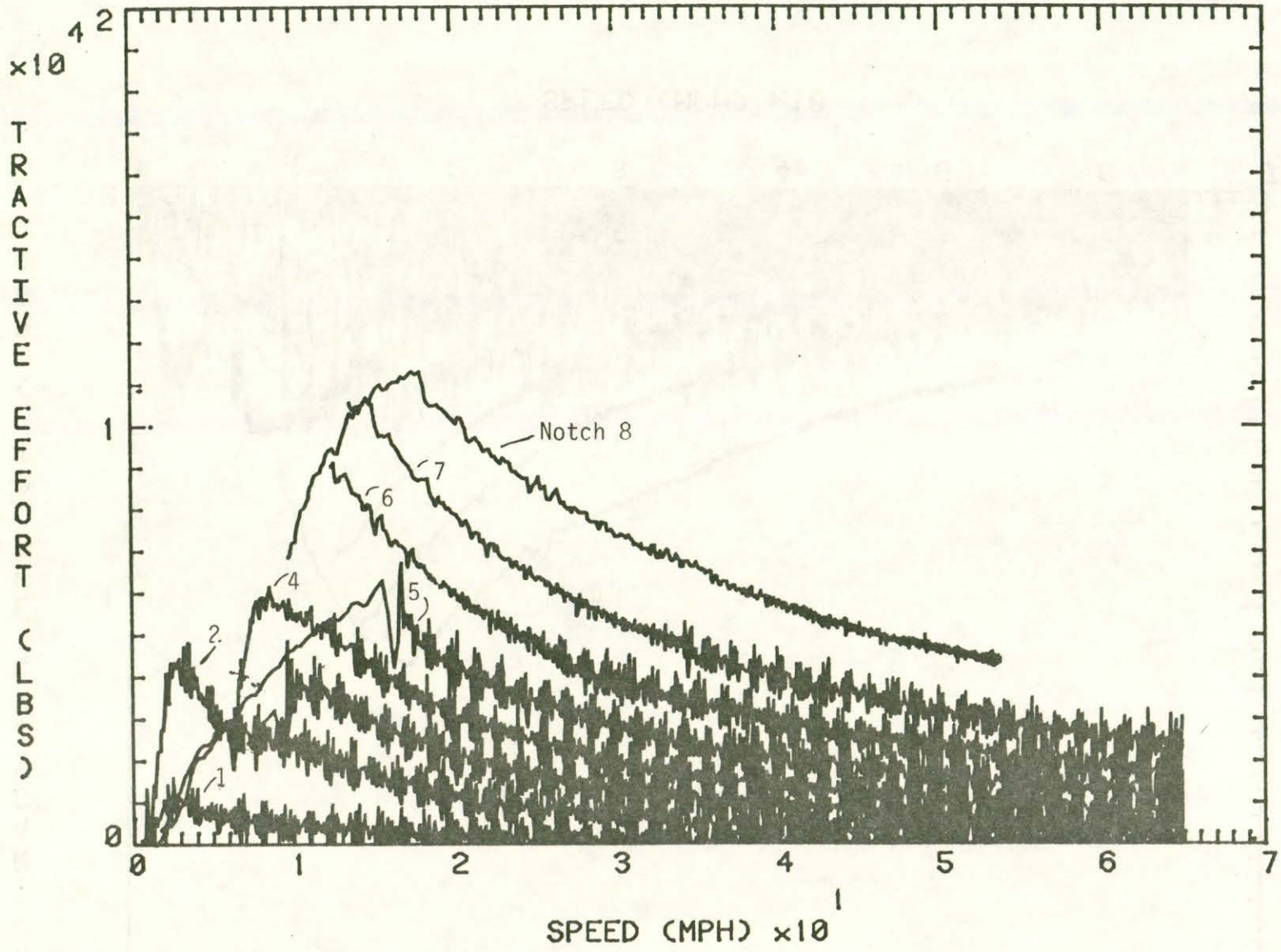

FIGURE 22 LOCOMOTIVE TRACTION MOTOR 1 NOTCHES 1-8 TRACTIVE EFFORT.

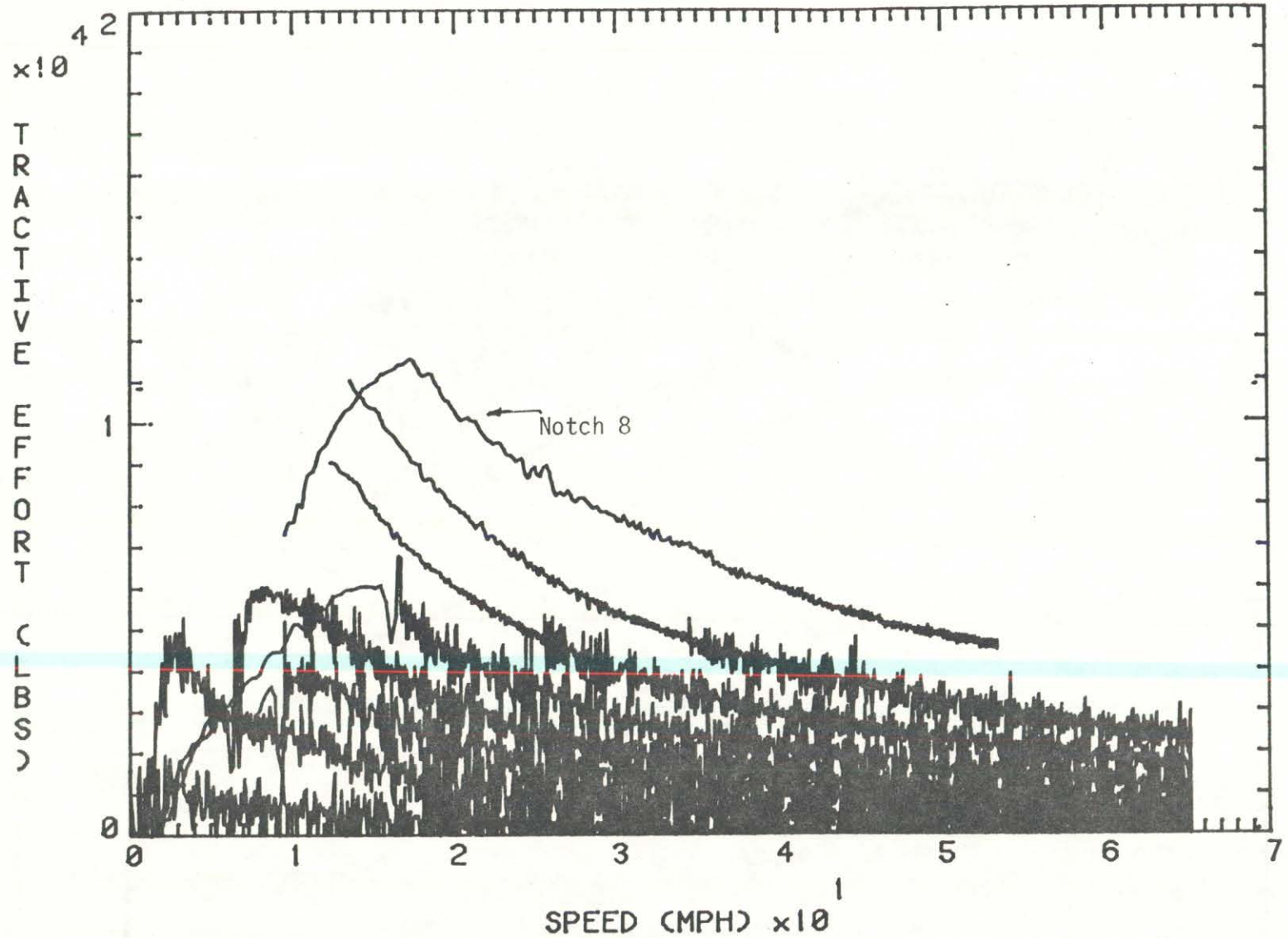

FIGURE 23. LOCOMOTIVE TRACTION MOTOR 2 NOTCHES 1-8 TRACTIVE EFFORT.

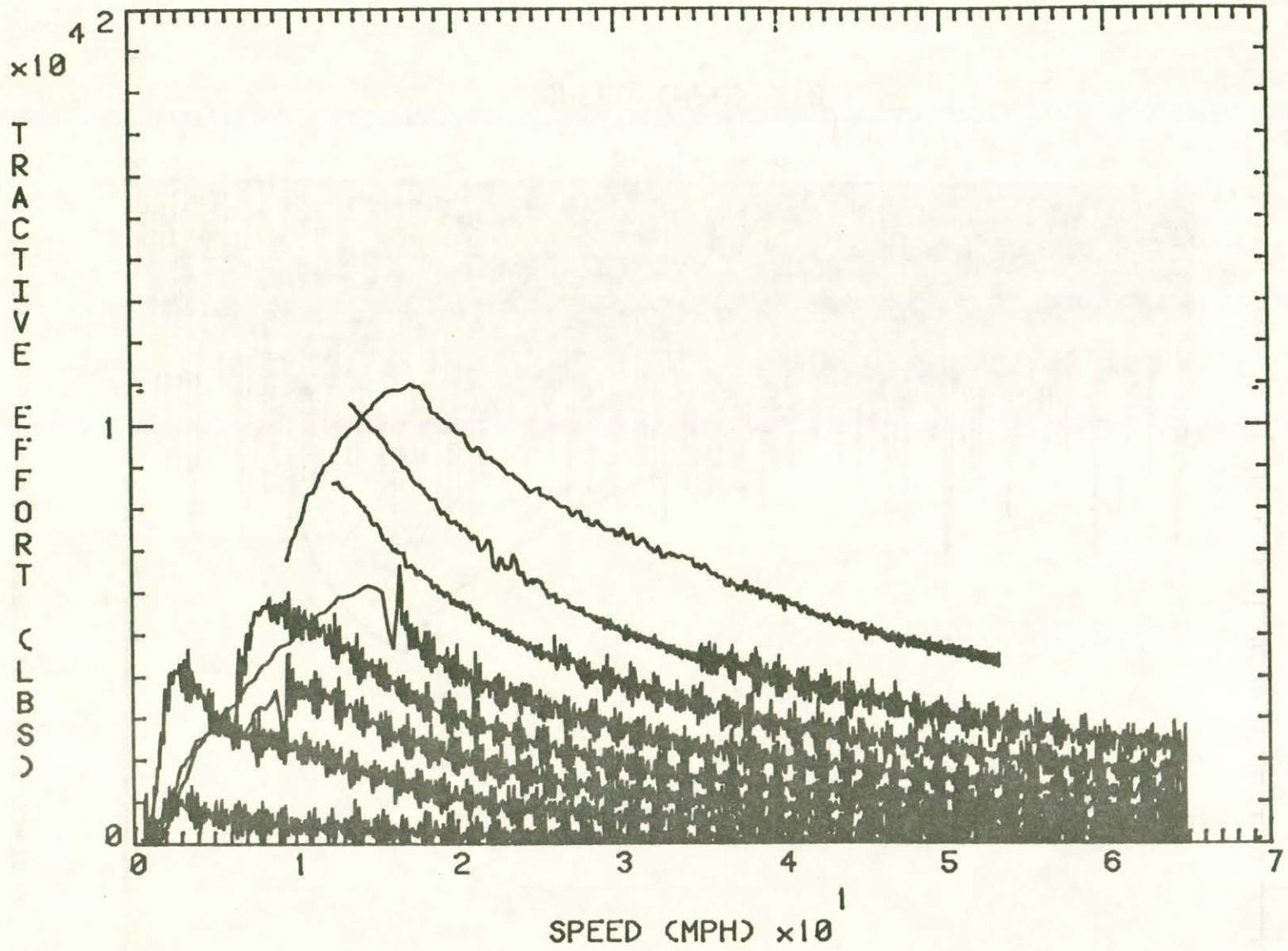

FIGURE 24. LOCOMOTIVE TRACTION MOTOR 3 NOTCHES 1-8 TRACTIVE EFFORT.

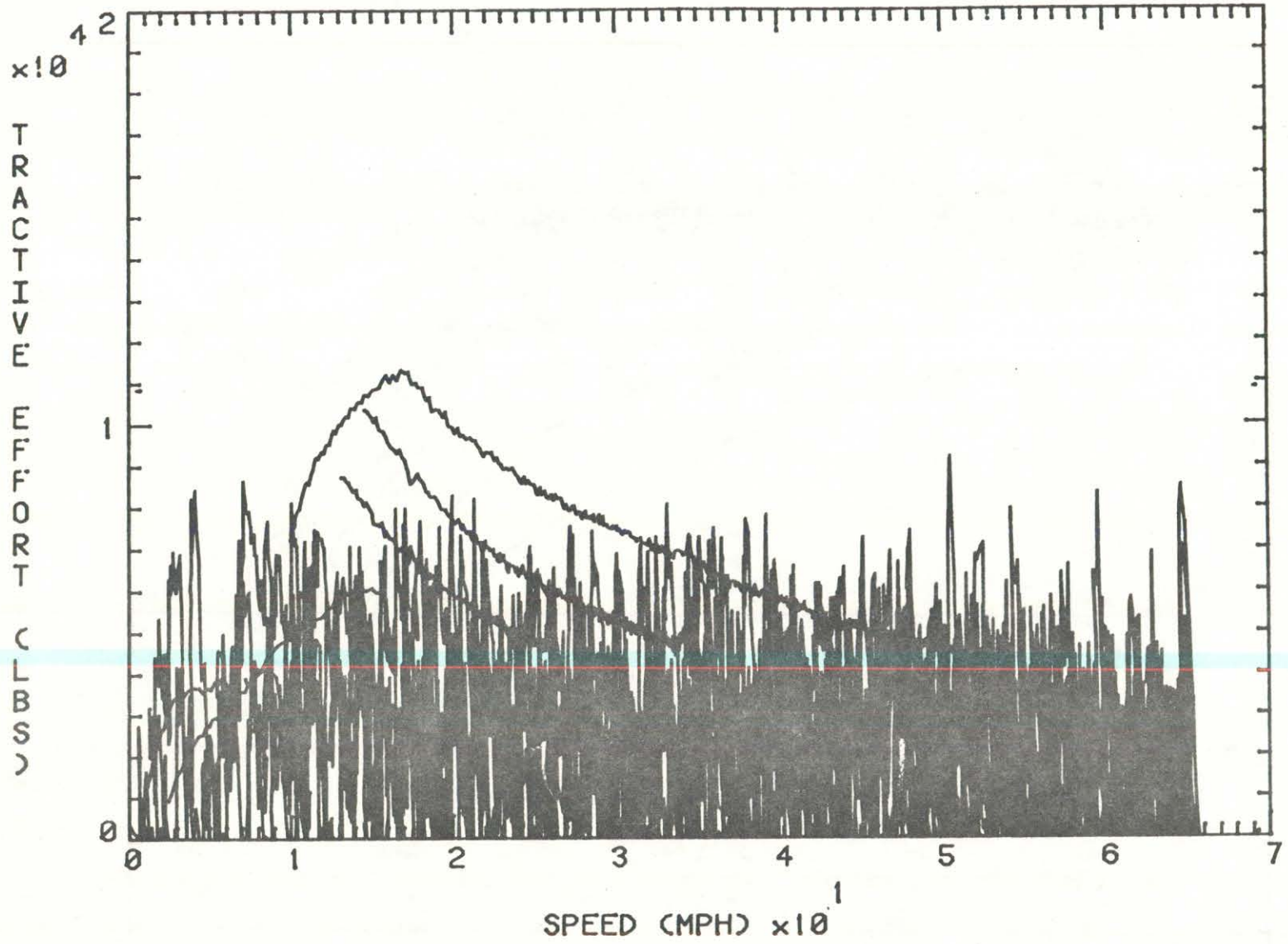

FIGURE 25. LOCOMOTIVE TRACTION MOTOR 4 NOTCHES 1-8 TRACTIVE EFFORT.

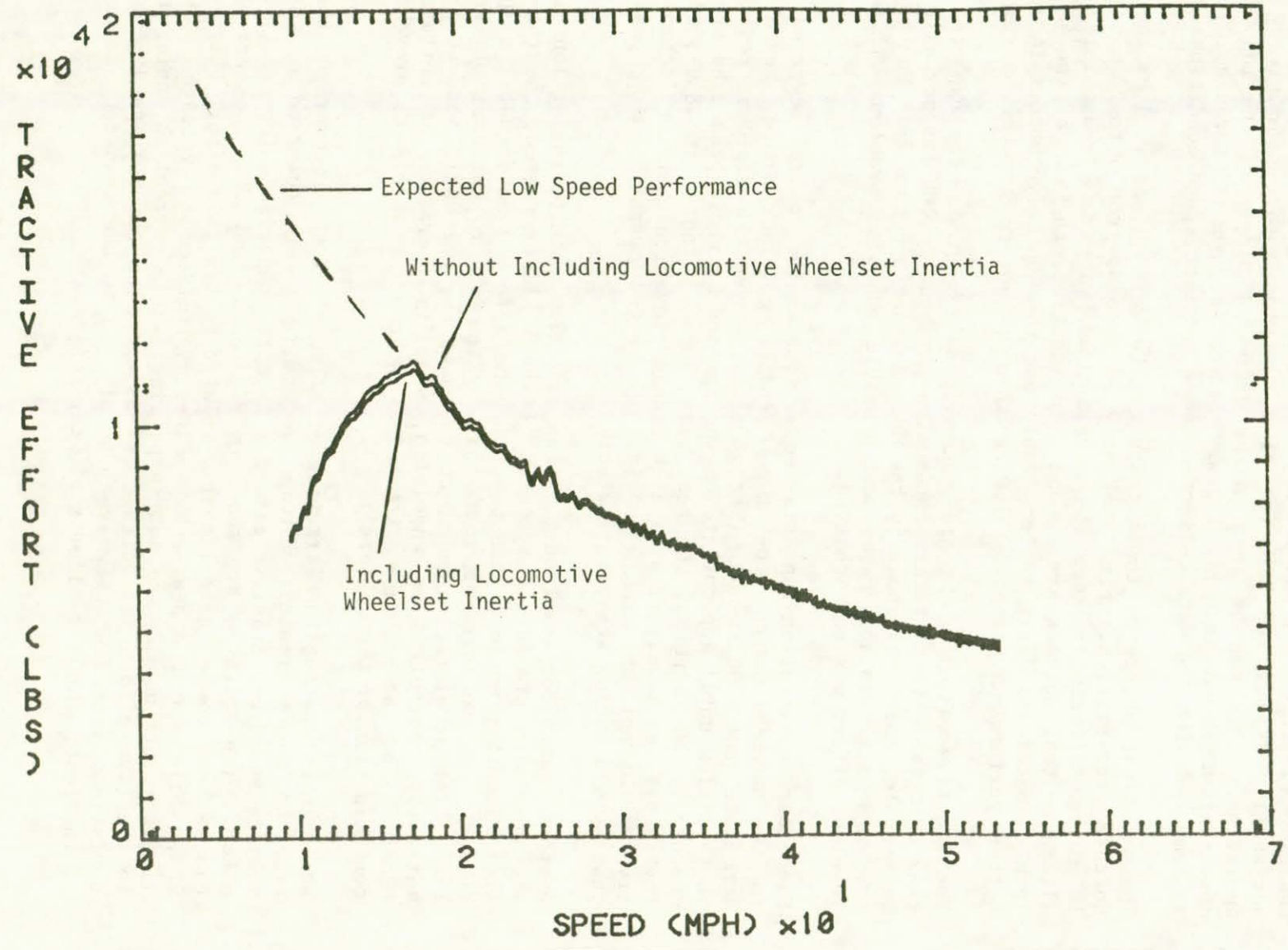

FIGURE 26. TRACTIVE EFFORT, LOCOMOTIVE TRACTION MOTOR 2 NOTCH 8, WITH AND WITHOUT LOCOMOTIVE WHEELSET INERTIA.

During this buildup of power, the traction motors are not in an equilibrium state. Thus, their response due to thermal changes, changing electrical fields in the various windings, etc., will not necessarily follow the behavior of a traction motor under steady operation. This can be seen in the different slopes of the input power-versus-output mechanical power curves (Figures 17 through 20) as compared with the data collected under constant speed conditions.

The transient nature of these tests can be well illustrated by the Notch 8 acceleration, which took only 20 seconds from 6 to 20 mph. In future efforts to keep the acceleration rate more reasonable, alternate test methods are needed. In addition, the use of the 42 inch diameter auxiliary rollers would put the RDU drive motors in a better performance range, allowing them to absorb greater power.

The tractive effort plots are generally as expected. The expected peak tractive effort of this locomotive is about 20,000 lbs per axle at very low speed, as shown by the dotted line in Figure 26. Due to the high acceleration rates and possible adhesion problems, this level of effort was not achieved.

Since our acceleration runs started as soon as the control lever was in the desired notch, the diesel engine governor would prevent immediate power build-up. (The governor prevents a rapid increase in fuel flow until appropriate engine rpm and manifold pressures are reached.) In addition, the test site, being situated at 4830-5300 feet above sea level, is at a high enough elevation that the locomotive would not be running at its full rated output. Thus, peak power would not be achieved instantly.

Another reason for lower output than expected would be the action of the wheelslip prevention system. If wheel slip occurred, the control circuitry would reduce power to the affected motor until slip ceased. It was evident that this system was operational during these high acceleration runs, as the sanders, which are also automatically controlled by wheelslip, were in operation at certain times. (The sanders were directed away from the wheels to prevent contamination of the rollers).

While investigating the 'armature efficiency' of the locomotive, the traction motor armature voltage and current were compared to the vehicle speed and tractive effort. Example comparisons for traction motor 2 (in Notch 8) are shown in Figures 27 and 28. The current can be seen to be quite linearly related to tractive effort (Figure 28), while speed appears less linearly related to voltage. The linear relationships are not surprising, since current is analogous to tractive effort and voltage is analogous to vehicle speed. The deviations from linearity are possibly due to the transient nature of the test, plus the effects of gear losses.

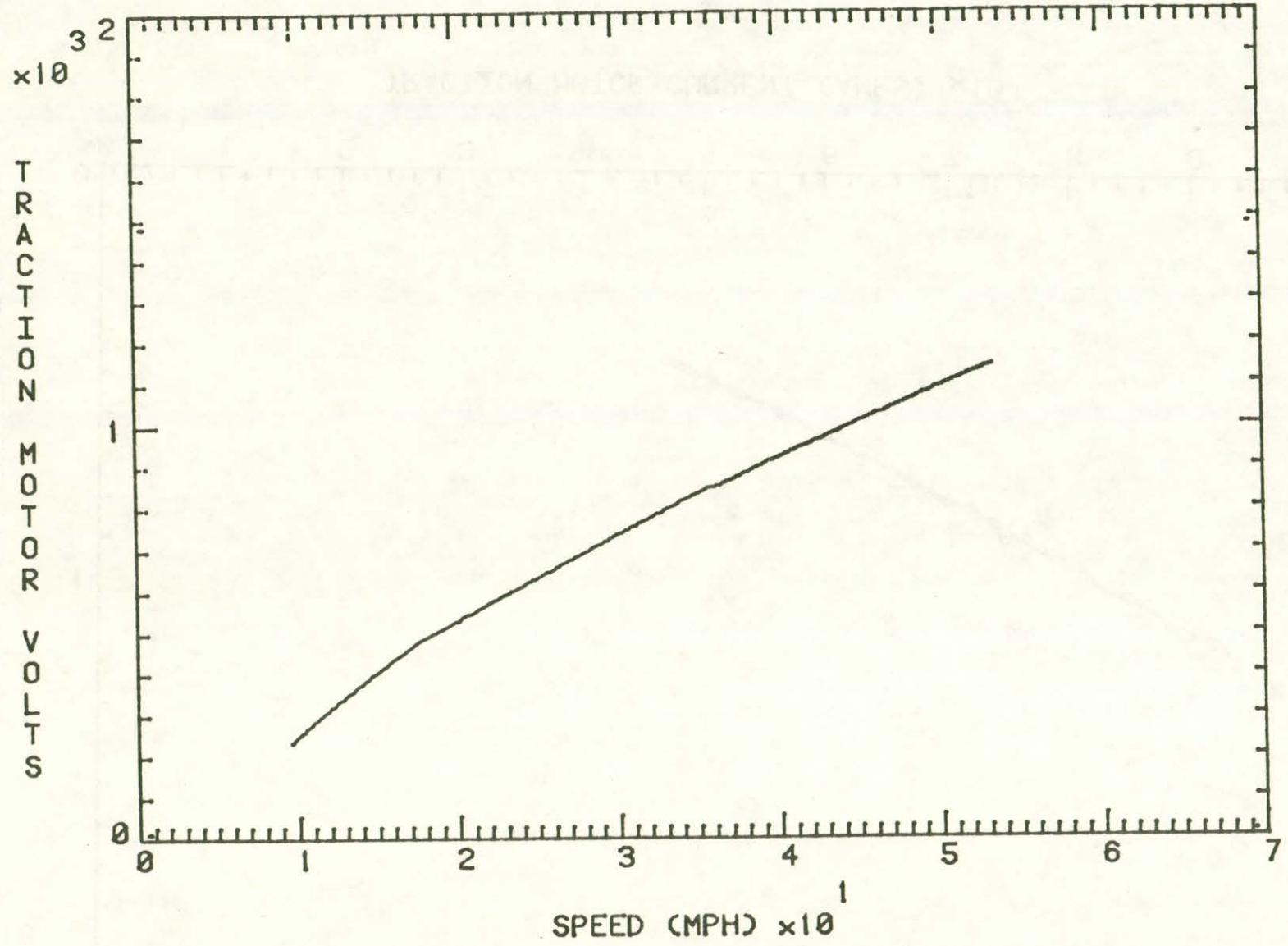

FIGURE 27. LOCOMOTIVE TRACTION MOTOR 2 NOTCH 8.

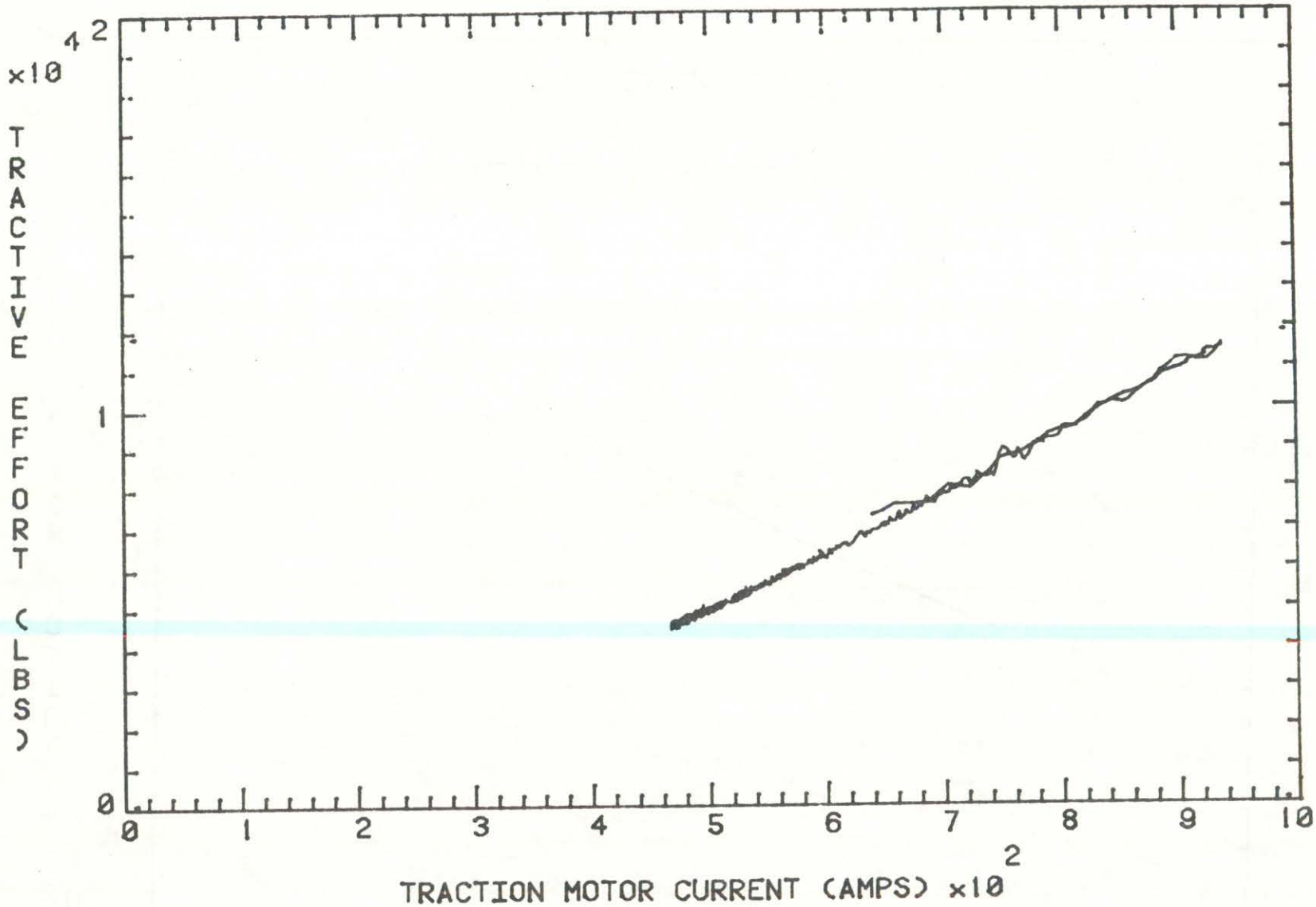

FIGURE 28. LOCOMOTIVE TRACTION MOTOR 2 NOTCH 8.

5.4 DYNAMIC BRAKING TESTS

This GP40-2 locomotive is equipped with a dynamic brake system, which allows the kinetic energy of movement to be dissipated by reversing the connections to the traction motors, thereby turning them into generators and dissipating their electrical energy as heat through resistance grids. Therefore, it was desirable to characterize traction motors as generators also.

Dynamic braking runs were accomplished by placing the RDU into its coast mode, running the locomotive up to speed, and then applying the locomotive dynamic brake until the rollers almost stopped. During each run, input voltage, current, and roller speed were measured.

During the first test series a fault developed in the RDU drive system, such that it was only possible to start braking below 30 mph. This, combined with the faults found in some of the series 1 data, made it necessary to redo these tests with an initial speed of 65 mph during the second test series. Six braking runs were made, one in each of the control positions from Notch 3 through 8.

5.4.1 Data Analysis and Results

Braking power and braking effort at the rails were calculated by differentiating the roller's speed to calculate its acceleration and multiplying the result by the inertia of the drive train and accounting for the roller gear losses using the following equations:

$$T = I \times \dot{\omega} \text{ (Eq. 1 from [1])} \qquad \text{(Equation 4)}$$

$$BE = (T + T_G)/2.5 \text{ ft} \qquad \text{(Equation 5)}$$

$$BP = (T + T_G) \times S \times \frac{1}{1257} \qquad \text{(Equation 6)}$$

where

BE = Braking Effort (lbs)

BP = Braking Power (kW)

T = Torque at the Rollers (ft-lbs)

T_G = RDU Gear Loss Torque (ft-lbs)

I = Rotating Inertia of RDU Drive Train Plus Locomotive Wheelset Gears and Armature

$\dot{\omega}$ = Roller Acceleration (2π rad/sec^2)

S = Roller Speed (rpm)

Figures 29 through 32 are curves of braking effort versus speed, while Figures 33 through 38 show the braking power versus traction motor armature output power (power dissipated by the dynamic brake grids) for axle 2. The braking power was similar for the other axles, as shown in Figures 39 through 41 for range 8 dynamic braking.

The braking effort curves match very closely with EMD's published curves for this locomotive (Figure 42). However, a discrepancy appears to exist in the designation of control lever positions. For example, range 7 and 8 data match EMD's range 8 and range 6 appears like EMD's range 7, range 5 like EMD's range 6, etc. For future testing, it is recommended that the resistance of the rheostat to which the lever is mounted be measured and referenced in some way that eliminates reliance upon the physical position of the handle.

The braking power data were fitted to linear power data by a "least squares" approximation. The inverse average slope for each of the eight curves is close to the slope of that same traction motor while driven at constant speed. The differences are probably due to the transient nature of the test performed. Since the speed, voltage, and current were continuously changing, transient effects in the traction motor would alter the 'armature efficiency' as in acceleration tests. These effects are probably not as severe as in the acceleration runs, but are due to deceleration rates that are higher than would usually be expected.

The slight dip in the braking power data of Figures 33 through 41 corresponds to the rounded peak in tractive effort shown in Figures 29 through 32. The GM data indicate a sharp point at this speed. This rounding is probably due to slightly reduced adhesion and increased creepage between roller and wheel at the high braking effort, and also to the mid-point derivative method used to calculate the accelerations.

The data shown were calculated using an inertia value that includes the inertia of the traction motor's armature gears, and wheelset. If one were to recalculate the braking effort and braking power using the reduced inertia values, results would be similar but at slightly reduced levels, as shown in Figures 43 and 44 for axle 2. These results are then the actual mechanical braking effort and power available at the wheel/rail interface during this test, whereas the earlier results are the effort and power available when running at constant speed in dynamic braking.

To avoid the problem of transient response in the traction motors due to non-steady state conditions, it is recommended that in future tests a series of constant speed dynamic brake runs be performed which are similar to the constant speed drive runs. This was attempted during the first series. Unfortunately, data quality, as explained previously, prevented the original data from being very useful. Lack of time prevented such runs from being performed during the second test series.

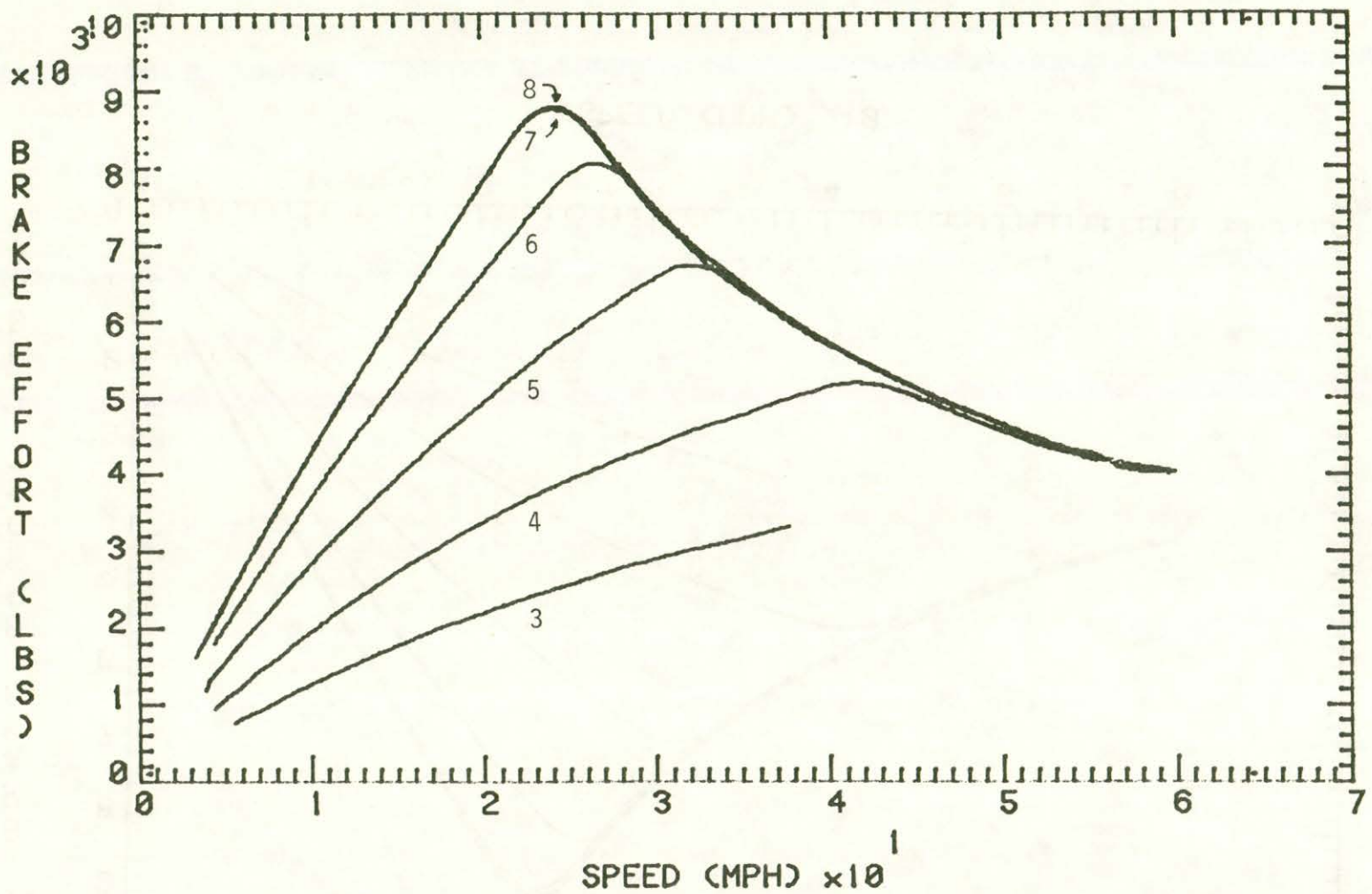

FIGURE 29. AXLE 1 DYNAMIC BRAKE EFFORT RANGES 3-8 WITH LOCOMOTIVE INERTIA.

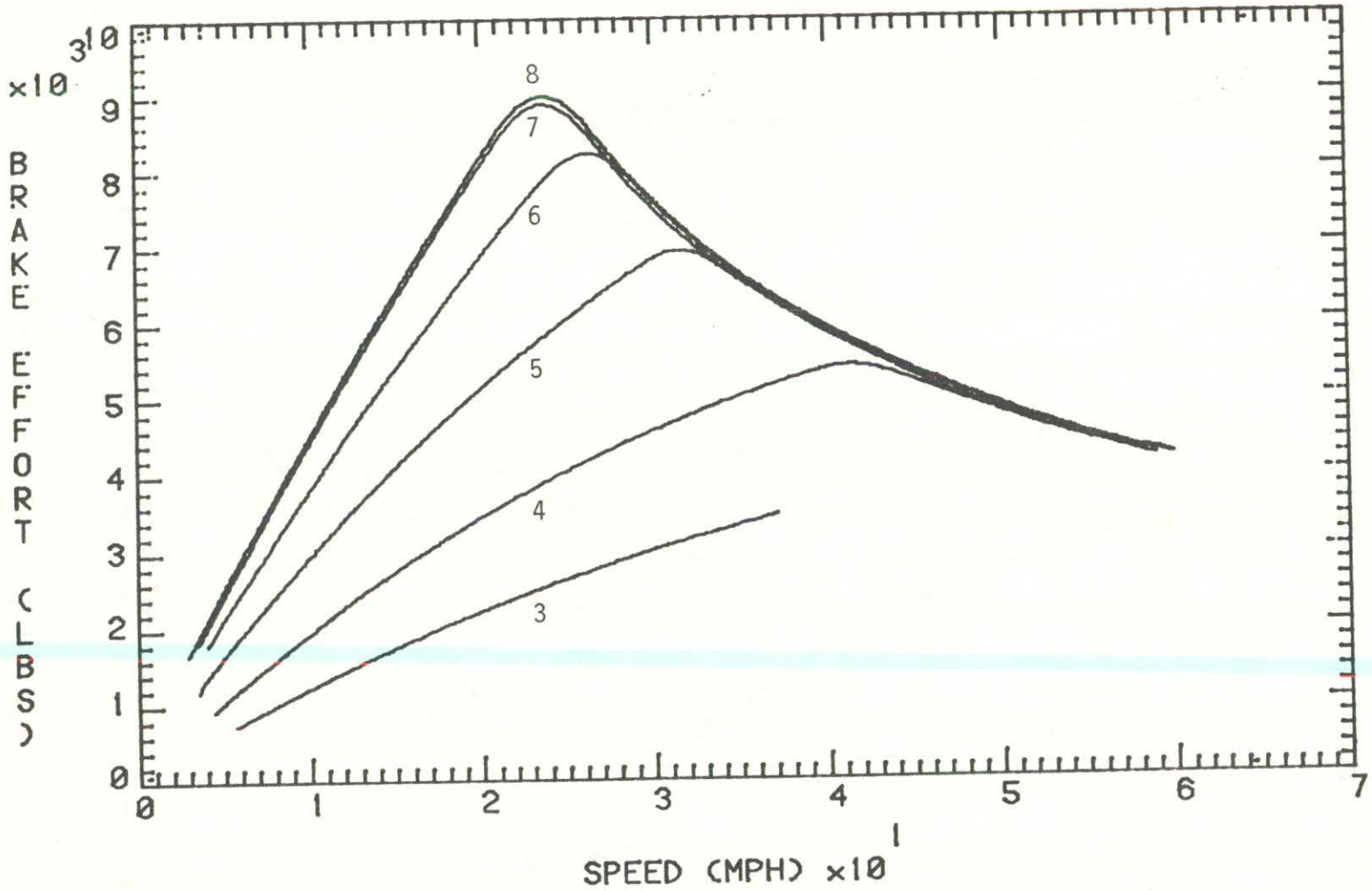

FIGURE 30. AXLE 2 DYNAMIC BRAKE EFFORT RANGES 3-8 WITH LOCOMOTIVE INERTIA.

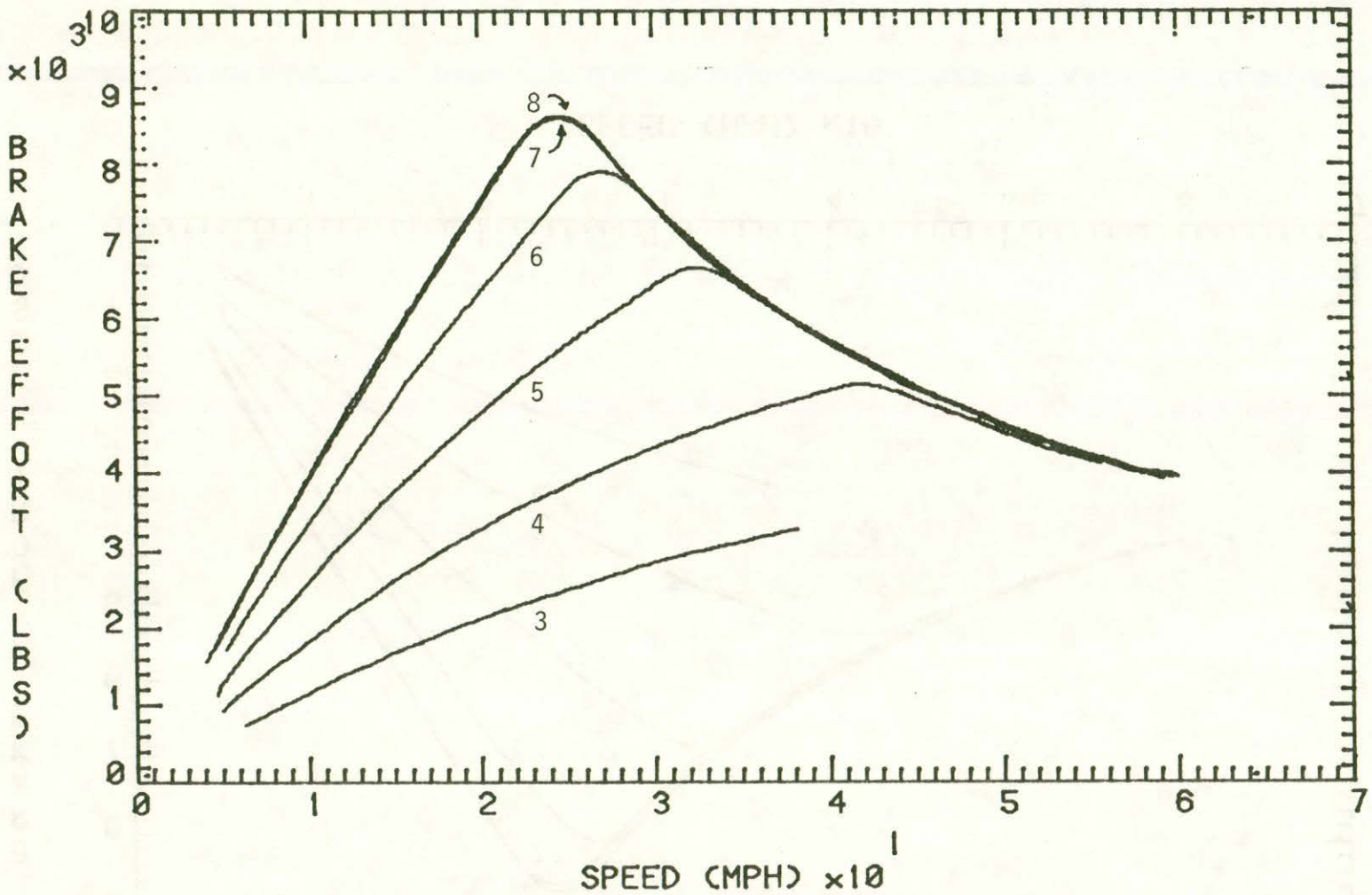

FIGURE 31. AXLE 3 DYNAMIC BRAKE EFFORT RANGES 3-8 WITH LOCOMOTIVE INERTIA.

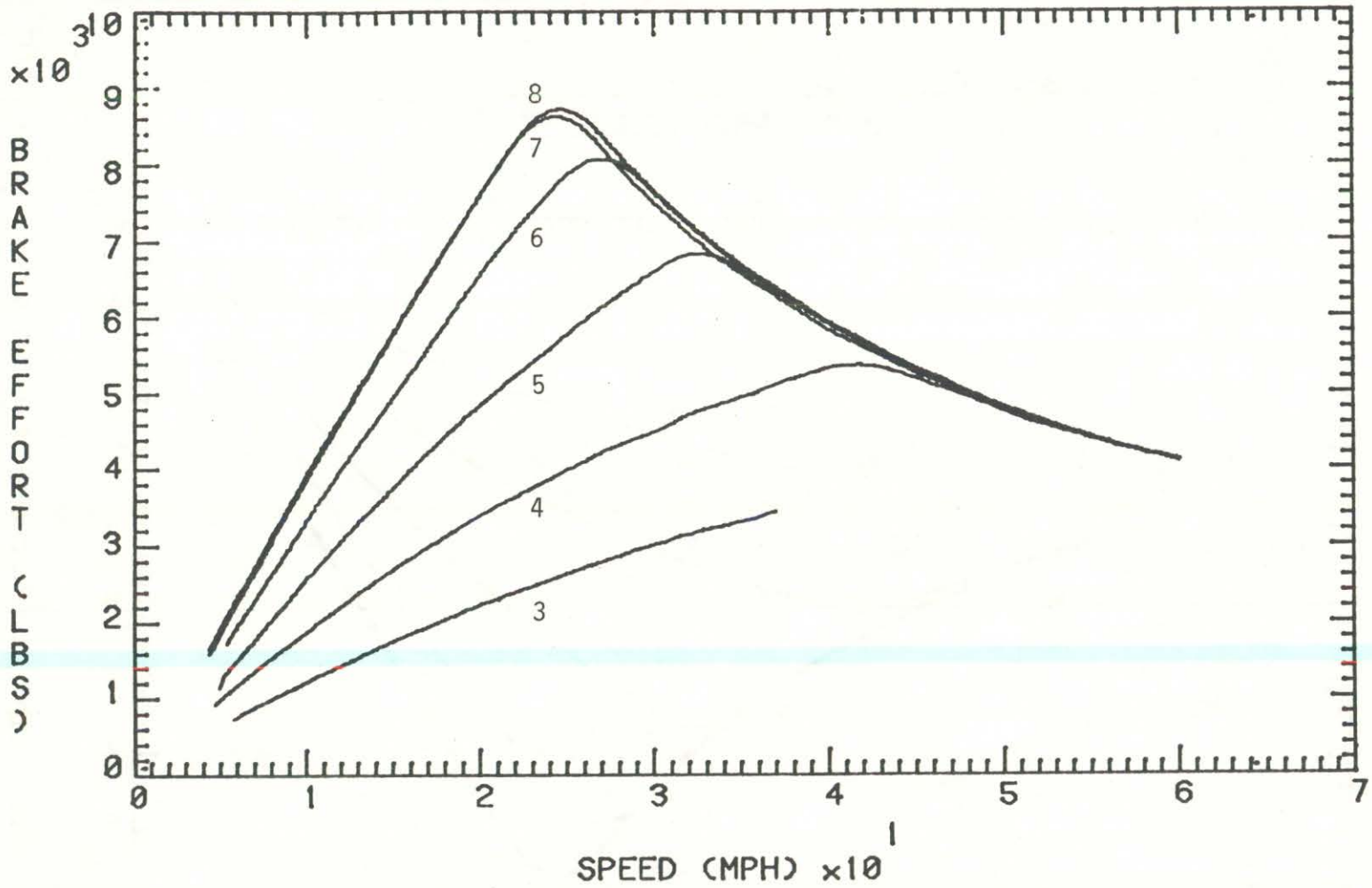

FIGURE 32. AXLE 4 DYNAMIC BRAKE EFFORT RANGES 3-8 WITH LOCOMOTIVE INERTIA.

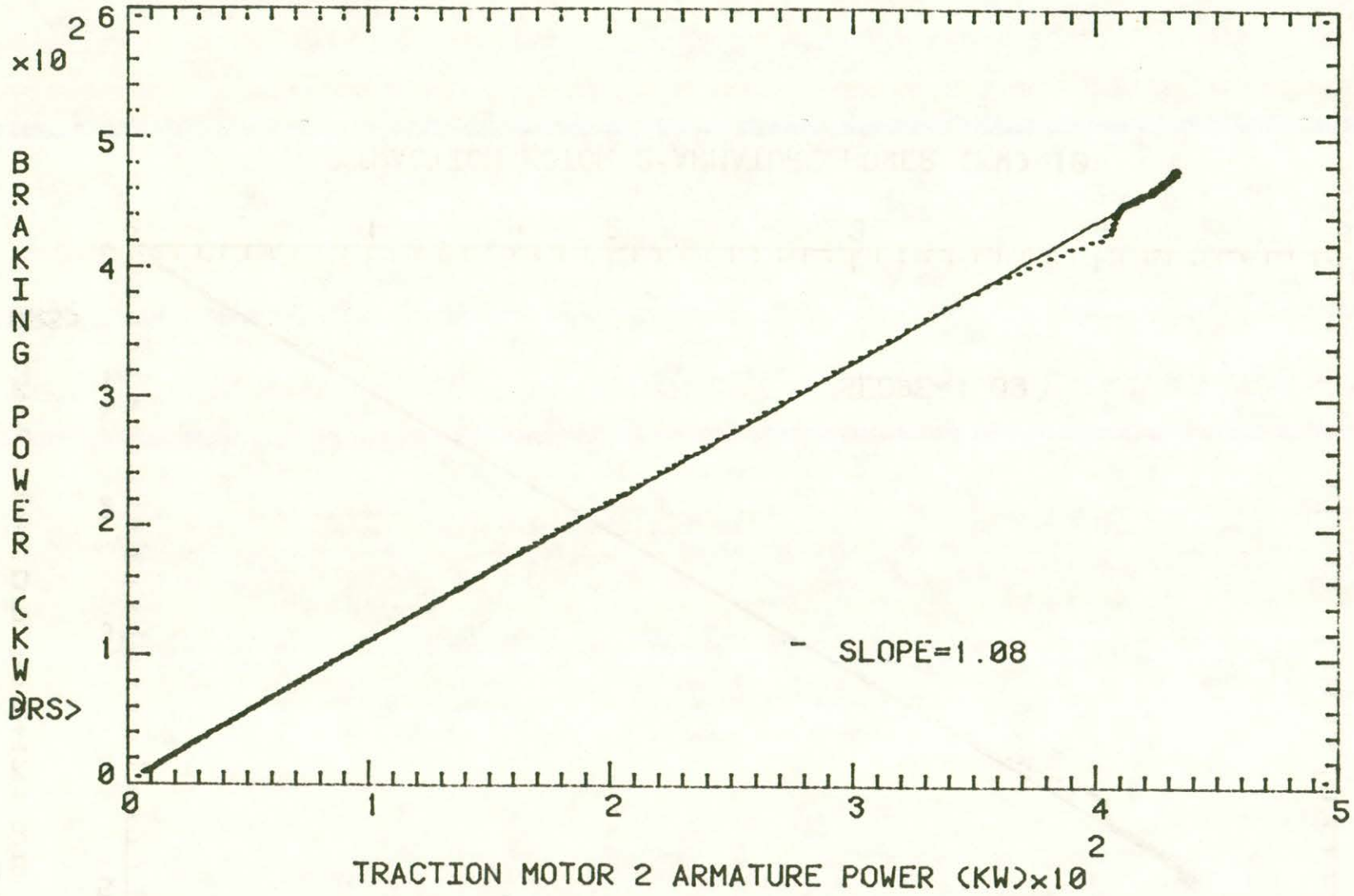

FIGURE 33. AXLE 2 DYNAMIC BRAKE POWER RANGE 8.

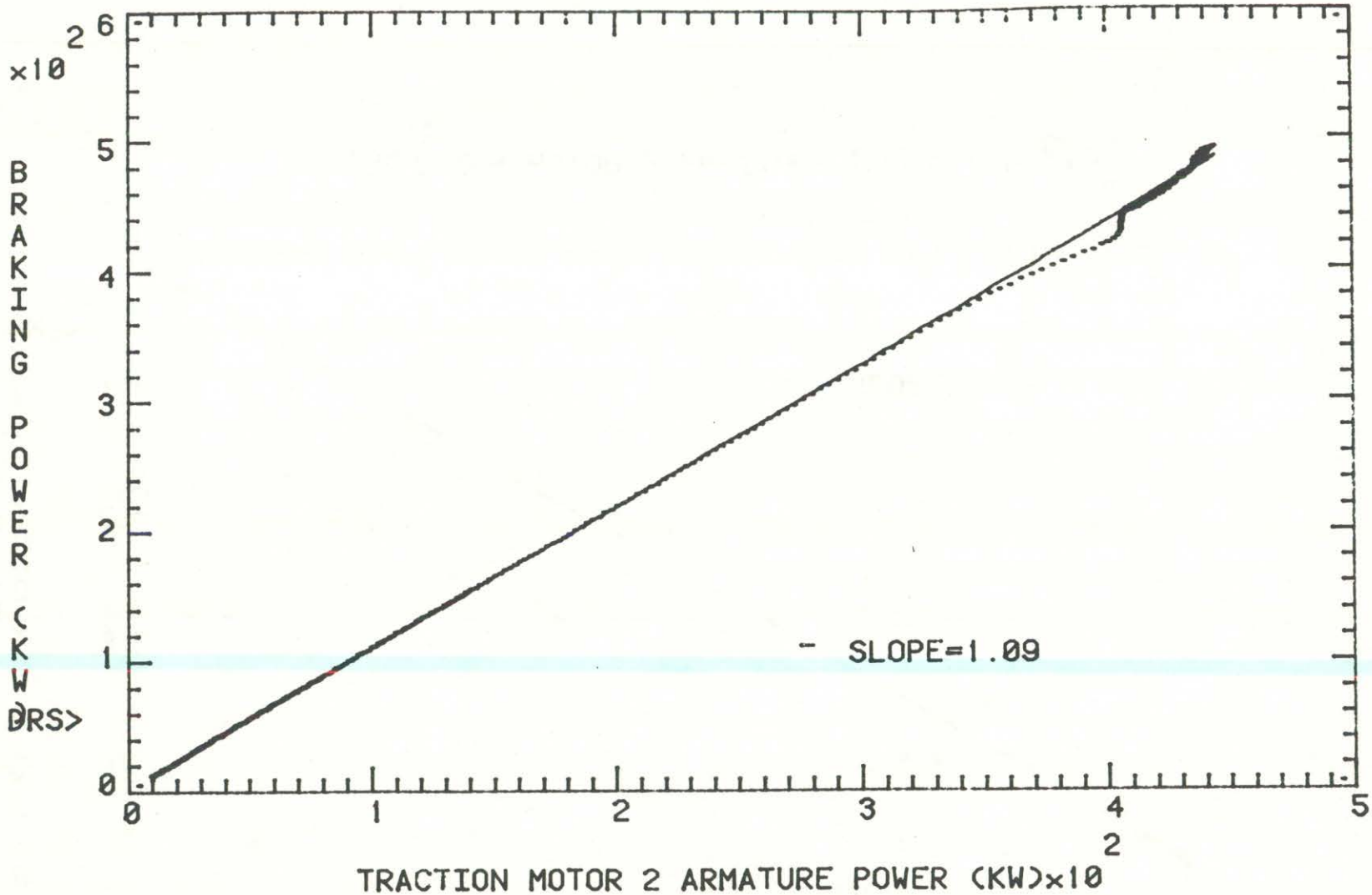

FIGURE 34. AXLE 2 DYNAMIC BRAKE POWER RANGE 7.

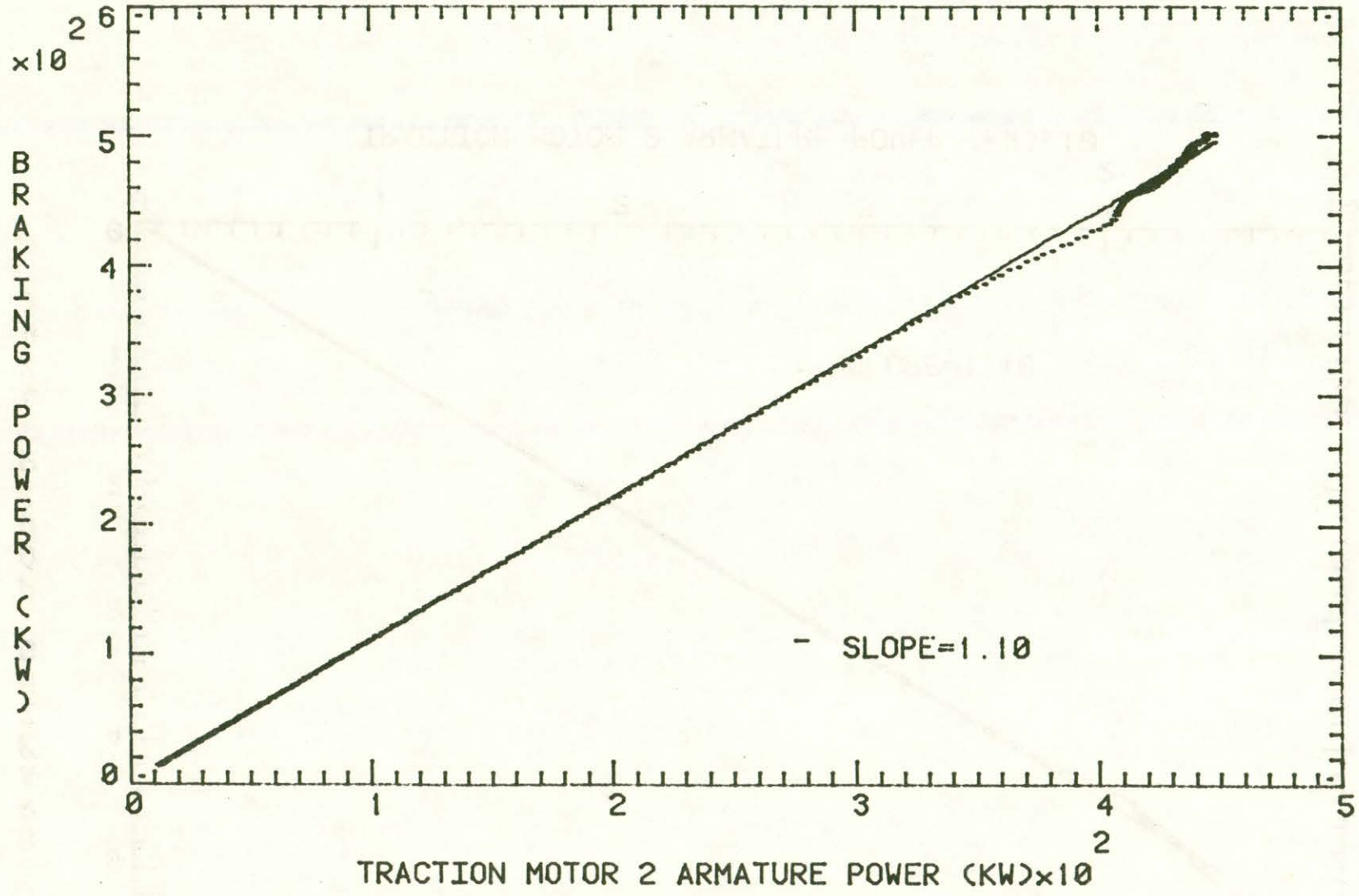

FIGURE 35. AXLE 2 DYNAMIC BRAKE POWER RANGE 6.

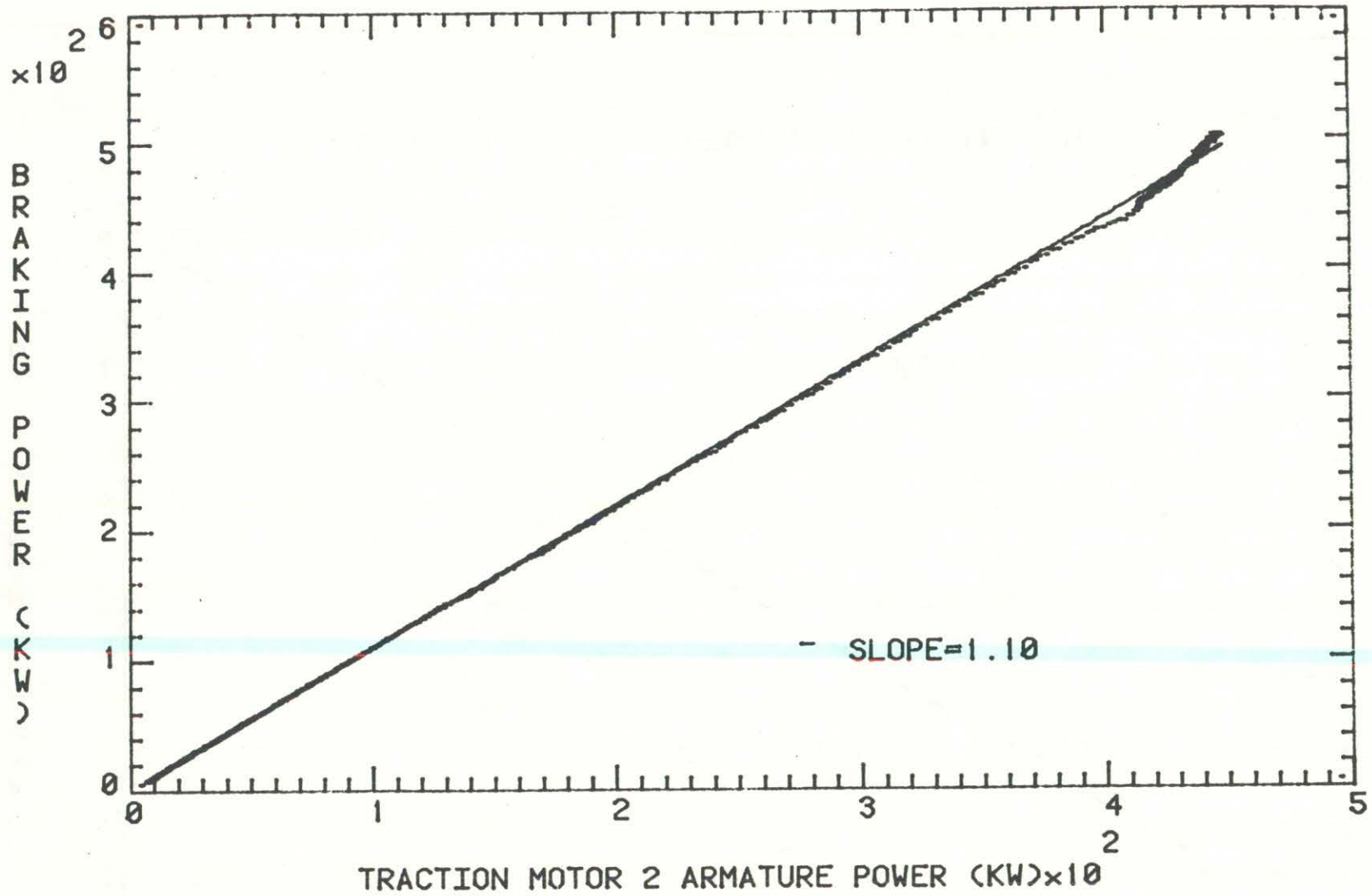

FIGURE 36. AXLE 2 DYNAMIC BRAKE POWER RANGE 5.

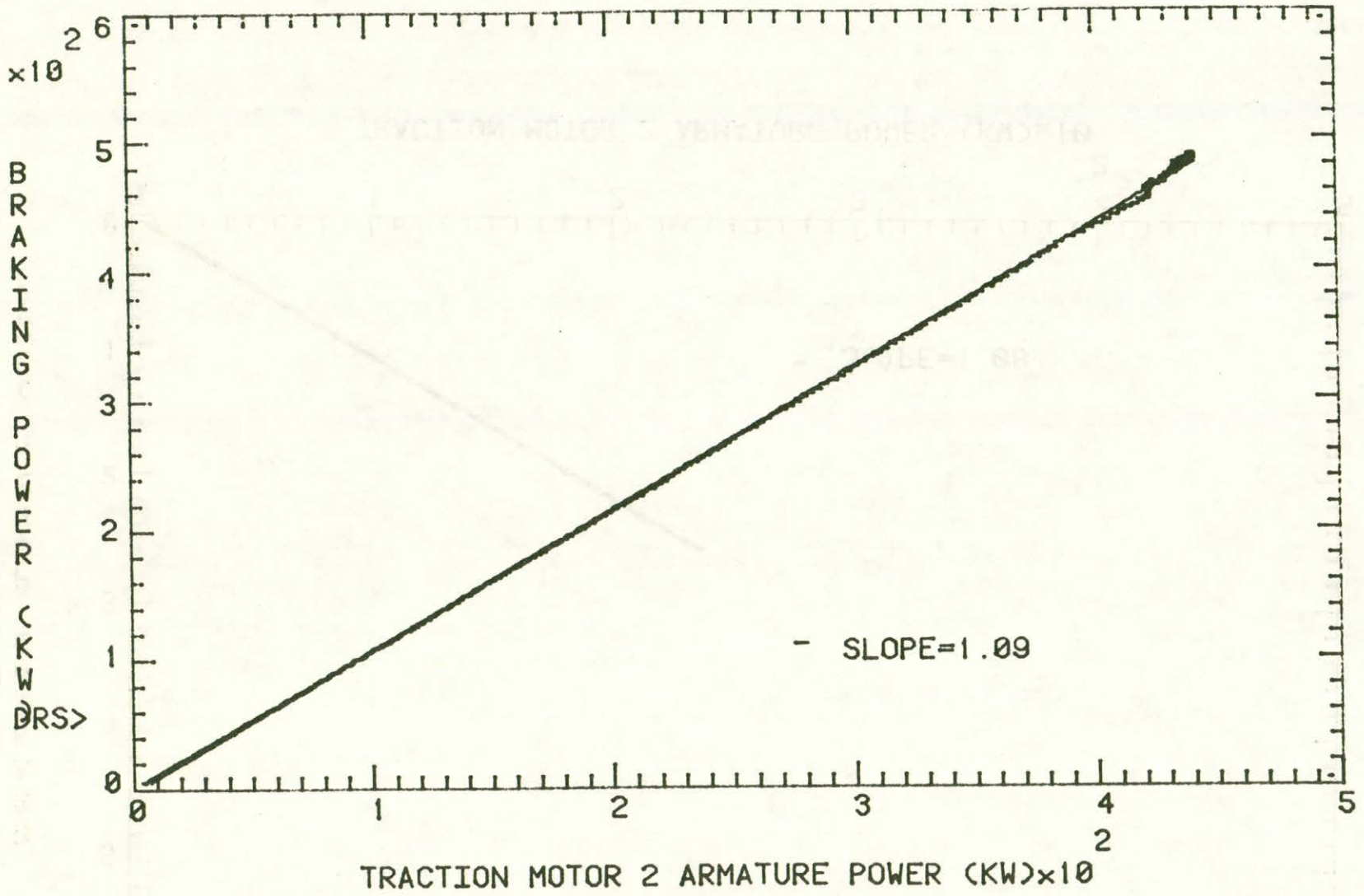

FIGURE 37. AXLE 2 DYNAMIC BRAKE POWER RANGE 4.

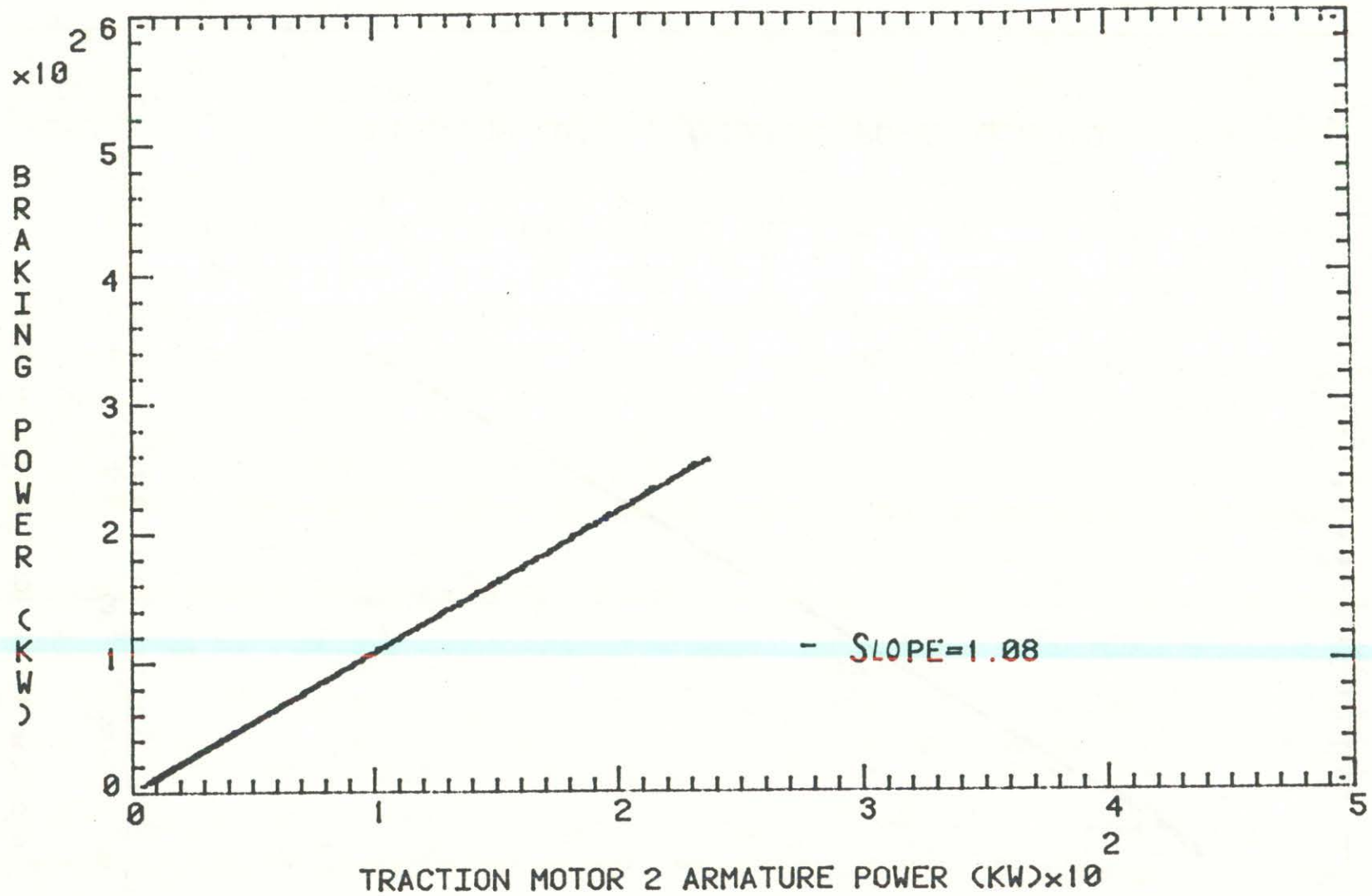

FIGURE 38. AXLE 2 DYNAMIC BRAKE POWER RANGE 3.

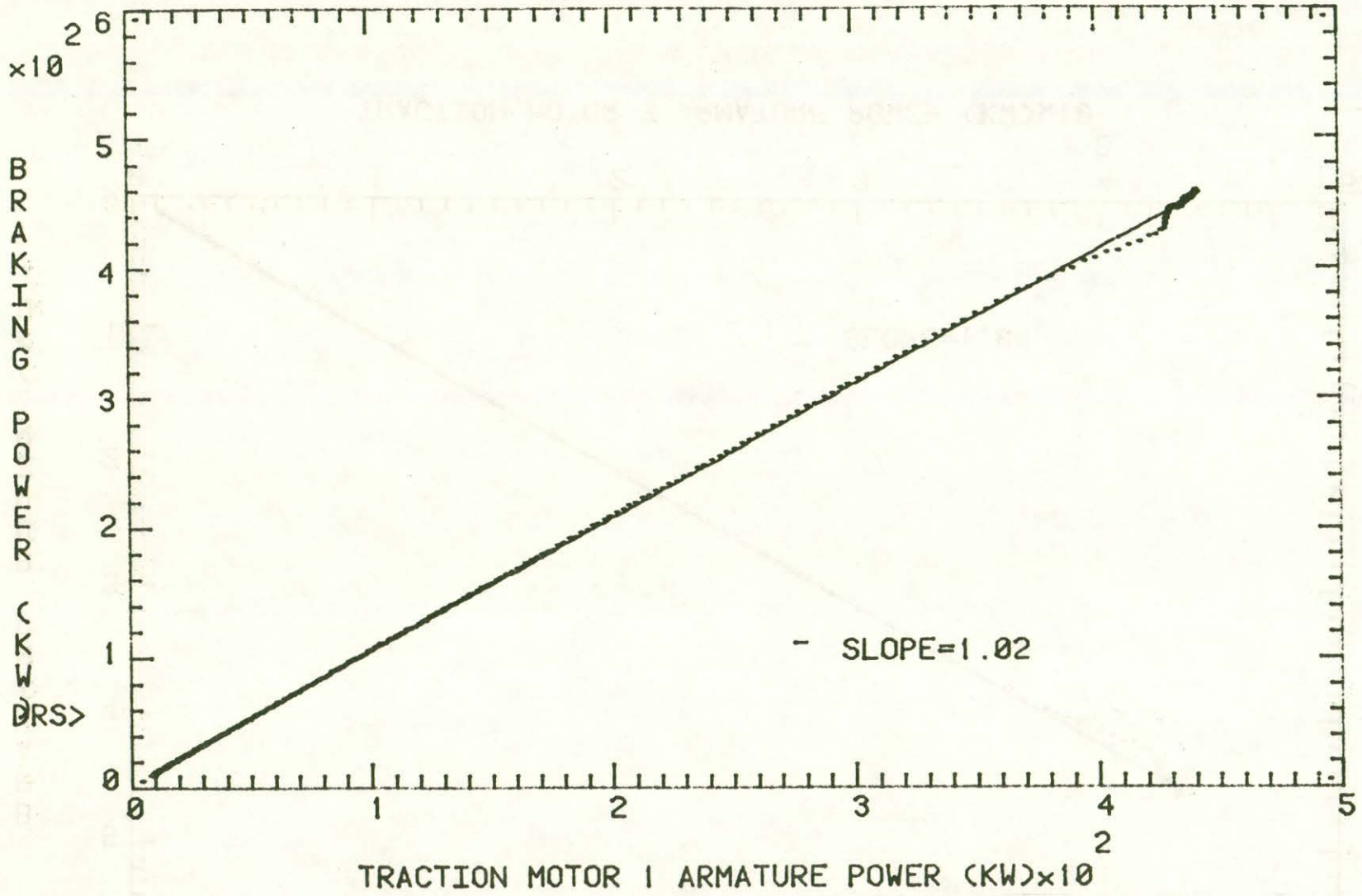
BRAKING POWER (KW)
×10 2
6
5
4
3
2
1
0
0
1
2
3
4
5
2
TRACTION MOTOR I ARMATURE POWER (KW)×10
SLOPE=1.02

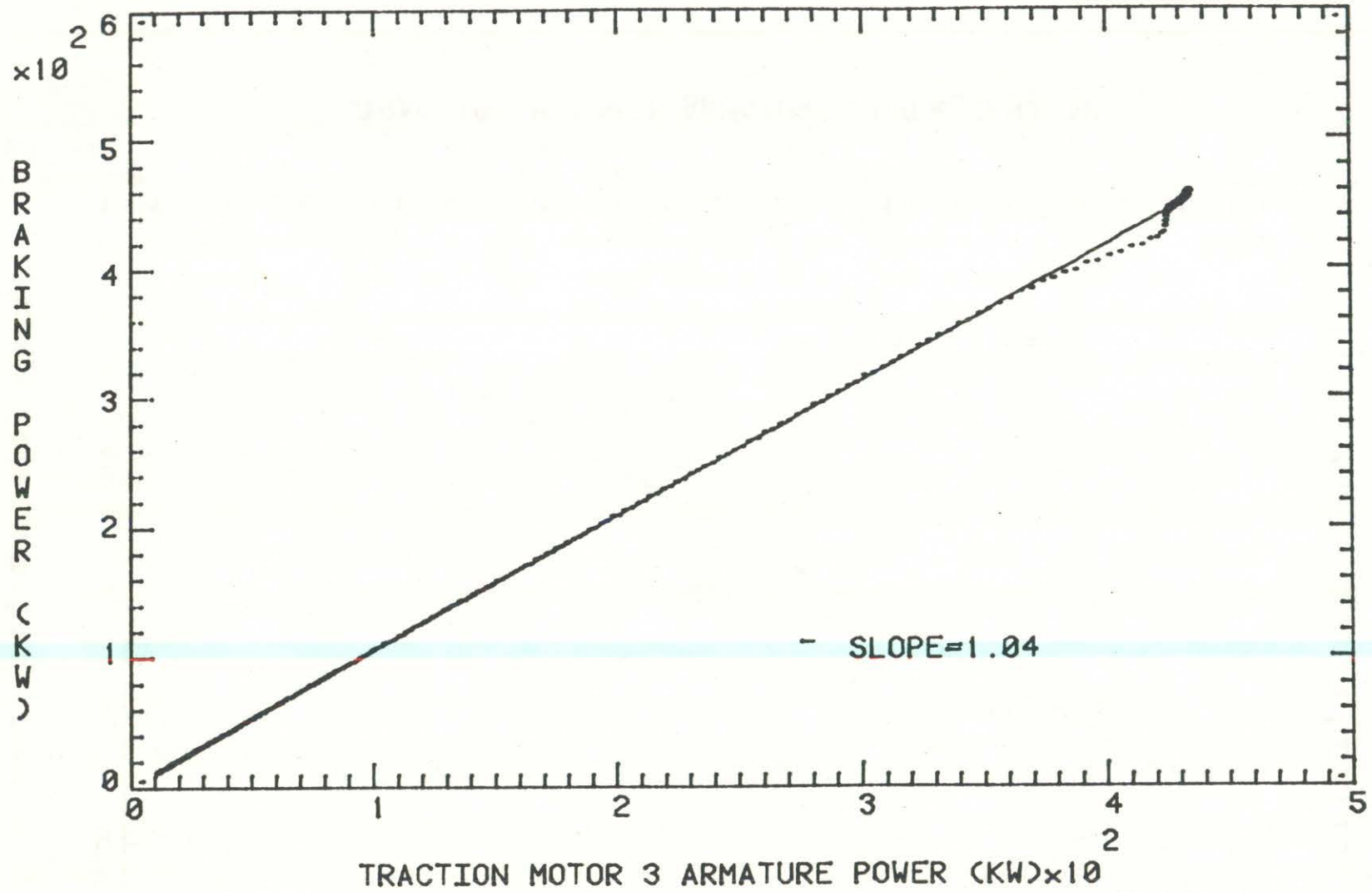

FIGURE 40. AXLE 3 DYNAMIC BRAKE POWER RANGE 8.

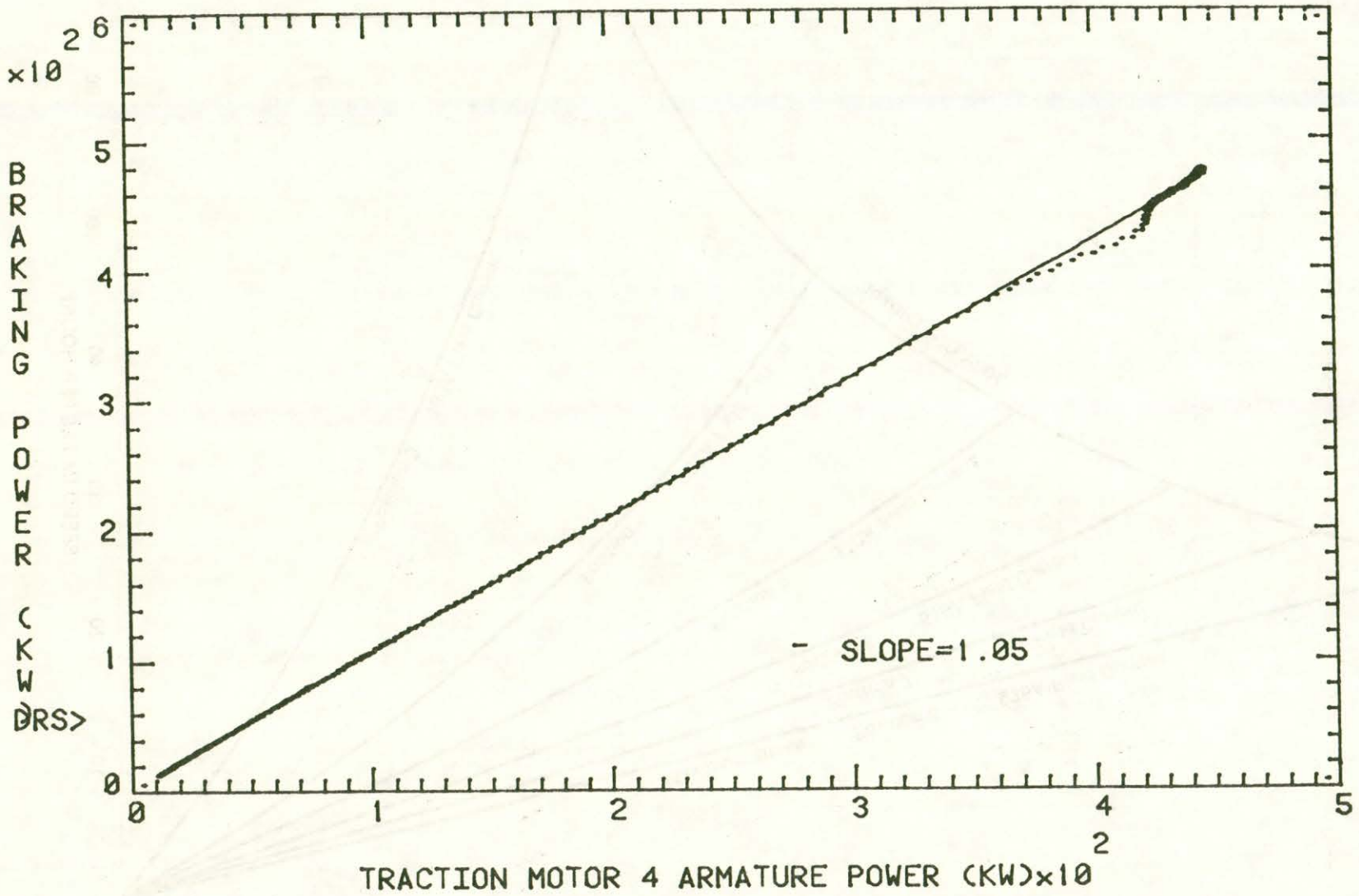

FIGURE 41 AXLE 4 DYNAMIC BRAKE POWER RANGE 8

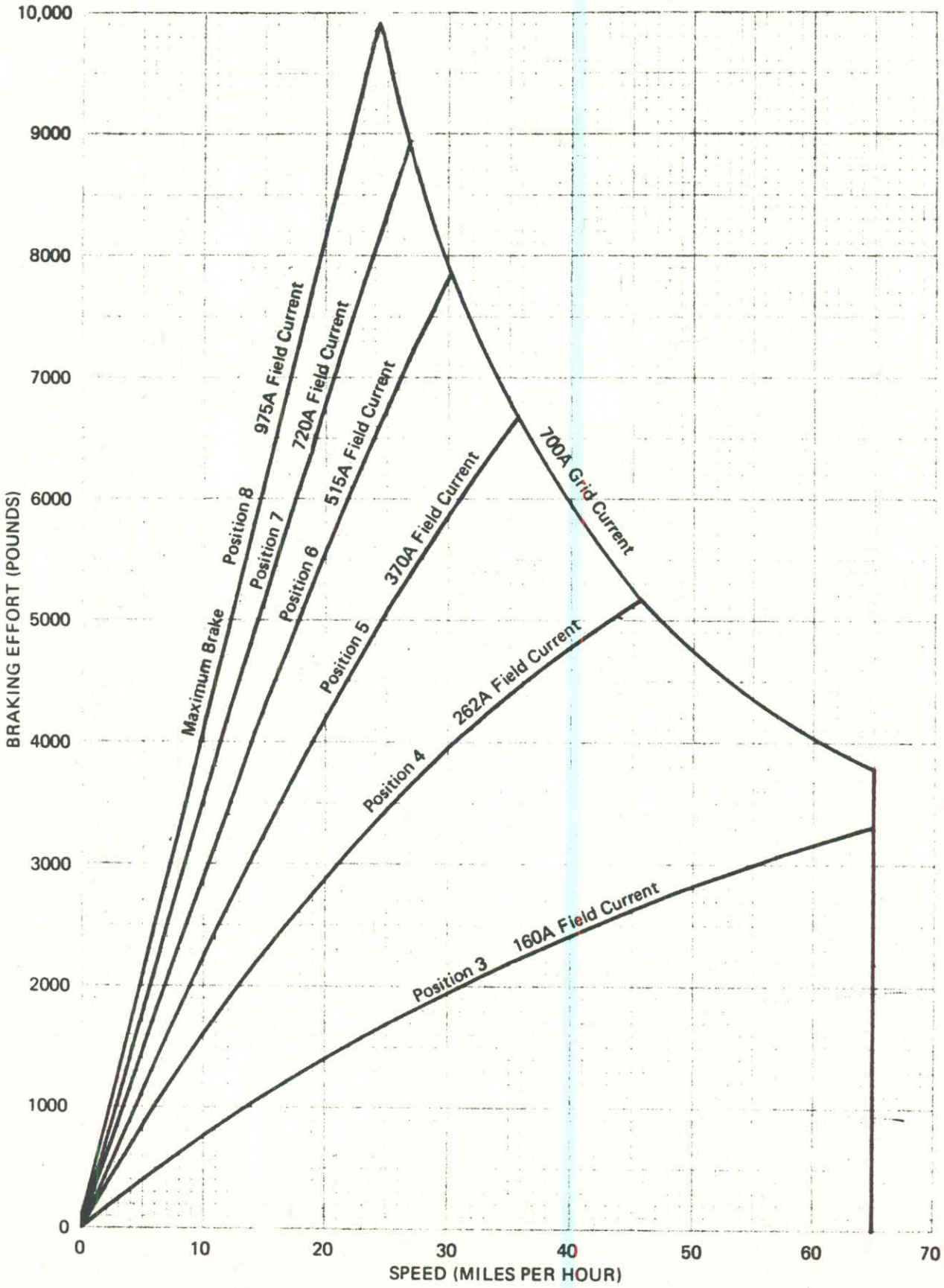

FIGURE 42. BRAKING EFFORT CURVES WITH DYNAMIC BRAKING.

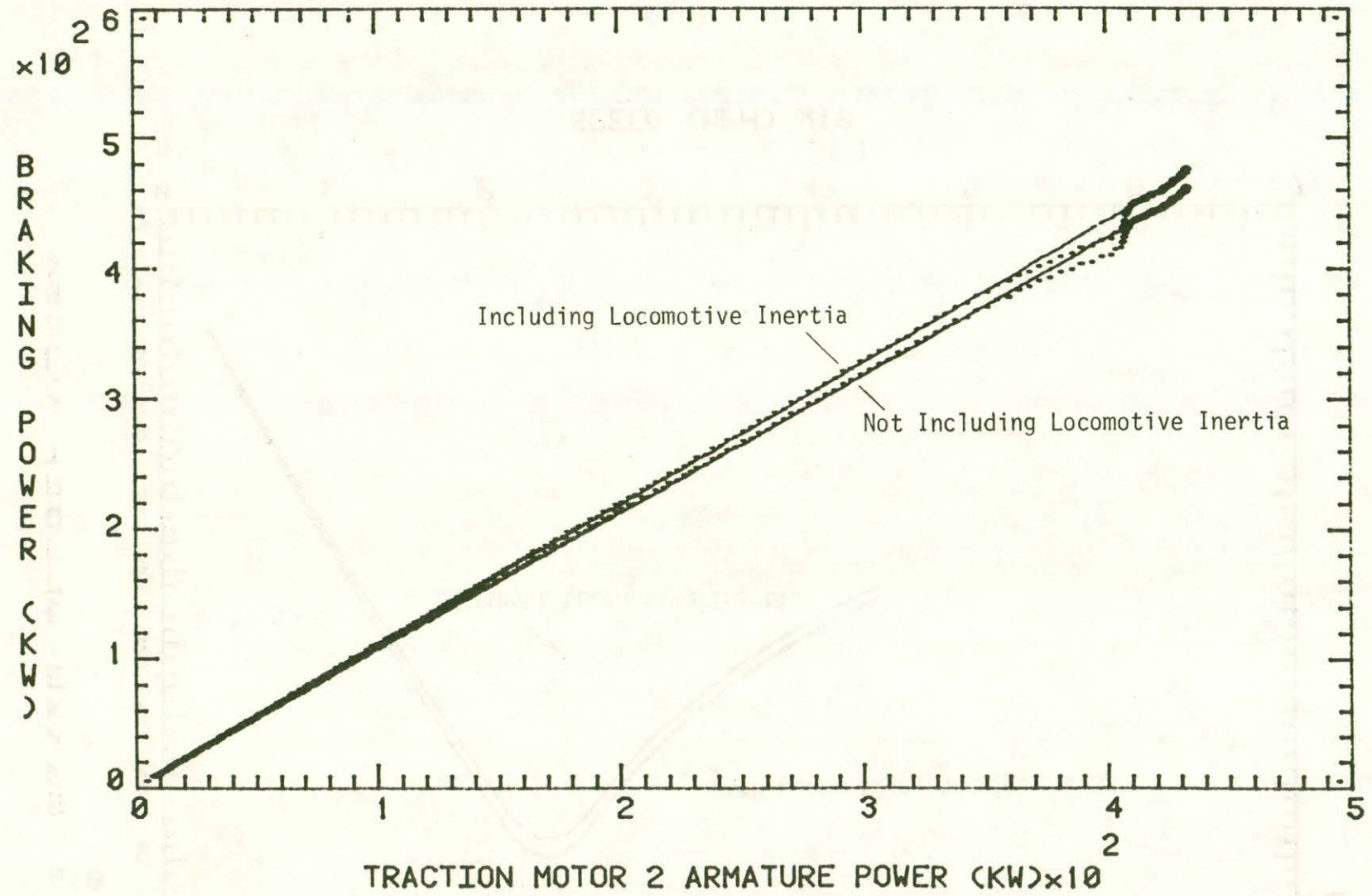

FIGURE 43. AXLE 2 DYNAMIC BRAKE POWER RANGE 8, WITH AND WITHOUT

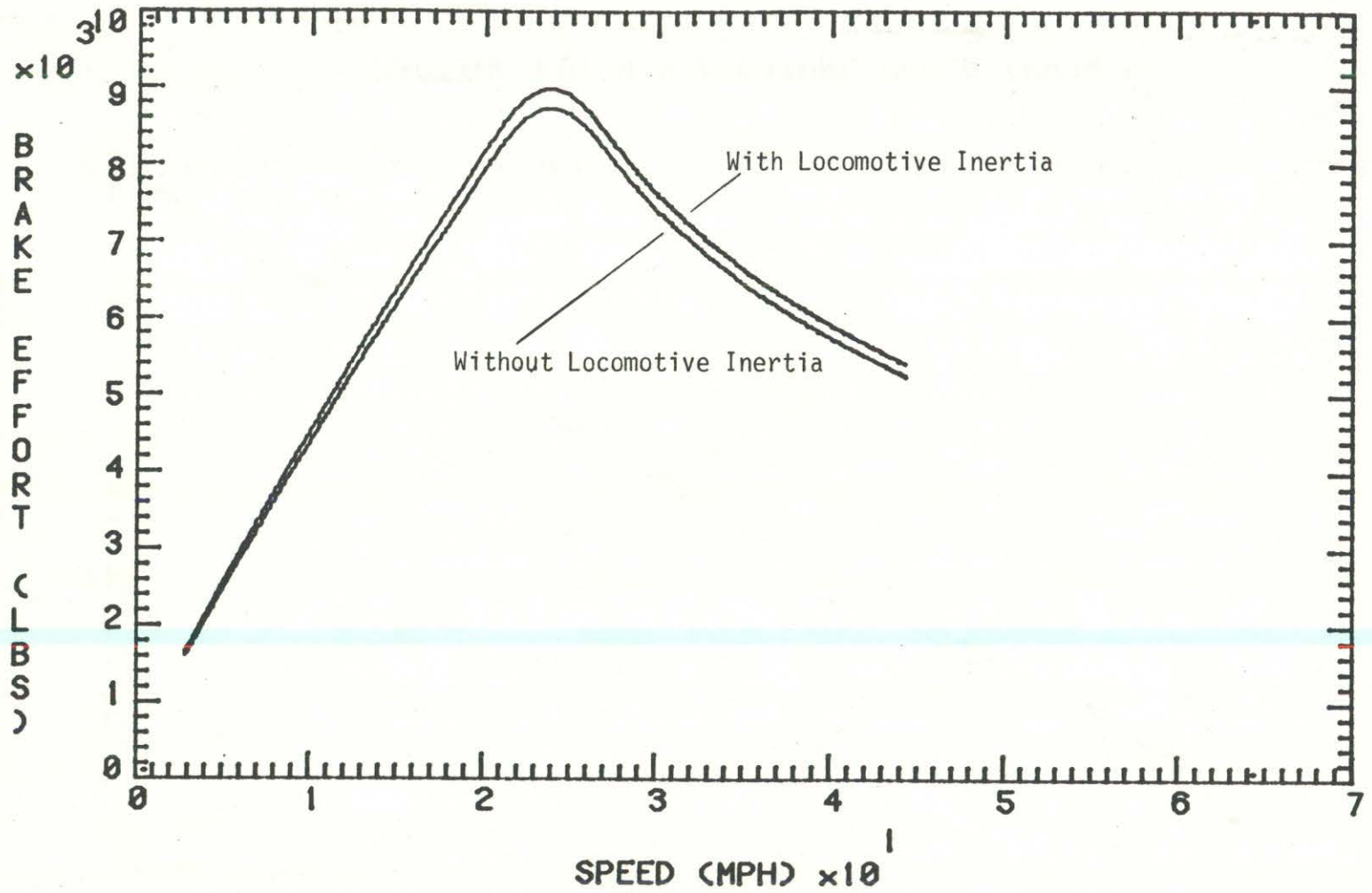

FIGURE 44. AXLE 2 DYNAMIC BRAKE EFFORT RANGE 8, WITH AND WITHOUT LOCOMOTIVE WHEELSET INERTIA.

6.0 ERROR ANALYSIS

To establish the accuracy of our measurements, the transducer accuracies were obtained from the calibration data and manufacturer's specifications. Typical full-scale errors are enumerated in Table 3.

TABLE 3. TYPICAL FULL-SCALE TRANSDUCER ERROR.

Instrument	Error % of Full-Scale
Max Flowmeter	0.5
Analog Devices 273 K Isolation Amplifiers	0.2
Current Shunts	0.2 (Estimated)
OSI VT7 Voltage Transducers	0.5
RDU Speedometers	0.1
RDU Torquemeters	0.5 (See Appendix A)
Data Aquisition System	0.1 (Estimated)

From these values the worst case expected error can be calculated for the constant speed drive mode tests. Error calculations were made for the power measurements based on the following equation [3] for error in the product of two measurements.

$$\sigma_{AB} = (A)^2 (\sigma_B)^2 + (B)^2 (\sigma_A)^2 \qquad \text{(Equation 7)}$$

where

σ_{AB} = Error for product A x B

σ_A = Error in Measurement A

σ_B = Error in Measurement B

A = Value for A

B = Value for B

The errors associated with each of the constant speed and control notch combinations can be calculated by substituting the full-scale error values shown in the table for σ_A and σ_B in Equation 7 and the corresponding measurement values for A and B. Results indicated that the maximum possible value of error input and output power was measured at notch 8 at 65 mph.

For example, for locomotive axle 2, with full-scale values of 2,000 amps armature current and 1,500 volts armature voltage, the possible error in current is 0.5% of 2,000 amps, or 10 amps. The possible voltage error is 0.6% of 1500 volts, or 9 volts. This resulted in a worst possible error of 13.4 kW for a maximum input power of 500 kW. This represents a possible error of 2.9%.

Similarly, the errors in speed (0.2%) and torque (0.6%) can be calculated from 25,000 ft-lbs. Thus, for a maximum output of 408.5 kW (uncorrected for RDU drive train gear loss), an error of 1.13% (4.6 kW) was calculated.

In addition to those errors, there is also the possible -0.5% error mentioned in Section 5.1, resulting from the method of calculating the input power.

The foregoing methodology outlines the means for establishing the worst case error of any particular power measurement. It does not establish the accuracy of each traction motor armature efficiency curve.

As can be seen in the figures presented, the fit of our data to the linear estimations is extremely good. This is verified by examining the statistical data generated by least squares linear regression, fitting the data to straight lines.

The slopes, R squared values, and errors for 95 and 99 percent confidence intervals, as calculated by the SPSS statistical package, are shown in Table 4.

TABLE 4. ERRORS IN CALCULATION OF THE SLOPE OF ARMATURE EFFICIENCY CURVES FOR CONSTANT SPEED DATA.

AXLE	SLOPE "Armature Efficiency"	R^2	ERROR IN SLOPE 95% Confidence	99% Confidence
1	0.931	0.99852	0.0122 (1.3%)	0.0164 (1.8%)
2	0.941	0.99903	0.010 (1.1%)	0.0143 (1.4%)
3	0.926	0.99913	0.009 (1.0%)	0.013 (1.4%)
4	0.925	0.99469	0.023 (2.5%)	0.031 (3.4%)

These data are from the constant speed drive mode runs. As can be seen, for three of the four axles, the confidence intervals are close to our target range of 1% accuracy.

This suggests that data from the braking and acceleration runs are of comparably high confidence since they evidenced generally lower scatter (even with more numerous data points) than is noted in the constant speed runs.

Improvements in accuracy are possible in several places. To reduce the magnitude of worst case error, it is advisable to set the full-

scale value of each transducer only somewhat greater than the maximum value expected. It is evident that some of our measurements could have been adjusted downward in this regard. For example, the full-scale setting for current should probably have been 1500 amps, not 2000.

Better instrumentation for measuring traction motor input power would be advisable, as well as better isolation amplifiers in order to reduce drift problems. Although it complicates the analysis procedure, drift is removed from the test data before analysis, and is therefore eliminated as a source of error. However, the use of two transducers to measure current provides two sources of error. Thus, highly accurate inductive current probes are recommended. This would also ease the installation. Otherwise, more accurate shunts and isolation amplifiers are suggested.

In the future, if the current shunts and isolation amplifiers are to be used, they should be calibrated together and kept for use in pairs. The accuracy of the two units together is probably better than the sum of the two individual manufacturer's specifications. This, however, cannot be verified without calibration. As it is now, the current shunts were not calibrated and their accuracies only estimated.

When the FAST track tests were performed, the instrumentation package differed somewhat (see Part 2), in that separate isolation amplifiers were not required because the data acquisition system was self-isolating.

Further checks on the accuracy of the voltage and current measurements were made by comparing the traction motor armature voltages with the generator voltage (Figures 45 through 48) and the sum of the four traction motor currents with the generator current (Figure 49).

All these data are from the constant speed tests. Results from the other test methods were similar.

As can be seen in Figure 49, our currents add up to almost exactly the generator current (only 1% error, which is within our measurement accuracy). Figures 45 through 48 support the linearity of our data. The slopes, as expected, are less than unity because the voltage drop across the traction motor fields is not being measured.

Further improvements in the accuracy of the RDU instrumentation are very limited due to the semi-permanent nature of their installation. If any instrumentation is to be upgraded, it is the Himmelstein torquemeters, which gave much trouble during the tests--the one on RDU axle 4 being the most unreliable.

In addition, for future reference work, the voltage and current transducers that measure the output of the RDU drive train motors should be calibrated. This would allow easier troubleshooting of the system in the event of other system failures.

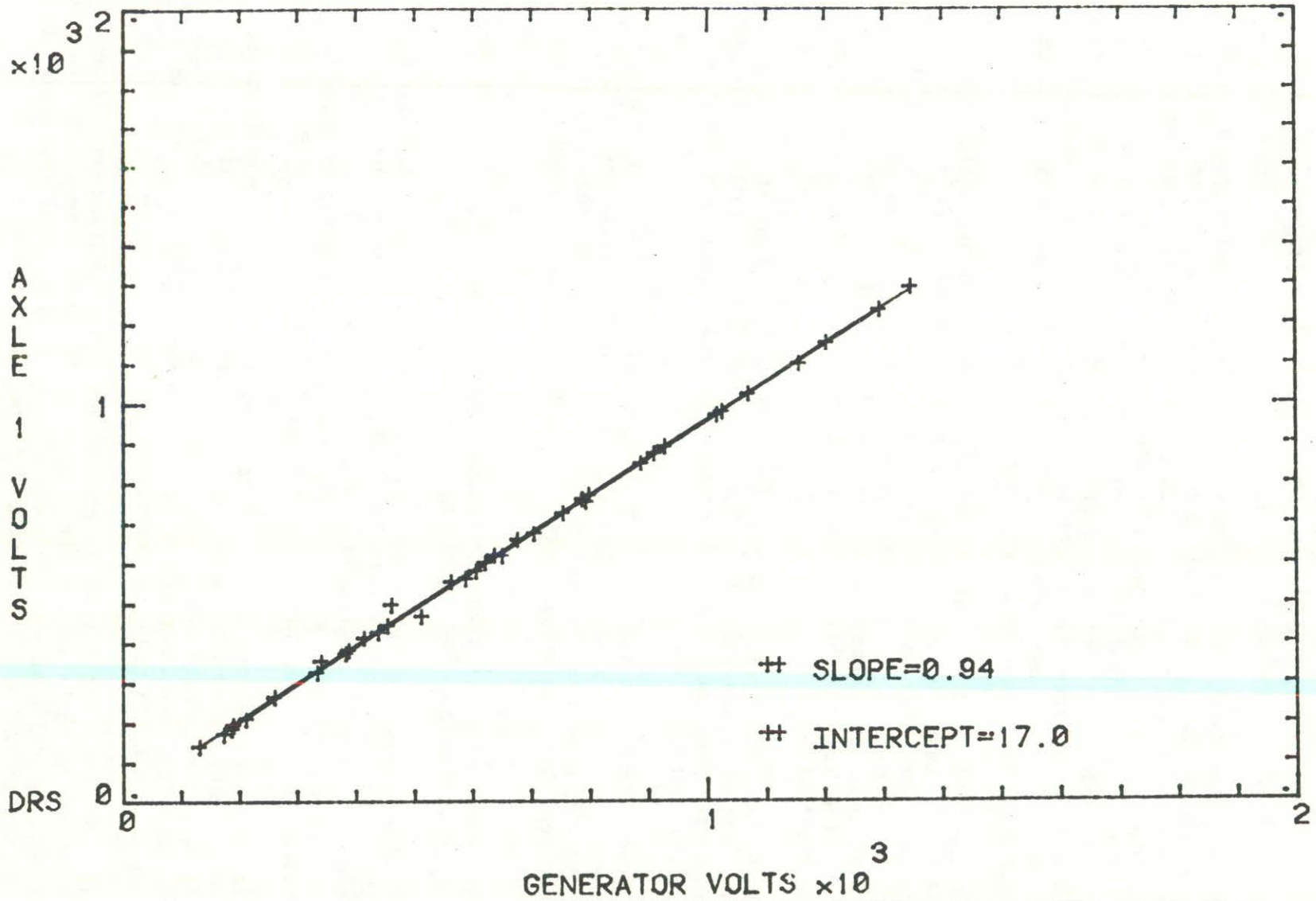

FIGURE 45. AXLE 1 GENERATOR VOLTAGE.

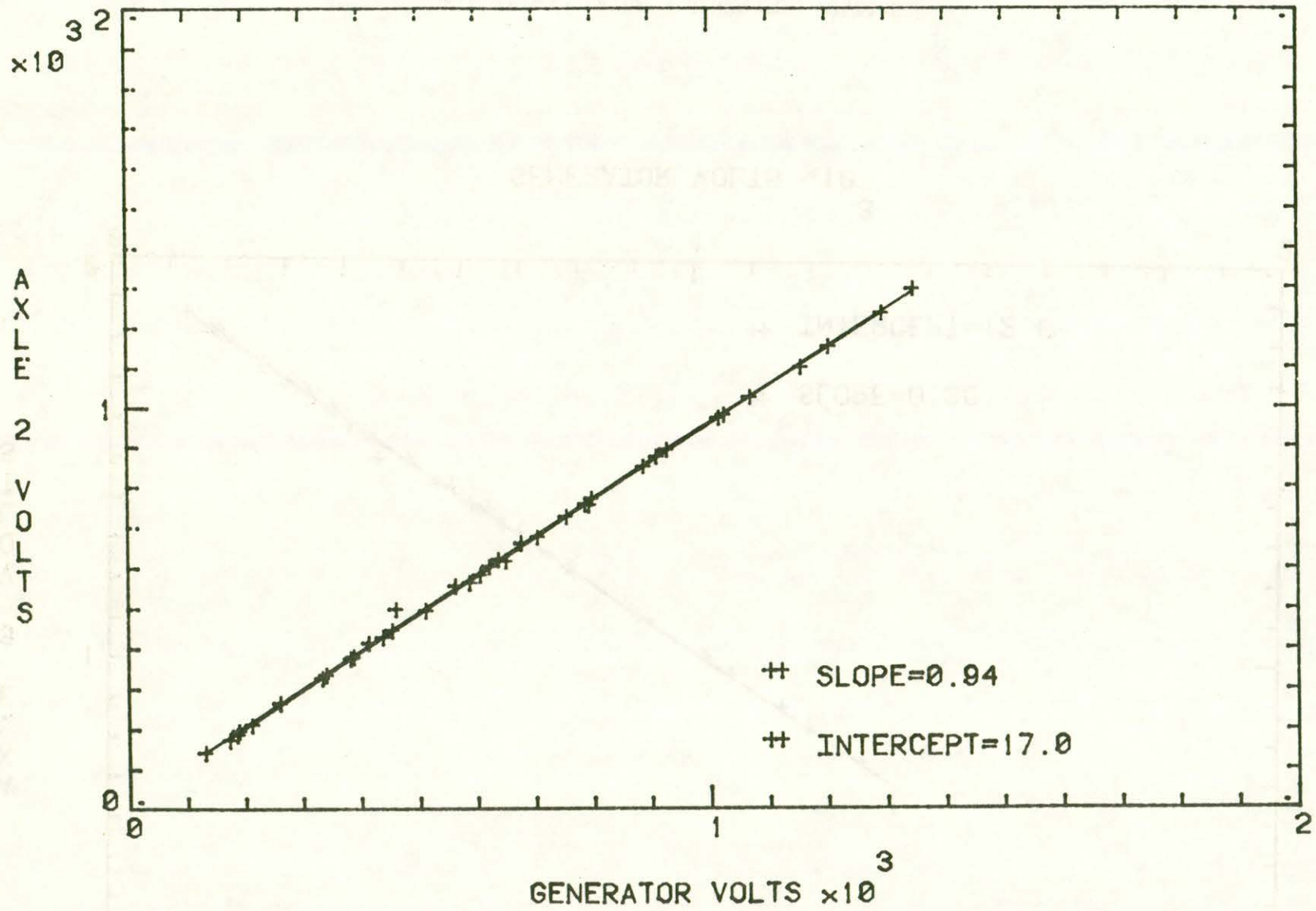

FIGURE 46. AXLE 2 GENERATOR VOLTAGE.

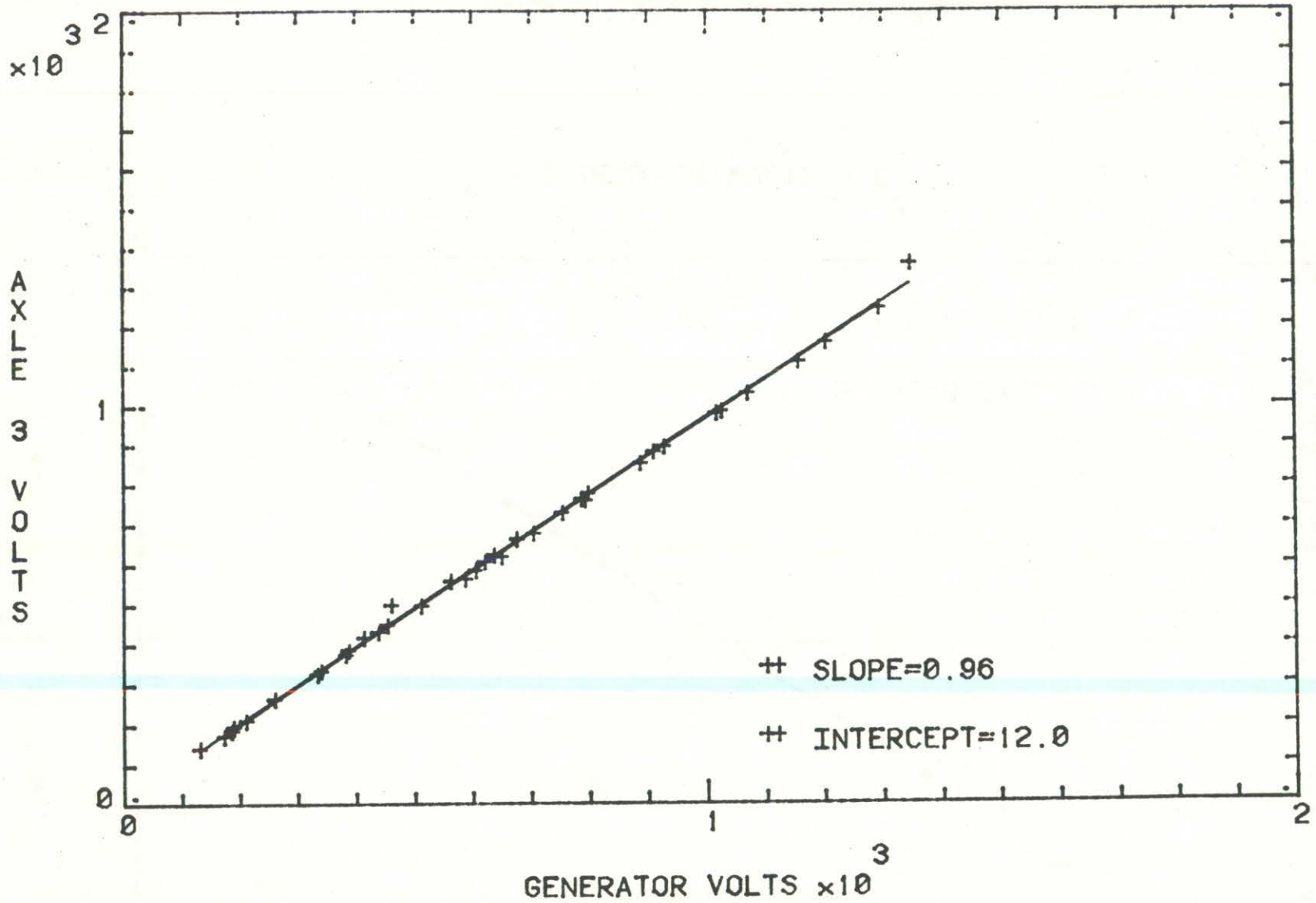

FIGURE 47. AXLE 3 GENERATOR VOLTAGE.

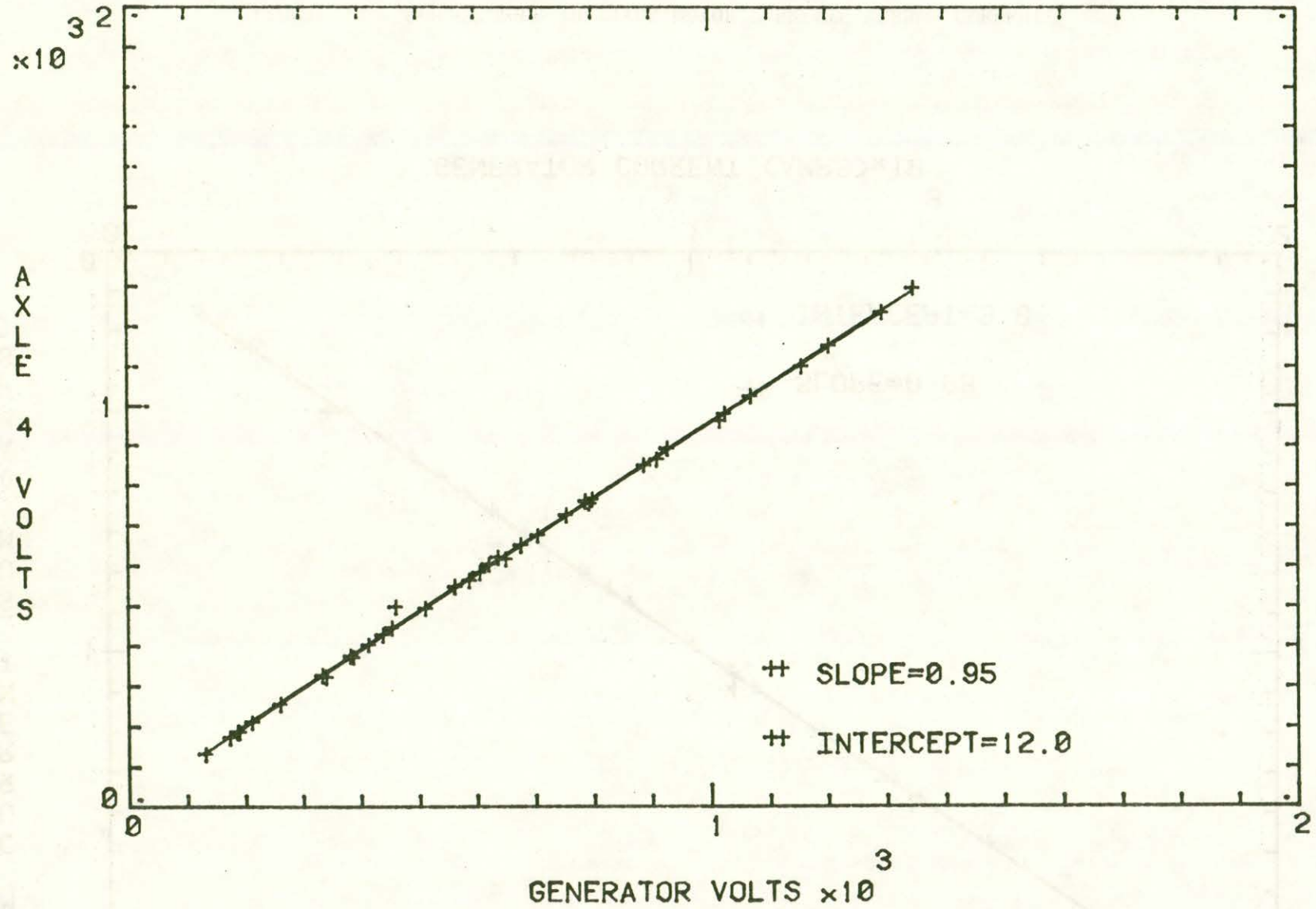

FIGURE 48. AXLE 4 GENERATOR VOLTAGE.

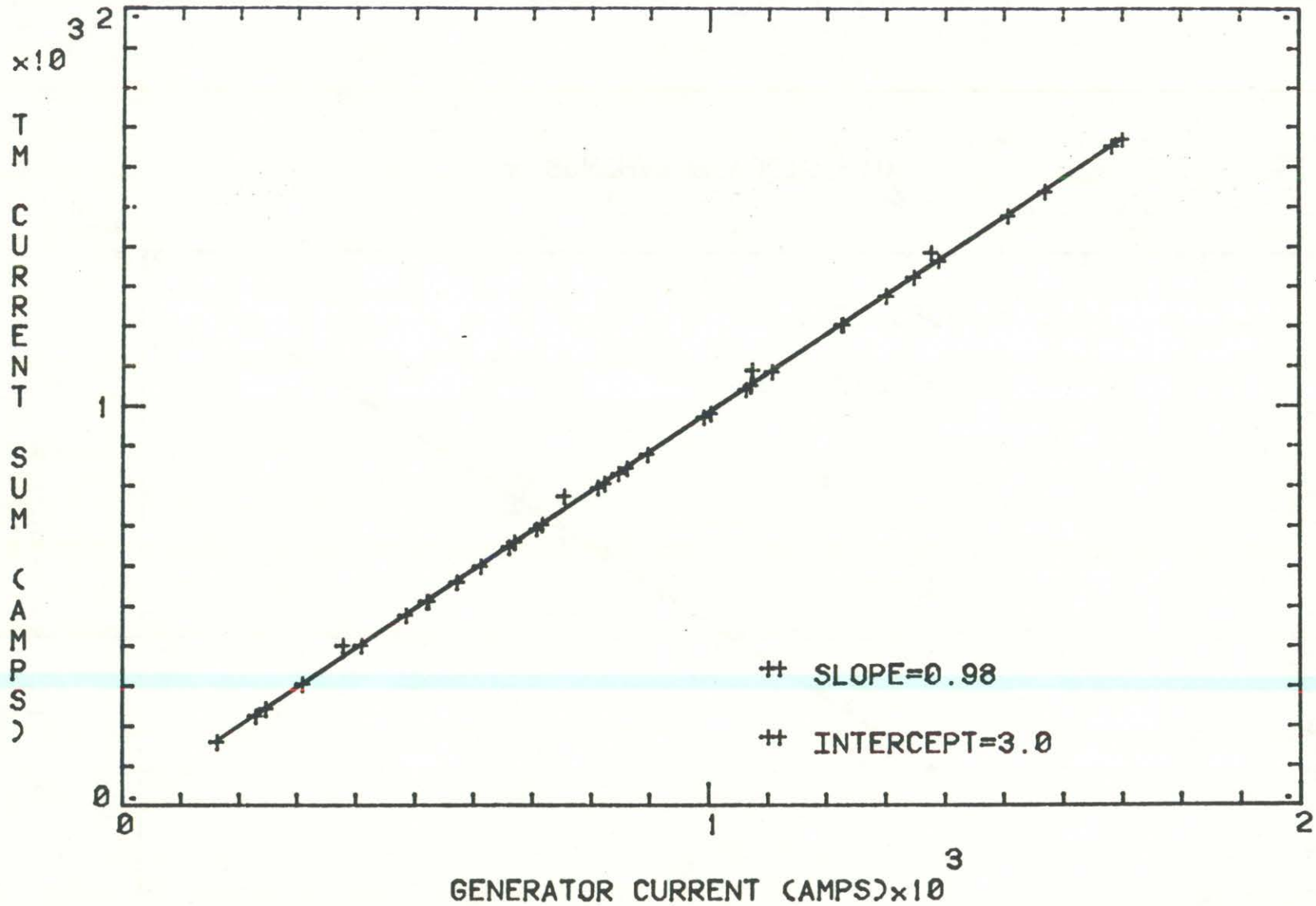

FIGURE 49. SUM OF FOUR TRACTION MOTOR CURRENTS VERSUS CURRENT.

7.0 DISCUSSION AND CONCLUSIONS

The slopes and intercepts of the 'armature efficiency' for each traction motor, as determined by each of the three test methods, are shown in Table 5.

TABLE 5. ARMATURE EFFICIENCY RESULTS

	Locomotive Axle	Test Method: Constant Speed Runs	Test Method: Dynamic Braking Range 8*	Notch 8 Acceleration
1.	Slope	0.931	0.972	0.889
	Intercept	-1.45	-2.10	-6.13
2.	Slope	0.942	0.916	0.913
	Intercept	-2.25	-0.38	-6.07
3.	Slope	0.926	0.952	0.923
	Intercept	-1.21	-0.53	-8.27
4.	Slope	0.925	0.949	N/A
	Intercept	-0.35	-0.56	Bad Data

*Slope of the braking data shown is the inverse of the slopes in Figures 33-41, (explained in Section 5.4.1).

As can be seen, the results for the braking and acceleration runs vary widely, both from each other and from the constant speed data. Due to the transient nature of these tests, their results are not included in the determination of the final calibration coefficients for each traction motor and wheelset.

Data from the constant speed drive mode tests thus result in a calibration equation (for each traction motor) of the following form:

$$TP = C_0 + C_1 (V \times A) - \frac{1}{2142} (IS\ ds/dt) \qquad \text{(Equation 8)}$$

where

TP = Tractive Power (kW)

V = Traction Motor Armature Voltage (volts)

A = Traction Motor Armature Current (amperes)

I = Traction Motor + Wheelset Rotating Inertia (ft-lbs-sec^2)

S = Speed (mph)

C_1 = Electrical to Mechanical Power Conversion Efficiency for Armature and Gear Train

C_0 = Constant Offset

Thus, tractive power may be determined by measuring locomotive speed and the traction motor current and voltage. The tractive effort at a given speed may be calculated by the following equation:

$$TE = 502.7\ TP/S \qquad \text{(Equation 9)}$$

where

TE = Tractive Effort (lbs)

Table 6 lists the traction motor armature and gear train efficiency (coefficient C_1 in Equation 8) for each traction motor, as well as the rotating inertia of that wheelset and motor.

TABLE 6. ARMATURE EFFICIENCY.

Axle	Offset (C_0)	Efficiency (C_1)	Inertia (ft-lbs-sec^2)
1	-1.45	0.931	515
2	-2.25	0.942	942
3	-1.21	0.926	772
4	-9.35	0.925	1355
Average	-3.57	0.931	896

The rotating inertia values were determined as explained in Appendix B by accelerating the RDU to speed under constant torque--first with, and then without the locomotive on the rollers. Inertia was calculated from the following equation:

$$I = (T - T_G)/\dot{\omega} \qquad \text{(Equation 10)}$$

The difference in inertia with and without the locomotive is the wheelset and traction motor inertia. As can be seen, the range for our calculated traction motor inertia is quite broad. This is because it is very small compared to the value of the RDU inertia which is on the order of 32,000 ft-lbs-sec^2. Thus, the error in calculating the traction motor and wheelset inertia is of a similar order as the quantity desired. In the future, a more accurate method of measuring wheelset inertia is desirable.

The inertia value is very small compared to overall train inertias and becomes important in Equation 8 only under high accelerations. Thus, the third term in Equation 8 can often be neglected.

It can be seen that the "armature efficiencies" for axles 3 and 4 are less than for axles 1 and 2. This is probably due to small electrical losses in the longer cables required to reach those axles. The offset values, C_0, also display a wide scatter. These values are small compared to the total output power; thus, their exact magnitude is close to the possible measurement error. Their sign is significant, however, showing that power must be applied to the traction motor before tractive power is developed.

The results of the error analysis show that, for three of the four axles, it was possible to determine the "armature efficiency" of the traction motors to within 2%. In addition, any individual power measurement can be made to within 3%.

With these results, accurate measurements of tractive power required to move a train are now possible.

For tests such as comparing the resistance of rails being lubricated or dry, the accuracy may be considered to be better than 2% (actually in the 1% range). This is because one does not then compare the tractive effort required, but only the variation of the inputs to the traction motor, allowing one to bypass the measurement error in the tractive effort determination and deal only with the measurement errors from the voltage and current transducers. Thus, very accurate comparisons can be made.

At present, the calibration figures given are valid only for relatively steady state conditions, without rapid changes in speed. The effects of transient response in the traction motors are not well documented. Since our transient tests were all performed under abnormally high accelerations, it is possible that the effects of transient response under more realistic conditions will be noticeable. Future testing is recommended to address these problems. Since all the FAST testing was performed at the most steady conditions possible, transient effects were minimal.

The calibration for tractive effort is only valid for a GP40-2 locomotive in good repair with the same gearing and traction motors. It is expected that, although other locomotives would have similarly linear performance curves, the actual coefficients would be different. The input power to the traction motors of other locomotives, if similarly instrumented, could be used for comparative resistance testing; the actual tractive effort would not be known.

Except for waveshape error associated with the diesel engine or generator of the locomotive (Section 5.1), these results are dependent only upon the characteristics of the traction motors and gear ratios. Thus, it is recommended that further calibrations be performed using most of the common traction motors currently in use by railroads, in order to extend these results to other locomotives. A comparison of new and well-worn traction motors is also recommended to establish any degrading of performance with age and use.

At the same time, it may be advisable to investigate other factors that affect locomotive performance, such as diesel engine performance and energy consumption by air compressors and other auxiliary equipment.

Such a major program of locomotive performance and calibration could be undertaken on the RDU and would permit the development of many instrumented locomotives.

PART 2: ON-TRACK TESTING

1.0 INTRODUCTION

Part 1 of this report details the successful attempt to establish the calibrated locomotive as an accurate measurement device for train resistance studies in the Rail Dynamics Laboratory (RDL). Part Two will describe the on-track application of this measurement scheme to document changes in train resistance due to track lubrication and a premium truck design.

2.0 BACKGROUND

The primary objective in establishing the calibrated locomotive as a 1% accurate measurement system is to be able to measure small changes in train energy requirements due to operational or equipment improvements.

Train resistance has been of great importance and interest to the railroad industry for more than a century. The knowledge and understanding of this resistance was initially needed to prepare the railway time tables and train schedules. Most of the earlier notable works in this field are attributable to Davis [1]*, Totten [2], and Keller [3]. In the last decade, train resistance has become more important from the energy point of view due to skyrocketing oil prices. The annual fuel bill for U.S. railroads is over 3 billion dollars; a small reduction in train resistance can lead to considerable financial savings for the industry.

Consequently, the railroad industry is beginning to examine the full effects of train resistance with a view to reducing the fuel costs. In recent years various analytical models (Train Performance Calculators, or Simulators), which were originally used to determine running times, have been modified to estimate fuel consumption. In most of these models, train resistance has been estimated by using the Davis equation [1], or some modified form of this equation [4]. The modified forms have resulted from the efforts of individual railroads and institutions, primarily when new equipment was introduced into service. The modifications reflected adjustments in coefficients of the Davis equation to provide the best fit through empirical data. The resulting equation, although it has limitations as described later, can, as shown by Radford [5], be used to estimate fuel consumption for different operating practices, provided that the set of conditions used for the estimation are comparable with the conditions which existed during the previous experiments to determine the equation.

To analyze train resistance and its influence on fuel consumption, the Davis equation in its general form can be written as:

---

*References are listed following the text of Part 2.

$$R = A + BV + CV^2 \quad (1)$$

where

R = Train resistance in lbs

A = Resistance component (independent of train speed)

B = Coefficient of train resistance (linearly dependent on train speed)

C = Coefficient of train resistance (parabolically dependent on train speed)

V = Train speed in mph

The terms A and B are partly composed of components which are strongly influenced by vehicle/track interactions. They depend on vehicle weight, dimensions, suspension stiffness and damping, track class, track stiffness and operating speed. All of these parameters influence the loads at the wheel/rail interface and the energy dissipated in the vehicle suspension. The C coefficient is generally used to describe the aerodynamic drag of a particular equipment type.

2.1 LIMITATIONS OF THE DAVIS EQUATION

Determination of the constants used in the Davis equation, both by Davis and by subsequent researchers, has been carried out by empirical means, typically by coast-down tests. Using this technique, a train is allowed to coast on level, tangent track while its speed is recorded as a function of time. Deceleration is obtained by differentiation and the retarding force is obtained by applying Newton's second law. A second procedure, which generally has more uncertainty, involves measuring the drawbar pull required to maintain constant speed on level track.

Thus, both methods treat the train as a complete system, without any attempt to separate the individual components of train resistance. Consequently, there is only a limited theoretical justification for either the choice of Eq. (1) as the function describing train resistance or the interpretation of the constants A, B, and C, although there has been qualitative rationalization of these components. Indeed, the following statement made by Wellington [6] in 1887 largely summarizes our state of knowledge one hundred years later:

> "Although over fifty years have passed since experimental investigations in respect to it began, there is no single element of train resistance whose laws can be said to be definitely known."

This is essentially true, despite a number of notable studies in this area in recent years, particularly by Bernsteen [7], Hammitt [8], Muhlenberg [9] and English, et al [10]. These studies relied primarily on theoretical analyses, with minimal, if any, on-track testing, (although the aerodynamic studies have employed data from small scale model wind tunnel tests).

The problem with not having a detailed knowledge of the individual components of train resistance which makeup the overall Davis equation is that, although improvements may be made in these individual components; e.g., through improved car and/or truck designs, there is no way to evaluate the overall effect of these improvements on energy or fuel consumption. For instance, aerodynamic train resistance includes not only friction (caused by moving the vehicle through the atmosphere), but also the train forces caused by the wind. The Davis equation assumes that all vehicles have an aerodynamic resistance directly proportional to the cross-sectional area of the vehicle. It ignores the shape of the vehicle, distance between vehicles, effect of adjacent vehicles, location and shape of outside appliances, and the effect of wind and other environmental conditions.

Curving resistance has been traditionally set at 0.8 lbs/ton/degree of curvature, and this value appears to be a reasonable estimate for vehicles fitted with conventional three-piece trucks with AAR 1-in-20 wheel profiles running on unlubricated track of good quality. However, this simplistic expression does not allow for calculation of the effects of variations about this set of conditions. For instance, it does not account for the effects of different wheel/rail profile and geometrical differences, rail gage variations, wheel flange lubrication, or suspension characteristics other than those characteristics of radial trucks. However, the determination by Elkins and Eickhoff [11], that the energy dissipated in the contact patch is a function of lateral and longitudinal forces and creepages, allows us to better understand these effects on both wheel/rail wear and train resistance.

Similar cases can be made for an incomplete knowledge of train energy requirements due to the effects of track structure, vehicle suspensions, bearing resistance, and vehicle dynamics.

It has become apparent that a very accurate method of measuring train resistance is required to document resistance savings due to engineering or operational variations not covered by existing quantitative work. It is also envisioned that this measurement scheme will be utilized to make improvements in our understanding of the various train resistance components.

To meet this perceived need for a portable and accurate energy consumption measuring system, the Transportation Test Center has developed the calibrated locomotive, as described in Part I of this paper.

To prove that this system would perform successfully in on-track testing, it was decided to use the calibrated locomotive to determine the train resistance savings due to two engineering variables already under study at the TTC:

1. Track Lubrication,

2. Self-steering Trucks

3.0 OBJECTIVES

It is known from past FAST* experience at the TTC that track lubrication provides significant savings in wheel and rail wear. It is also known that self-steering trucks provide substantial wheel wear savings in the FAST environment. These savings must manifest themselves in decreased train resistance. The objectives of the on-track testing portion of the Traction Motor Characterization test were:

1. to demonstrate that the onboard data collection system will stand up to on-track service, and

2. to document the amount of train resistance savings due to the aforementioned variables.

4.0 TEST DESCRIPTION

On-track testing was accomplished at the TTC, utilizing the calibrated locomotive and a mini-train consist of six loaded 100-ton open top hopper cars. See Figure 50.

All of the testing was performed on the 4.8 mile FAST loop. This loop consists of approximately 50% tangent track and 50% curve track, with curves ranging from three to five degrees. Grades up to 2½% are encountered. (Figure 51, 2 parts.)

The test laps were conducted at 40 miles per hour, with operators instructed to maintain a constant speed by use of engine power or dynamic braking.

---

*The FAST track is a specially constructed 4.8-mi loop divided into 22 sections where specified combinations of track components and structures are installed for testing. It contains 2.2 mi of tangent, 0.4 mi of 3° curve, 0.3 mi of 4° curve, and 1.1 mi of 5° curve; the remaining 0.8 mi being transitional spirals.

Mechanical components are tested in the FAST consist, which is made up of 4-axle locomotives normally hauling a 75-car, 9500-ton train. Cars are available from a pool of about 90 cars assigned to FAST. The majority are 100-ton hopper or gondola cars, and the remainder are 100-ton capacity tank cars and laden trailer-on-flat-cars.

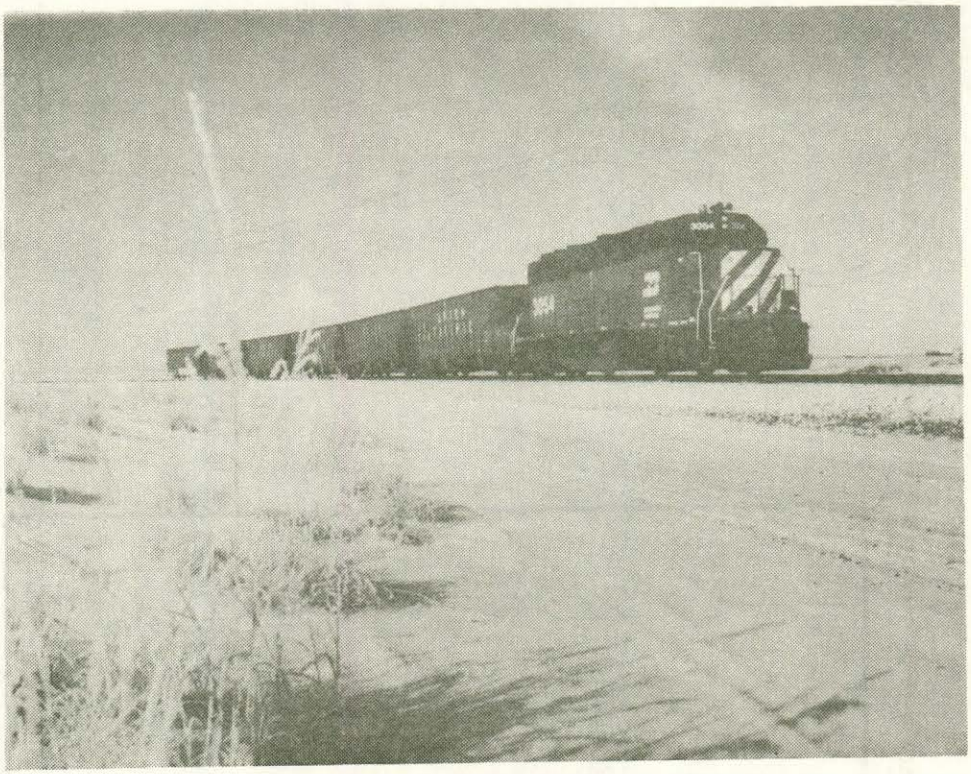

TTC N83-1910

FIGURE 50. MINI-CONSIST USED IN TRAIN RESISTANCE TESTING.

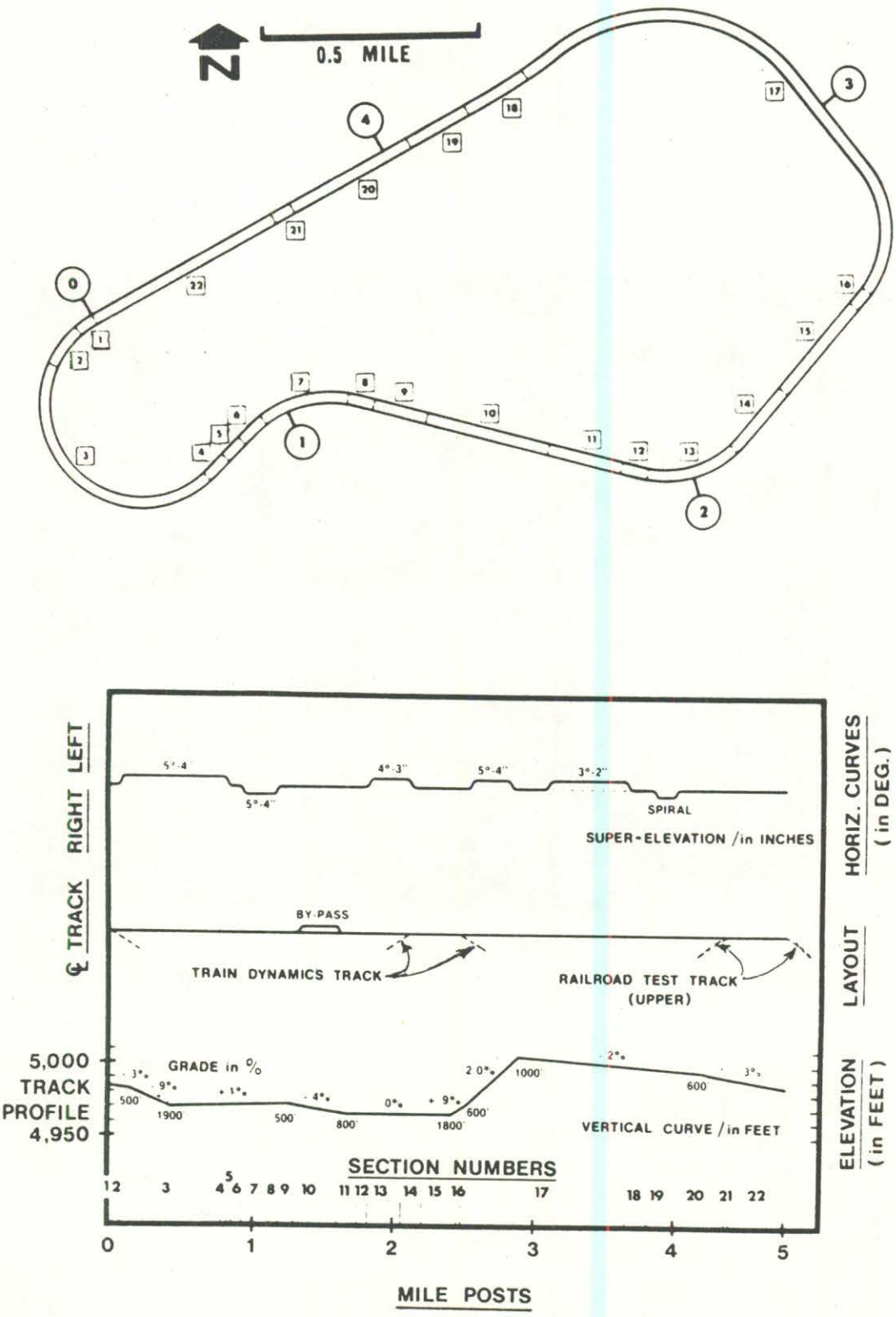

FIGURE 51. FAST TRACK PROFILE.

4.1 TEST MATRIX

Test Number	Track Condition	Truck Design
1	Unlubricated	Standard 3-Piece
2	Lubricated	Standard 3-Piece
3	Unlubricated	Self-Steering (Radial)

4.2 TEST EQUIPMENT

Lubrication was applied by a vehicle-borne system lent to the Test Center by the Norfolk Southern Railroad (see Figure 52). This system, which is mounted in a railroad boxcar, pumps grease onto the wheel flange surface.

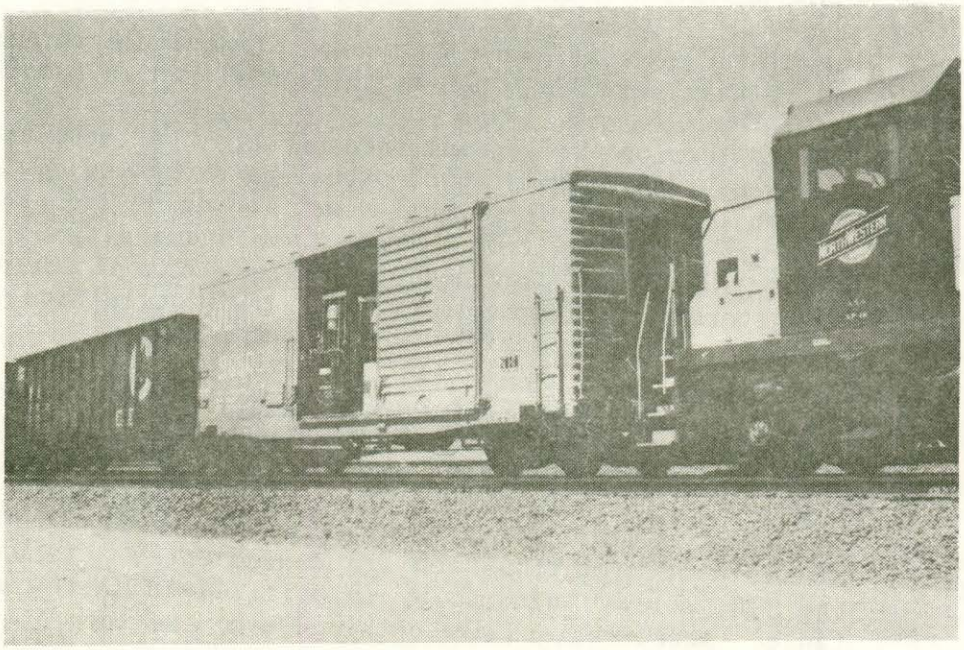

TTC N83-1167

FIGURE 52. NORFOLK SOUTHERN LUBE CAR IN MINI-CONSIST.

The pump is activated by a cable system running from the carbody to the truck sideframe. As the boxcar enters a curve, the truck rotates, thus activating the pump. The pump is controlled mechanically to squirt grease on the wheel flange at chosen (adjustable) increments. The wheel then smears the grease on the wheel/rail interface. In a short period of time the grease migrates through the train to cover the rail gage face and the wheel flange surface. Experience at FAST with several types of lubrication application schemes is that the grease pattern on the rail can be controlled to keep it off the rail head where it would impede locomotive traction. Due to the fact that FAST is a closed loop and because the lubricator frequently interpreted vehicle dynamic motions as track curvature, the tangent track sections are also well lubricated. It has been observed that one greasing of the FAST track provides adequate lubrication for several train passes. The lubricated test runs described in this report were accomplished on residual grease from the previous evening of operation.

4.3 TRUCK DESIGN

Test #3 was performed utilizing self-steering or radial trucks. The unique feature of these radial trucks is the use of wheel/rail forces to cause the axles to align themselves radially in curving. This feature reduces or prevents flanging of the wheelsets during curving. Three of the vehicles had trucks with the retrofit design (Figure 53) and three were the x-linked design of radial trucks (Figure 54). A complete description of these two designs is available in [12].

4.4 INSTRUMENTATION - ONBOARD SYSTEM

The transducers utilized to measure traction motor armature current and voltage were the same as those utilized in the RDL calibration.

Data collection was accomplished onboard the locomotive utilizing an Analog Devices Micromac 4000 signal conditioning device and an HP-85 desktop computer. The signal conditioning device provided filtering at 2 Hz, isolation from high voltage and analog-to-digital conversion. The HP-85 provided conversion to engineering units. Data were stored on floppy disks. The data collection system is shown mounted in the locomotive cab in Figure 55.

Figure 56 is a schematic of the locomotive-based measuring system. Note that fuel consumption from a flowmeter, and main generator current and voltage were also measured.

The on-track measurement accuracy is highly dependent upon knowledge of train accelerations and track gradients. For on-track tests at the TTC, survey information is utilized to factor out grade resistance. Accelerations are obtained from the locomotive-mounted speed sensor.

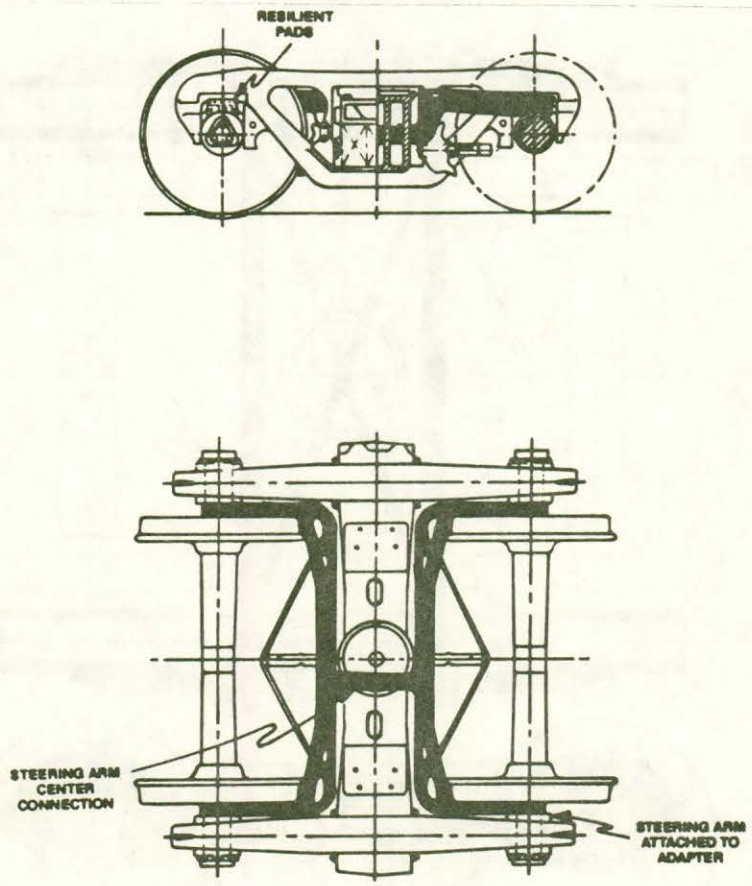

FIGURE 53. RETROFIT RADIAL TRUCK.

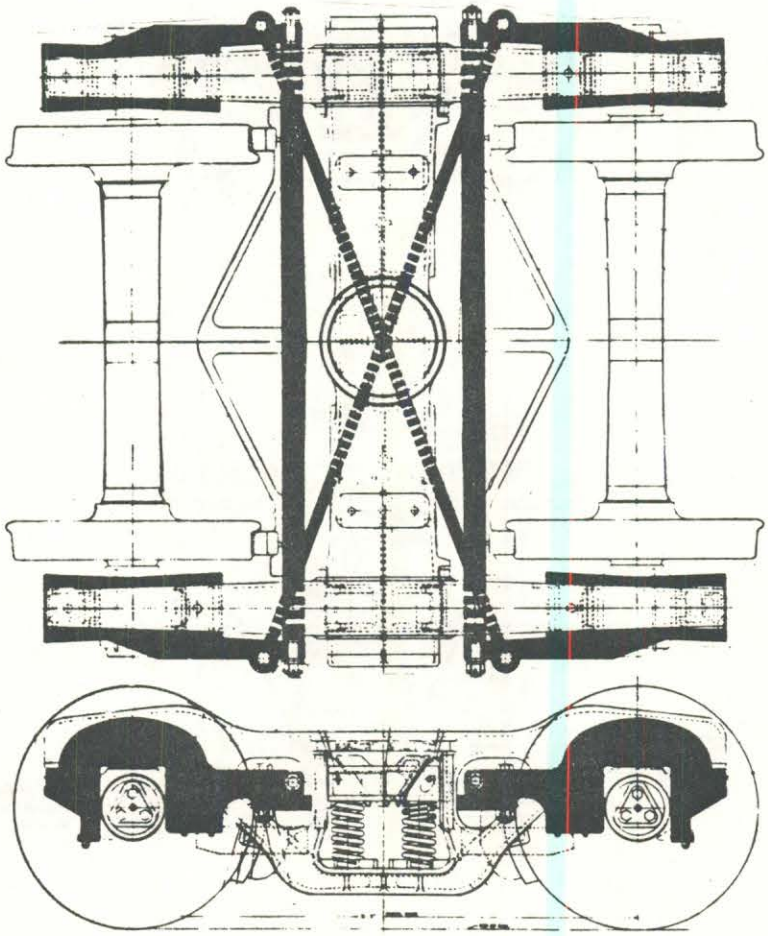

FIGURE 54. CROSS-LINKED RADIAL TRUCK.

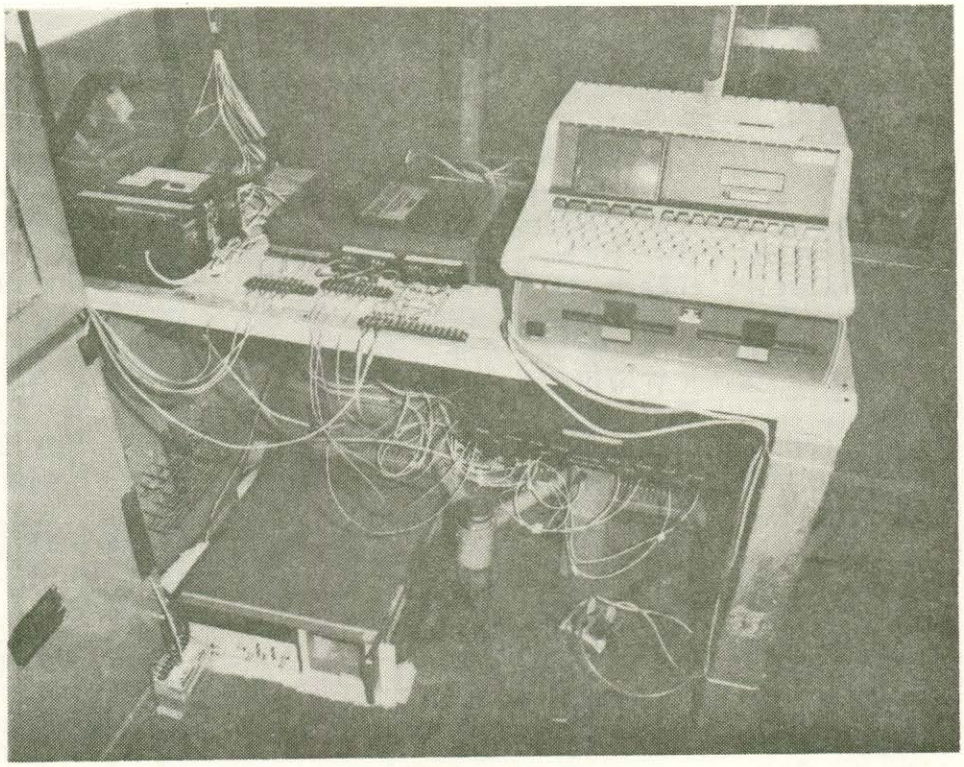

TTC N83-0949

FIGURE 55. ON-BOARD DATA COLLECTION SYSTEM.

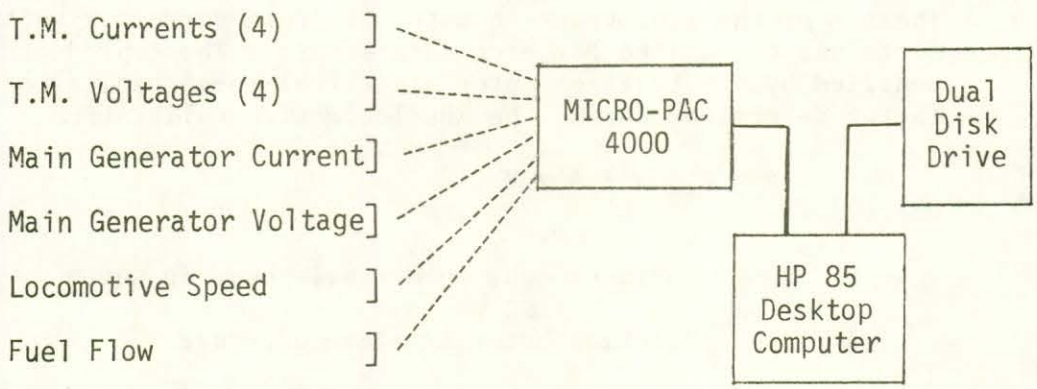

FIGURE 56. ON-BOARD MEASURING SYSTEM SCHEMATIC.

For track gradients in excess of 0.25 percent, the train resistance equation is generally dominated by the gradient term. If the calibrated locomotive (or any other) system is to be utilized to gather absolute energy consumption information over unknown routes, the development of a locomotive-based gradient sensor is very desirable. Comparative energy measurements over identical track can be accomplished without this added feature.

4.5 TEST TRACK LOCATIONS

The test sections identified by FAST track section are listed below. Individual data reduction was done for each test section.

Section Number	Curvature	Length (Ft)
3	5°	3786
7	5° R	1033
17	5°	1561
13	4°	1580
17	3°	3198
20	Tangent	1982
22	Tangent	1890
10	Tangent	2920
Non-test	Variable	7259

5.0 CALCULATIONS

Resistance data were reduced on the HP-85 desktop computer. Average resistance in pounds was calculated for each test section for each train lap. Resistance for each entire lap of FAST was also calculated.

5.1 POWER CALCULATIONS

The sum of the four traction motor armature current x voltage products was calculated for each data sample. These products were modified by the traction motor electrical-to-mechanical efficiency factor determined during the RDL locomotive calibration.

$$P = E_{ff} \times \Sigma A \times V$$

where

P = Instantaneous wheel/rail power in watts

A = Traction Motor Armature amperage

V = Traction Motor Armature voltage

E_{ff} = Ratio of power at the wheel rail interface to the input electrical armature power. In this case .93 for traction, 1.075 for dynamic braking.

The power was averaged for each test section.

5.2 RESISTANCE CALCULATIONS

Dividing the power in kilowatts by speed in miles per hour yields a resistance number expressed in kilowatt-hours per mile. Multiplying this result by a constant (502.681) yields a resistance number in pounds.

$$R_p = \frac{P}{S} \times K$$

where

R_p = Train resistance (lbs)

P = Power (kW) at the wheel/rail interface

S = Speed in (mph)

$K = \frac{3600}{5280} \times \frac{550}{.746} = 502.681$

$\frac{3600}{5280}$ converts hours per mile to seconds per foot

$\frac{550}{.746}$ converts kilowatts to pounds-feet per second

5.3 ACCELERATION CALCULATIONS

Train resistances caused by unwanted train accelerations are subtracted from each data sample to allow comparison from section-to-section on a constant speed basis. The expression used is:

$$R_A = M \times a$$

where

R_A = Resistance due to acceleration

M = Mass of the train

a = Train acceleration

5.4 GRADE RESISTANCE CALCULATIONS

Grade resistance is factored out by combining the resistance data from clockwise and counterclockwise operations.

6.0 TEST RESULTS

Three separate tests were conducted on the FAST track. Since these tests were designed to demonstrate the measurement system on track only, one train speed was accomplished for each test configuration. The results are not intended to be typical of the full range of train speeds.

6.1 TEST #1 - STANDARD THREE-PIECE TRUCKS ON UNLUBRICATED RAIL

This test was intended to provide a baseline for comparison to the results obtained in Tests #2 and #3. Resistance for individual test sections are shown in Table 7. Test data for individual runs are found in Appendix D.

The average power consumption to move the test consist around the FAST loop at 40 mph was found to be 414 kilowatts. The Davis approximation for this loop is 442 kilowatts.

6.2 TEST #2 - STANDARD THREE-PIECE TRUCKS ON LUBRICATED RAIL

Testing on lubricated rail yielded substantial train resistance savings for the entire FAST loop as expected. At 40 mph the lubricated rail train resistance was reduced by 34.9%. This compares favorably with fuel savings of 32% noted during FAST operations covering several months[13] of alternating dry and lubricated operation.

Unlike the testing described in the report, which used a vehicle-mounted[14] lubrication system, the lubrication was applied by wayside devices during the operating period where measured fuel savings were noted. (4 locomotives, 70 loaded 100-ton open top hoppers.) It should be noted that, although an even band of grease was evident on both rails, no attempt was made to quantify the effectiveness of track lubrication at a particular test site. From the test data it was evident that lubrication was effective in reducing train resistance in all test zones and all test laps. This savings was smaller than expected in the 4° curve in Section 13. It is apparent from test data that six of the eight test laps were poorly lubricated in this section.

Table 7 summarizes the train resistance figures for each test section and for the entire FAST loop. Data for individual runs are listed in Appendix D.

It is well known that fuel consumption is closely related to throttle position for a properly performing diesel locomotive. Observations from the Train Operations Recording Systems (TORS) are shown in Figure 57. The solid line indicates the throttle positions utilized when four locomotives are pulling a seventy car FAST train around the loop on relatively "dry" track.

TABLE 7. COMPARISON, LUBE TRACK TO DRY TRACK RESISTANCE AT 40 MPH.

Section No.	Curve	Resistance (lbs) Dry Track	Resistance (lbs) Lube Track	Ratio (Lube/Dry)
3	5°	7543.31	3761.39	.4990
7	5° (R)	8004.60	3265.25	.4079
17	5°	6615.91	3984.25	.602
13	4°	6899.16	3731.70	.541
17	3°	5542.15	2720.79	.491
20	Tangent	4736.62	3037.60	.640
22	Tangent	4509.53	2870.31	.637
10	Tangent	2869.37	2604.20	.907
Total FAST*		5239.61	3410.65	.651
Non-Test Zones		4135.13	3611.78	.873

---

*Author Note: Total FAST resistance number for lube track includes data from Section 3, 4° curve when it was poorly lubricated. The data displayed for Section 3, 4° curve is from adequately lubed runs only.

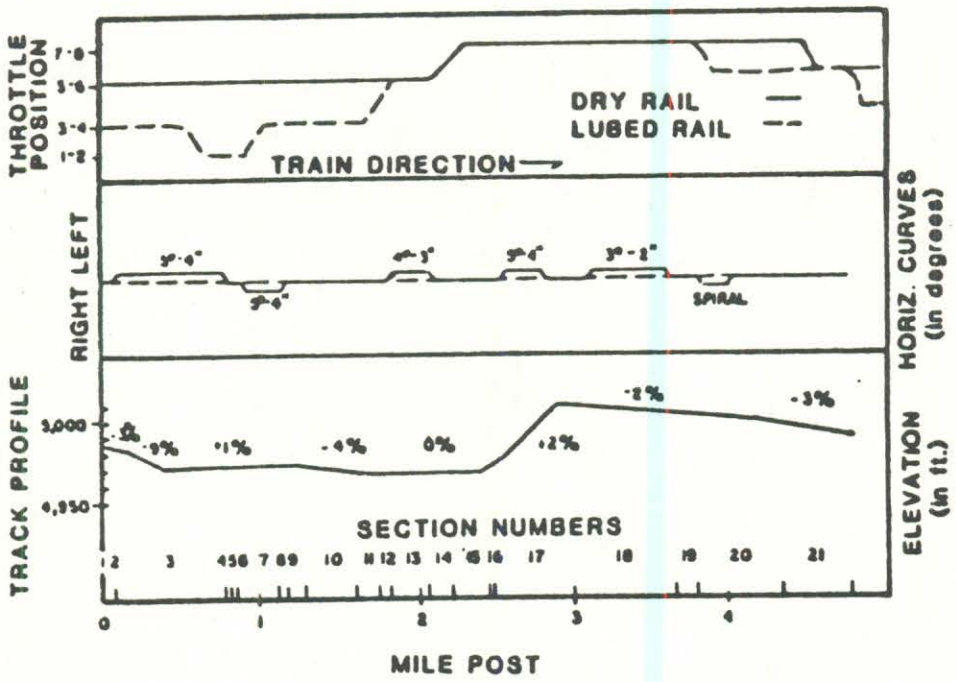

FIGURE 57. FAST PROFILE, SHOWING THROTTLE POSITIONS, LUBED AND UNLUBED TRACK.

The dotted line shows the throttle positions utilized to pull the same train under lubricated track conditions. In this case, lubrication was applied by a wayside system, but other methods of grease application have been tested at the TTC, including locomotive-mounted and Hy-railer systems.

As documented by Table 7, significant resistance savings were produced for all FAST test sections as well as for the entire loop. Although several of the test sections were quite short compared to the length of the train, repeatable data were obtained for each. Comparing like segments, it appears that the dry rail resistance data for Section 17 - 5° curve and Section 10 tangent may be on the low side. There is, however, no documentation to support this.

To illustrate these on-track savings, the desktop computer has been programmed to generate a time-based plot of any of the measurement channels.

Figure 58 is an overlay of traction motor input power for identical consists on lubricated and unlubricated track at FAST. Two consecutive laps are shown for each condition. Individual data points have been corrected to eliminate train resistance due to undesired accelerations. The difference between these power time histories is the savings due to lubrication, 34.9%. The time history of speed for the same operations is shown below.

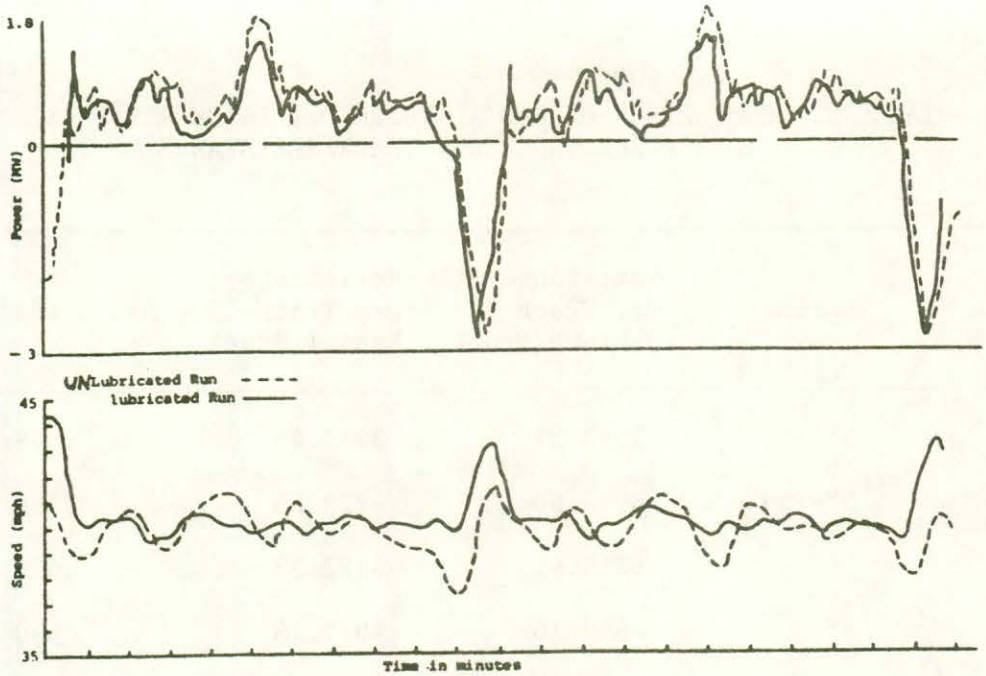

FIGURE 58. TRAIN RESISTANCE TIME HISTORIES ON FAST TRACK, STANDARD TRUCK, LUBED AND UNLUBED.

Note that train resistance during dynamic braking (which is current-limited) was greatly reduced for the lubricated run. This is manifested in the higher train speed for that track section.

The time histories displayed are for two laps at FAST.

6.3 TEST #3 - RADIAL (SELF-STEERING) TRUCKS ON UNLUBRICATED RAIL

It was apparent from Test #2 that substantial savings could be realized by careful lubrication of curve and tangent track by wayside or vehicle-borne lubrication. Similarily, it was felt that substantial savings might be realized by vehicles with trucks designed to reduce wheel flanging in curves and on tangent track.

Train resistance testing was conducted on the FAST track utilizing six open top hoppers equipped with self-steering (radial) trucks. As stated in 4.3, the unique feature of these radial trucks is the use of wheel/rail forces to cause the axles to align themselves radially in curving. This feature reduces or prevents flanging of the wheelsets during curving.

Three of the vehicles had trucks with the retrofit design and three had x-linked design radial trucks.

Table 8 documents the train resistance summary of each test section as equipped with radial trucks operating on dry rail. Resistance data for standard three-piece truck operation on dry rail are included for comparison. Individual test run data are listed in Appendix E.

TABLE 8. COMPARISON OF RADIAL TRUCK DRY TRACK RESISTANCE TO 3-PIECE TRUCK DRY TRACK RESISTANCE.

Section No.	Curve	Resistance Dry Track 3-Piece Truck	Resistance Dry Track Radial Truck	Ratio (Radial/Dry)
3	5°	7543.31	3917.45	.519
7	5° (R)	8004.60	4723.65	.590
17	5°	6615.91	4122.33	.623
13	4°	6899.16	4071.18	.590
17	3°	5542.15	2709.93	.489
20	Tangent	4736.62	3363.23	.710
22	Tangent	4509.53	3922.17	.870
10	Tangent	2869.37	3025.37	1.054
Total FAST*		5239.61	3535.10	.675
Non-Test Zones		4135.13	3437.96	.831

As expected, the self-steering trucks showed a substantial resistance savings over the 3-piece design on dry rail. For the entire FAST loop, a savings of 32.5% was achieved. In one tangent segment (Section 10), the self-steering train had greater resistance, by a small amount, than was exhibited by the train equipped with 3-piece trucks. This may be a further indication that the dry track resistance measured in this section is too low. It may also be an indication that the trucks (standard 3-piece) were aligned better in this tangent section than in the others; in other words, tangent track train resistance may be affected by residual vehicle misalignments set up in curving.

Figure 59 is an overlay of traction motor input power for the standard six-car consist on unlubricated rail and a radial truck-equipped, six-car consist on dry rail. The difference between the power time history lines represent the savings due to self-steering trucks. The data shown are for two laps on FAST.

Figure 60 is an overlay of traction motor input power requirements for six cars equipped with standard 3-piece trucks on lubricated rail and six cars equipped with self-steering trucks on unlubricated rail. Again, the data shown represent two laps at FAST. The power requirements are quite similar for these two scenarios, which may indicate that track lubrication and self-steering trucks are effectively attacking the same resistance problems. The savings obtained by lubrication cannot be added to the savings obtained by the premium truck design.

The closeness with which the speed time histories follow each other also indicates that the train handling requirements for the two test configurations were quite similar.

7.0 CONCLUSIONS

The Locomotive Traction Motor Characterization study provided a useful tool for measuring the potential benefits of operational and engineering changes in railroad practice. It also helped to illustrate the potential benefits available from specific existing technologies.

The onboard data collection system was shown to be a durable and reliable method for collecting train resistance data in the railroad environment. The system has subsequently been utilized in several revenue service applications.

Self-steering or "radial" trucks were also shown to be a viable means of reducing operating costs.

Although track lubrication was originally chosen as just a variable for testing the reliability of the calibrated locomotive system, it has proved to be an effective and readily available means for significantly reducing railroad operating expenses.

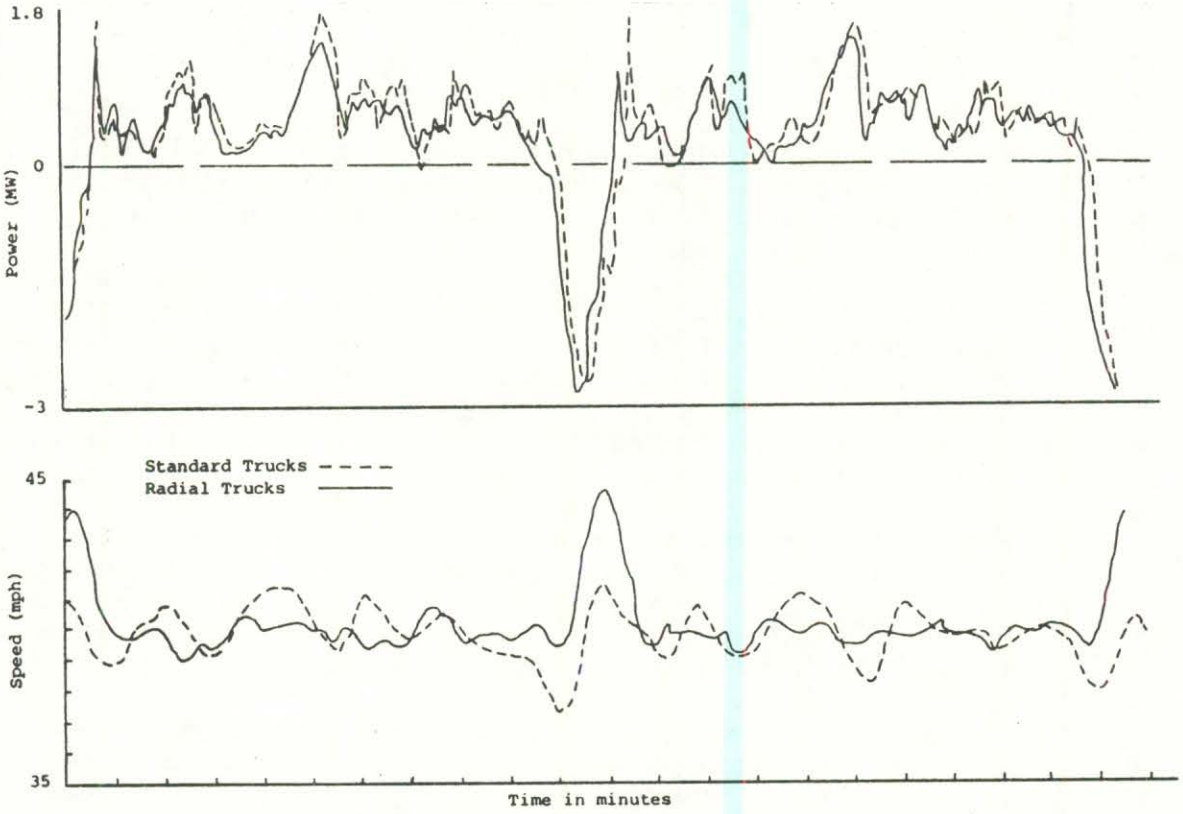

FIGURE 59. TRAIN RESISTANCE TIME HISTORIES ON FAST TRACK, RADIAL AND STANDARD TRUCKS, UNLUBED.

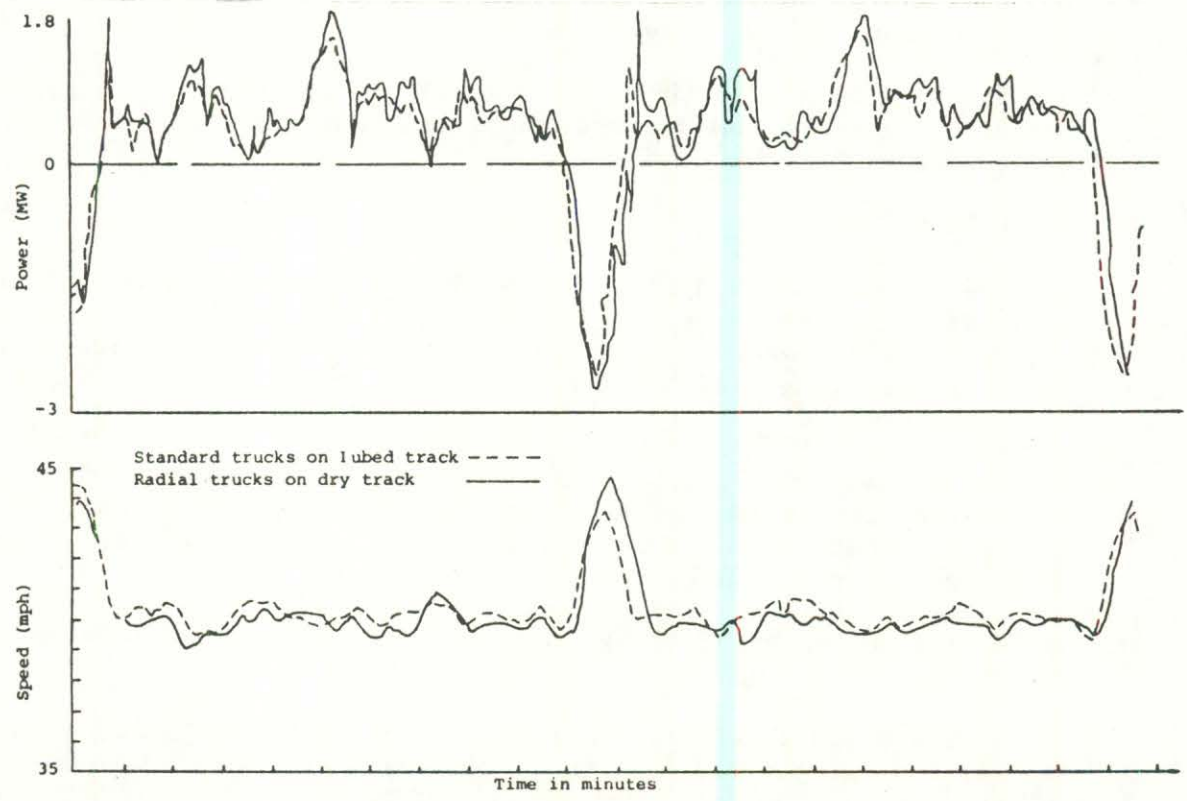

FIGURE 60. TRAIN RESISTANCE TIME HISTORIES ON FAST TRACK, RADIAL TRUCKS ON DRY TRACK, STANDARD TRUCKS ON LUBED TRACK.

REFERENCES, PARTS 1 AND 2

Part 1

1. Irani, F. D., Washburn, R., Peters, A. J., and Ball, D., RDU Dynamometer Test, DOT Report No. FRA/ORD-84/03, May 1984.

2. Irani, F. D., Flow Meter Evaluation for Railroad Locomotive Appications Using the RDU, Association of American Railroads Report No. AAR-597, December 1984.

3. Abernethy, R. B., et al, Measurement Uncertainty Handbook, revised 1980, NTIS No. AEDC-TR-73-5.

Part 2

1. Davis, W. G., "The Tractive Resistance of Electric Locomotives and Cars," General Electric Review, October 1926.

2. Totten, A. I., "Resistance of Lightweight Passenger Trains," ASME Conference, Detroit, MI, May 17-21, 1937.

3. Keller, W. M., "Variables in Train Resistance," ASME Publications, Paper 58-A-265, Railroad Division, ASME Annual Conference, New York, NY, November 30 - December 5, 1958.

4. Howard, S. M., Gill, L. C., and Wong, P. J., "Railroad Energy Management, Train Performance Calculator: A Survey and Assessment," DOT Report No. FRA/ORD-81/02, 1980.

5. Radford, R. W., "Fuel Consumption of Freight Trains Hauled by Diesel Electric Locomotives," ASME Publications 83-RT-9, ASME/IEEE Joint Railroad Conference, April 1983.

6. Wellington, A. M., "The Economic Theory of Railway Location," J. Wiley & Sons, 1887.

7. Bernsteen, S. A., Uher, R. A., and Romualt, J. P., "Interpretation of Train Rolling Resistance from Fundamental Mechanics," ASME/IEEE Joint Railroad Conference, April 1980.

8. Hammitt, A. G., "Aerodynamic Forces on Freight Trains," DOT Report No. FRA/ORD-76-295111.

9. Muhlenberg, J. D., "Resistance of a Freight Train to Forward Motion," DOT Report No. FRA/ORD-78/04, April 1978.

10. English, G. W., Young, J. D., Boumeester, H., Schwler, C., Roney, M. D., and Bunting, P. M., "Railway Linehaul Energy Intensity: An Analysis Leading to Design of a Train Simulation Software Package," Canadian Institute of Guided Ground Transport Report No. 80-15, February 1981.

11. Elkins, J. A., and Eickhoff, B. M., "Advances in Non-Linear Wheel/Rail Force Prediction Methods and their Evaluation, "ASME Winter Annual Meeting, New York, NY, 1979.

12. Elkins, J. A., Rownd, K. C., Leary, J. F., and Jollay, J. P., "A Generalized Truck Wheel Wear Predictor-Extensions from FAST," from The Economics and Performance of Freight Car Trucks, Montreal Truck Conference, 1983.

13. Steele, R. K. and Reiff, R. P., "Rail: Its Behavior and Relationship to Total System Wear," Proceedings of the Second International Heavy Haul Railway Conference, Paper No. 82-HH-24, September 1982.

14. Reiff, R. P., Southern Lubricator Car Operation on FAST, TTC Report No. TTC-006(FAST-TN84), AAR/Transportation Test Center, Pueblo, Colorado, June 1985.

APPENDIX A

HIMMELSTEIN TORQUEMETER VERIFICATION AND CALIBRATION,
ROLL DYNAMICS UNIT, RAIL DYNAMICS LABORATORY, TTC

1. On September 21 and 22, 1983, the Himmelstein torquemeters on the four RDU drive trains were checked and calibrated using a locally-manufactured fixture. The purpose of this exercise was fourfold.

   a. Validate the concept of a local, accurate, and repeatable calibration capability.

   b. Validate the merit of the fixture manufactured at the TTC.

   c. Determine the percent of error that may have existed in the torquemeter calibration during previous RDL testing.

   d. Recalibrate the torquemeters as accurately as possible.

   Prior to this effort, there was no local method for calibrating the torquemeters. Each transducer had to be removed from the drive train and returned to Himmelstein for calibration. Upon return, the electrical setup for the torquemeters was determined from calibration data furnished by Himmelstein. This procedure had not been done in over three years. Moreover, there is always the element of doubt as to the possibility of damage during the return shipment; or changes in scaling, for example, that might have occurred because of differences between the calibration and application environments. A local procedure would therefore have the distinct advantage of calibrating the torquemeters in place, on the machine.

2. The locally-manufactured fixture, shown in Figure A-1, consisted of a beam bolted to the input side of the torquemeter, a MTS (Lebow) 5.5 KIP load cell mounted 22 inches out from center of the beam, a 9-ton hydraulic cylinder and an Enerpac hand pump. The value of 22 inches from center was determined by the physical constraints of the drive train structure. All data were taken with the load cell in tension. The load cell was calibrated by the TTC Metrology Lab and conditioned using B & F signal conditioning equipment. The output side of the torquemeter was locked in place mechanically and the torque output was read on the Himmelstein indicators located in the drive train power control rooms. This configuration produced a scale of 1 lb force = .545454 ft-lb of torque.

3. The fixture was first installed on drive train 4, since analysis of test data had determined that drive train 4 had the largest percent of error. Three data runs, each consisting of 8 data points, were made in approximately 500 ft-lb steps from 0 to 3500 ft-lbs. A regression analysis was done for each data run and a correlation coefficient of .9999, or better, was determined in each run. The slope for run 1 was 1.1299, for run 2 it was 1.1233, and for run it 3 was 1.115. The average slope for the three runs was 1.1227. From these data, we determined that the Himmelstein calibration resulted in a reading 12.277% higher than the true torque.

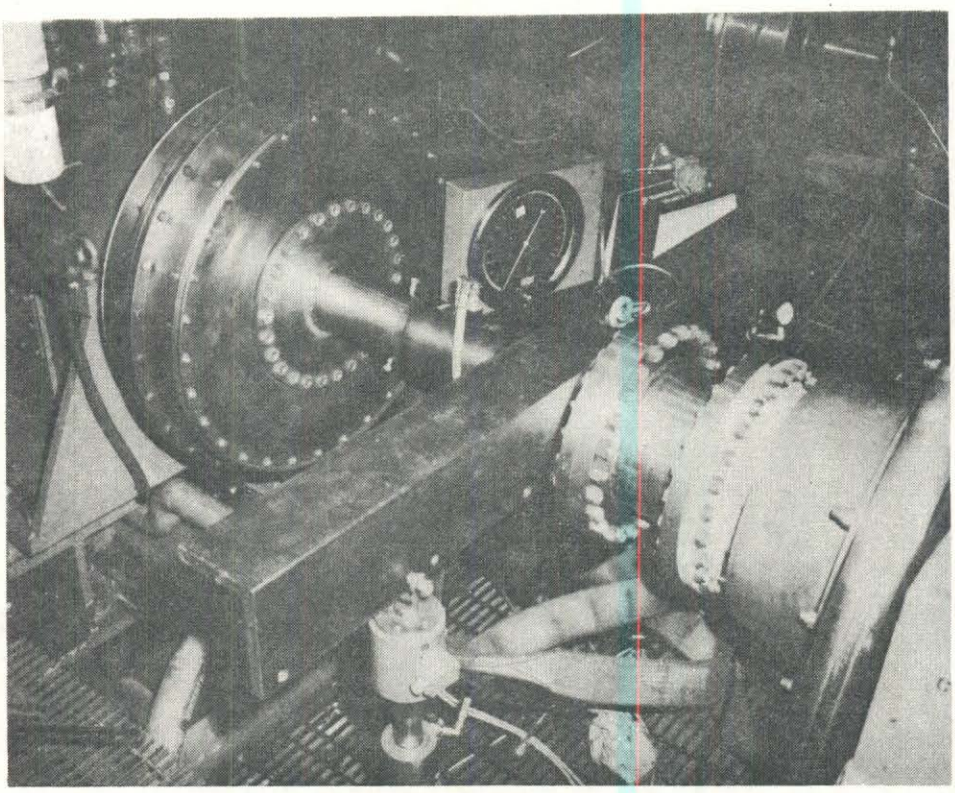

TTC N85-1873

FIGURE A-1. LOCALLY-MANUFACTURED TORQUEMETER CALIBRATION FIXTURE IN TYPICAL RDU APPLICATION.

This was consistent with the analysis of previous test data. The above test was made in the positive direction. The same test was repeated in the negative torque direction with essentially the same results.

4. The fixture was then removed from drive train 4 and installed on drive train 1. Each drive train, 1 through 4, was then checked and recalibrated. On all drive trains, the scaling factor was set in the positive torque direction. The results are as follows:

Drive Train 1

Correlation Coefficient .9999
Slope: .9953943; % deviation from 1.: -.004627%
% deviation from Himmelstein Cal: +2.6%
% deviation, - from + torque: -.0017%

Drive Train 2

Correlation Coefficient .9999
Slope: .9940934; % deviation from 1.: -.00594%
% deviation from Himmelstein Cal: +.00853%
% deviation, - from + torque: +.01041%

Drive Train 3

Correlation Coefficient .9999
Slope: .9969414; % deviation from 1.: -.00307%
% deviation from Himmelstein Cal: +.00197%
% deviation, - from + torque: +.0147295%*

Drive Train 4

Correlation Coefficient .9999
Slope: .9979241; % deviation from 1.: -.00208%
% deviation from Himmelstein Cal: +12.277%
% deviation, - from + torque: -.00339%

From the above data, it is apparent that significant errors resulted in data taken on drive trains 1 and 4 using the Himmelstein calibration data. It is also apparent that now, after the calibration, the torquemeters should be capable of measuring torque to within 1/2 of 1% and that + and - torques can be measured to within 1.47% on drive train 3* and much closer on the other three units.

Immediately after the final Phase 2 tests were completed, the calibration of all 4 torquemeters was checked. All 4 were found to be within 0.1% of the above values.

The calibration fixture is simple and takes little time to use. It is therefore recommended that a calibration check be made of the RDU torque meters prior to, and just subsequent to, any test that requires high resolution torque data.

APPENDIX B

MEASUREMENT OF LOCOMOTIVE AND RDU GEAR LOSSES AND ROTATING INERTIA

After the torquemeters were recalibrated it was necessary to recalculate the RDU and locomotive gear losses and rotating inertias, since the old values were based on the old torquemeter calibrations. The gear and bearing losses were measured by running the RDU up to 65 mph. The RDU was then placed into the coast mode and allowed to coast to a stop. The roller speed was recorded at 2 samples per second on digital tape. This was done with locomotive off the rollers first, and then with the locomotive on the rollers. Three runs were made in each configuration.

The torque due to gear loss was calculated using the following formula:

$$T_G = -I\,\dot{\omega} \qquad \text{(Equation B1)}$$

where

T_G = Gear Loss Torque (ft-lbs)

I = Rotating Inertia (ft-lbs-sec2)

$\dot{\omega}$ = Acceleration Rate of Rollers (2π rad/sec2)

As can be seen, these calculations required the knowledge of the rotating inertia values which were determined by accelerating the rollers from 0 to 65 mph with constant torque being applied by the RDU motors. Torque and speed were recorded on digital tape. This test was done with and without the locomotive on the rollers, and at two levels of torque: 1500 and 2500 ft-lbs.

Rotating inertia was calculated from the following formula:

$$I = \frac{T - T_G}{\dot{\omega}} \qquad \text{(Equation B2)}$$

where

T = Measured Torque

This calculation can be seen to depend on the gear loss torque. Therefore, the calculations were performed iteratively, starting with an assumed value of inertia, then calculating gear loss, recalculating inertia, and so on, until no changes in the results occurred.

For the two configurations of locomotive on and off the rollers, three coast runs and two acceleration runs were made. Thus, six combinations for each configuration were possible. The results of the six combinations were combined to produce an average value for each configuration. The difference between results of the two configurations represents the locomotive wheelset and traction motor gear losses and rotating inertia.

Typical plots of gear loss versus speed for RDU axle and locomotive axle 4 are shown in Figures B1 and B2. These show the gear losses in terms of horsepower and the tractive resistance in terms of torque. The data were fit to second-order and third-order polynominals, respectively, by the least squares method.

Thus, gear loss is characterized as follows:

$$T_G = A_o + A_1 S + A_2 S^2 + A_3 S^3$$

where

T_G = Gear Loss Torque (ft-lbs)

S = Speed (mph)

and the coefficients A_o - A_3 are as shown in Table B1 for the various RDU and locomotive axles.

By subtracting the various coefficients, a set of coefficients for locomotive gear loss alone was also determined.

The plot of rotating inertia versus speed for the same axle is shown in Figure B3. As can be seen, the calculated value does not hold perfectly steady. Therefore, the mean value was used. The inertia values for the two configurations plus the difference between the two, which is the locomotive wheelset and traction motor inertia, are tabulated in Table B2.

The values for locomotive inertia can be seen to be quite variable. This is because they are quite small compared to the overall system inertias. Thus, they are of the same order of magnitude as the possible measurement errors. In the future, more accurate methods of measuring locomotive inertia are desirable.

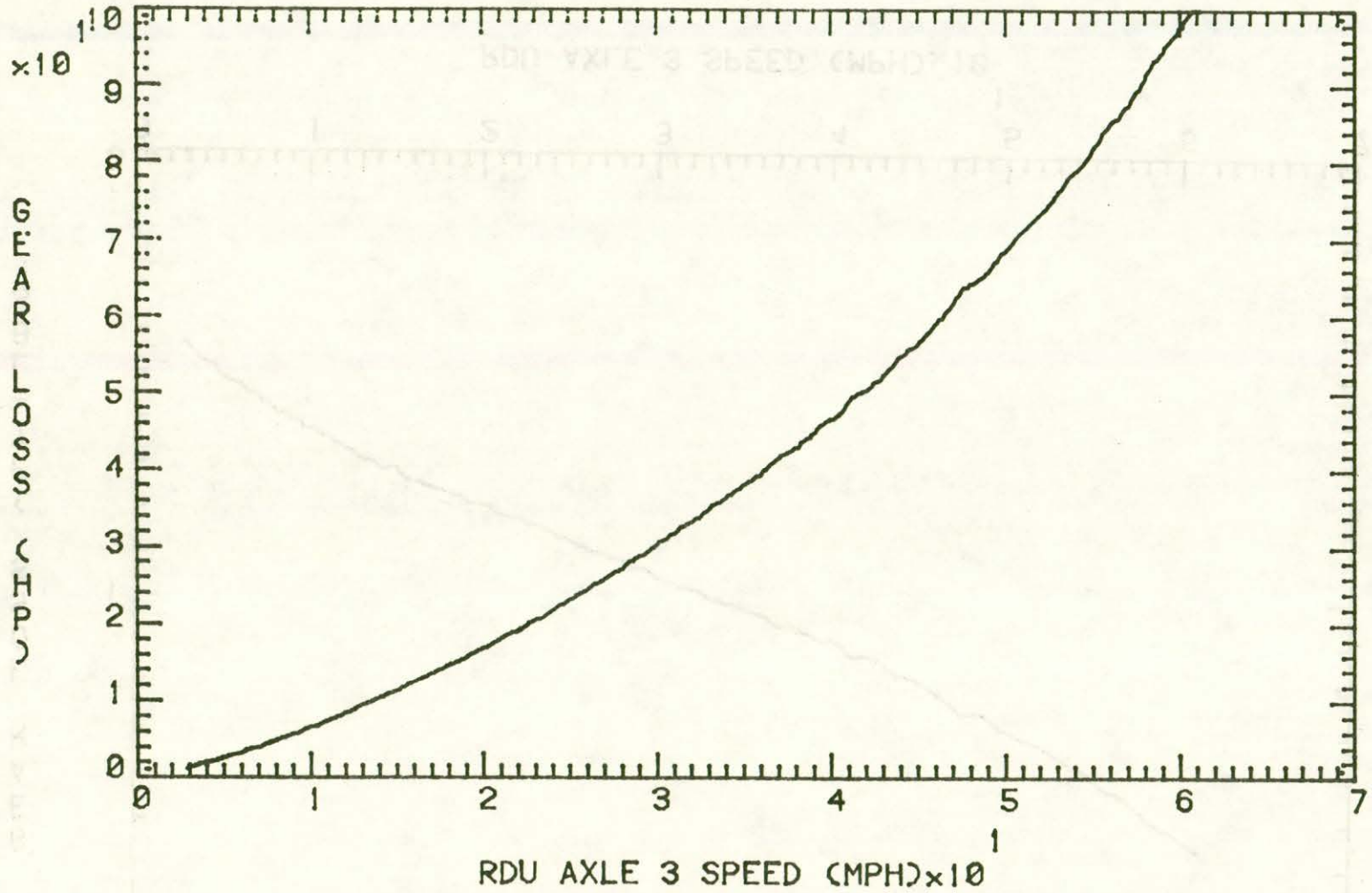

FIGURE B-1. RDU AXLE 3 AND LOCOMOTIVE AXLE 2 GEAR LOSSES.

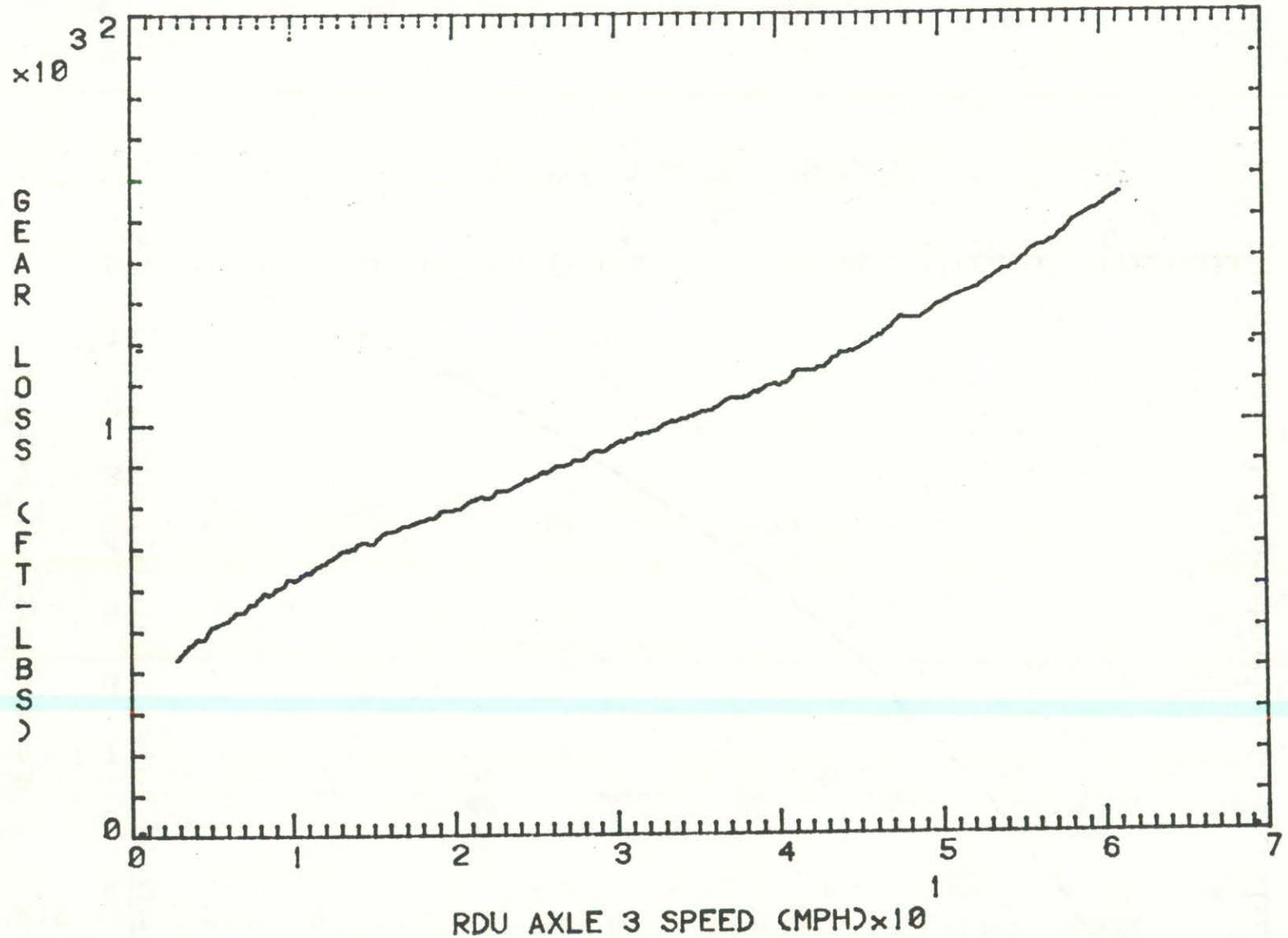

FIGURE B-2. RDU AXLE 3 AND LOCOMOTIVE AXLE 2 GEAR LOSSES.

TABLE B-1. GEAR LOSS COEFFICIENTS.

$T_G = A_0 + A_1S + A_2S^2 + A_3S^3$

T_G = Gear Loss Torque (ft-lb)
S^G = Speed (mph)

Loco Axle with	RDU Axle	A_0	A_1	A_2	A_3
1	4	373.124	23.907	-0.2564	0.6028
2	3	368.193	27.6841	-0.4276	.0044944
3	2	327.022	28.9476	-0.4839	.00476528
4	1	291.561	29.2474	-0.431604	.00351015
RDU Axle Only					
4		241.372	19.3511	-0.1547	0.0013
3		227.127	23.6462	-0.3448	0.0032814
2		197.918	20.881	-0.24771	0.002214
1		173.100	22.0781	-0.29248	0.0023782
Loco Axle Only					
1		131.752	4.6359	-0.1017	0.0015
2		141.066	4.0379	-0.0828	0.0012
3		129.104	8.0666	-0.2362	0.0026
4		118.461	7.1693	-0.1391	0.00113

TABLE B-2. ROTATING INERTIA, FT-LB/SEC^2.

Loco Axle with	RDU Axle	RDU Only	RDU + Loco	Loco Only
1	4	32130	32645	515
2	3	32383	33325	942
3	2	31636	32407.5	771.5
4	1	31780	33135	1355
Average		31982	32878	896

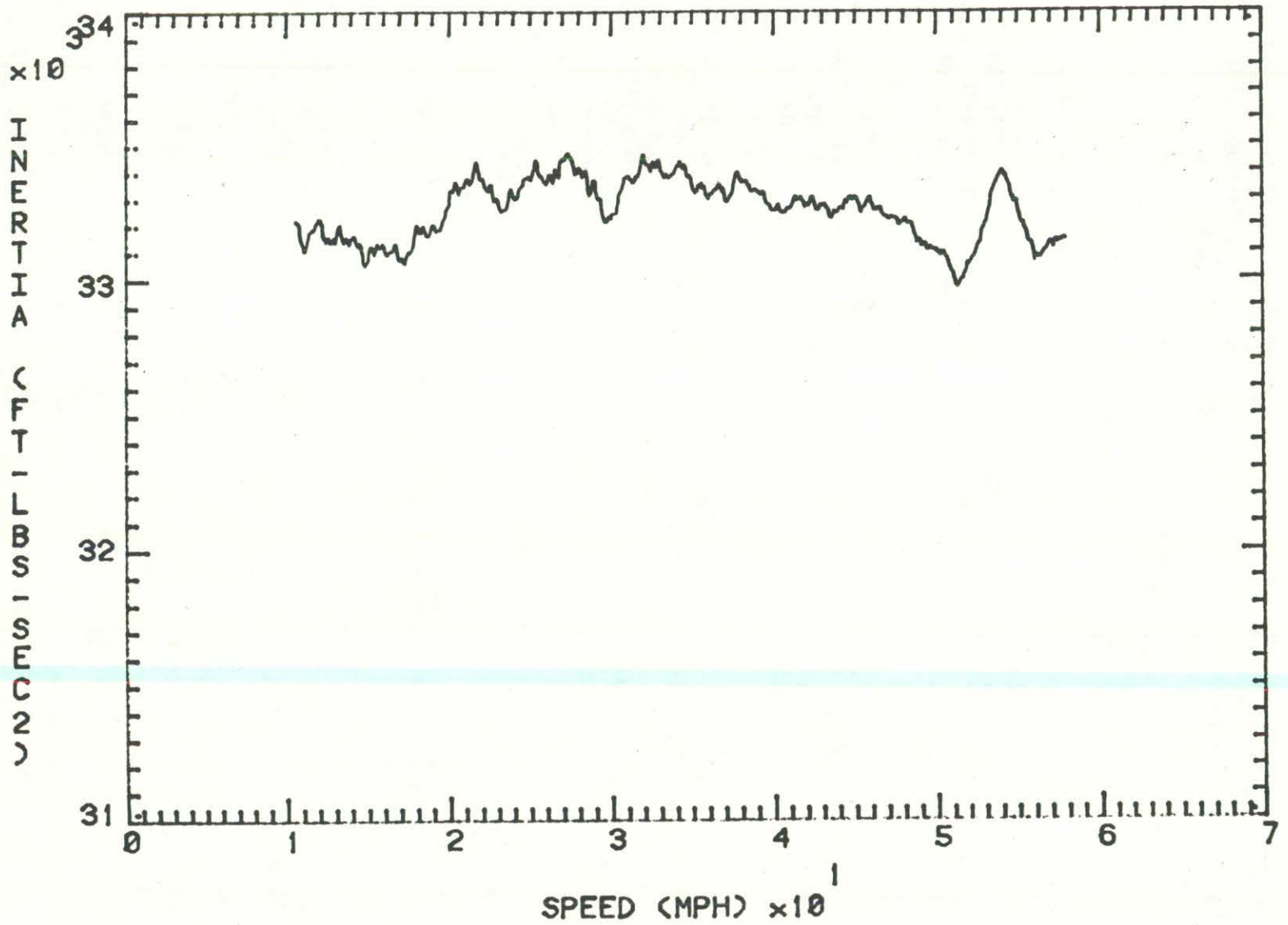

FIGURE B-3. RDU AXLE 3 WITH LOCOMOTIVE AXLE 2 INERTIA.

APPENDIX C

INCIDENT REPORT: RDU ROLLER BURN WITH BN-3054 LOCOMOTIVE

On October 24, 1983, the BN-3054 locomotive was in the process of completing the tractive effort portion of the test on the Roll Dynamics Unit (RDU). The locomotive was driving at 5 to 6 mph, in notch 3 position, with brakes applied for drag. At the moment of brake release and throttle advance to Notch 8, a negative 3,000 ft-lb torque was applied. The first run produced no problems, but in the second test, when RDU Drive Train 1 stopped, locomotive axle 4 continued to drive (momentarily) before it dropped out in routine response to the locomotive wheel slip detection system. The result was that the rollers incurred a typical burn of approximately 1/16" depth, as shown in Figure C1.

It has been determined that oil, dripping from the locomotive and onto one roller, was probably the major cause of this slip. We have also determined to alleviate this occurrence in the future by cleaning the rollers periodically and running the system above 10 mph, which can safely be done without detriment to the test. The locomotive wheels were not damaged or in need of reprofiling. Photos were taken and will be available upon request at a future date.

The repair of the two rollers (on RDU axle 1) was accomplished as follows:

Machine Shop personnel (T. Melton and M. Mauger) were consulted to see if the repair of the rollers could be accomplished either by grinding or cutting the surface of the rollers. It was concluded that cutting was the best alternative, and that the setup illustrated in Figure C2 should be attempted.

The bracket, cutting, etc., resulted in the following. (Approximately three days)

1.	Machine Shop		56 m/h
2.	RDL Technicians		32 m/h
3.	RDL Engineering		12 m/h
		Total	100 m/h
4.	Material (Bracket)		$100.00

Approximately .100" of material was removed from the diameter of the rollers.

The results of this correction, accomplished in place (on the RDU), saved the cost of removal, shipment, resurfacing, reinstallation, and downtime. The ballpark estimate of the savings approaches $10,000, with approximately four weeks downtime.

This correction was found to be cost effective and completely successful. The author wishes to commend those persons who contributed to its success.

The bracket, photos, and method used have been documented, in the event that the rollers need resurfacing in the future.

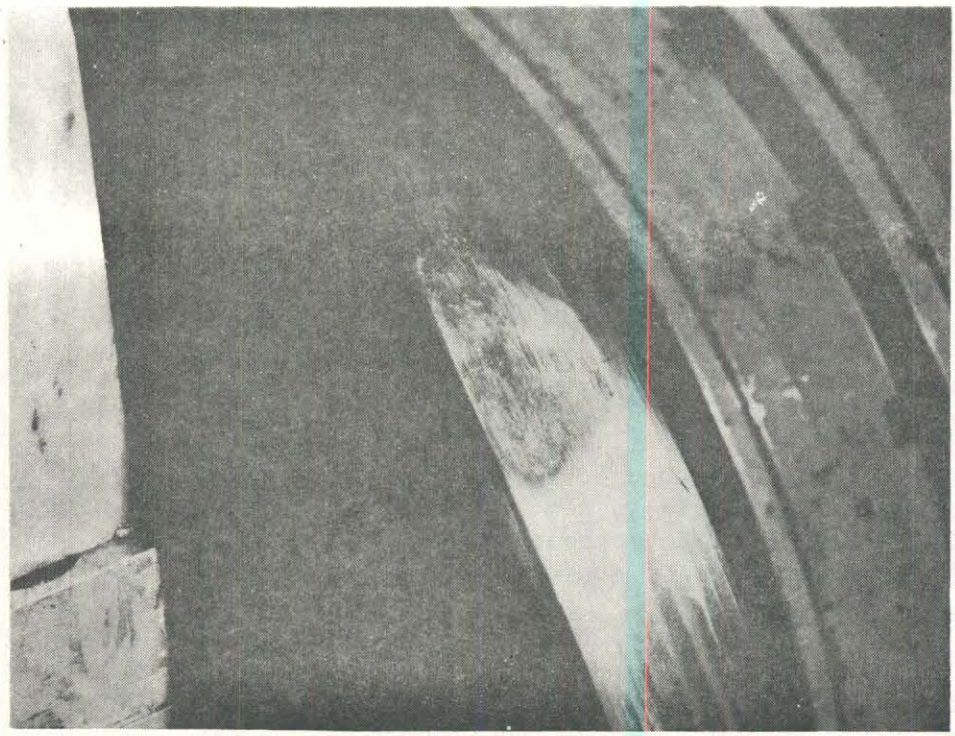

TTC N83-1676

FIGURE C-1. BURN ON RDU ROLLERS.

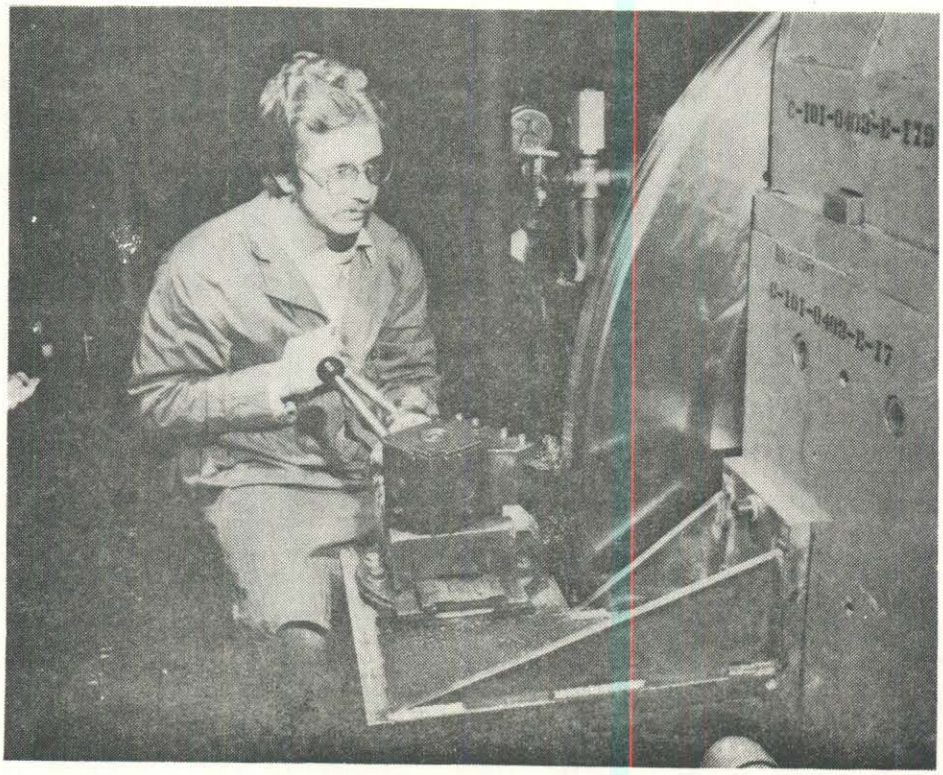

TTC N83-1678

FIGURE C-2. SETUP FOR RESURFACING RDU ROLLERS IN SITU.

APPENDIX D

TRAIN RESISTANCE TABLES, CONVENTIONAL TRUCKS ON LUBRICATED AND DRY TRACK

Table D-1 presents train resistance data for test consists with conventional 3-piece trucks operating at 40 mph over curved and tangent sections of lubricated and unlubricated track. Running took place on the Facility for Accelerated Service Testing (FAST) track at the Transportation Test Center (TTC) in Pueblo, Colorado.

Train resistance values were determined using a diesel-electric locomotive on which the traction motor characteristics had previously been established. This resulted in the ability to determine the amount of train resistance (the energy required to operate the train) simply by measuring the input current and voltage to the armatures of the locomotive traction motors.

The aforementioned runs were, in fact, made to (1) establish the durability of data-gathering systems placed onboard the locomotive and (2) demonstrate the ease with which train-operating variables could be evaluated for their effect on train resistance.

TABLE D-1. CONVENTIONAL 3-PIECE TRUCKS ON DRY AND LUBRICATED TRACK.

(Train Resistance, Loco + 6 Cars)

Section 3 - 5° Curve

	Lube Data (Pounds)		Dry Data (Pounds)	
	Clockwise	Counterclockwise	Clockwise	Counterclockwise
	9512.22	- 2024.70	13411.53	1707.61
	9598.90	- 2136.10	13667.90	1925.02
	9641.42	- 1697.45	13039.97	---
	9445.38	- 2248.54	12961.84	---
Avg	9549.58	- 2026.70	13270.31	1816.31

Combined Avg 3761.39 Combined Avg 7543.31

Ratio = .4986
Savings = 50.14% (3781.92 pounds)

Section 7 - 5° Curve

	Lube Data (Pounds)		Dry Data (Pounds)	
	Clockwise	Counterclockwise	Clockwise	Counterclockwise
	1613.60	4292.90	6784.04	9409.16
	2890.42	4071.72	6805.71	9455.43
	1429.36	4314.90	5946.72	---
	3470.72	4038.37	6771.11	---
Avg	2351.03	4179.47	6576.90	9432.29

Combined Avg 3265.25 Combined Avg 8004.60

Ratio = .4079
Savings = 59.2% (4739.35 pounds)

Section 17 - 3° Curve

	Lube Data (Pounds)		Dry Data (Pounds)	
	Clockwise	Counterclockwise	Clockwise	Counterclockwise
	6198.06	- 346.85	8962.80	2598.86
	5941.69	- 573.06	8801.94	2980.90
	6148.22	- 951.84	7770.10	---
	5942.70	- 592.57	7642.81	---
Avg	6057.67	- 616.08	8294.41	2789.88

Combined Avg 2720.79

Combined Avg 5542.15

Ratio = .4909
Savings = 50.01% (2821.36 pounds)

Section 17 - 5° Curve

	Lube Data (Pounds)		Dry Data (Pounds)	
	Clockwise	Counterclockwise	Clockwise	Counterclockwise
	-23431.97	32689.35	-24239.28	40113.94
	-23208.78	30492.63	-23585.79	38867.29
	-25325.07	32689.35	-27456.44	37741.29
			-27421.25	
Avg	-23988.61	31975.11	-25675.69	38907.51

Combined Avg 3984.25

Combined Avg 6615.91

Ratio = .602
Savings = 40% (2631.66 pounds)

Section 13 - 4° Curve

Lube Data (Pounds)		Dry Data (Pounds)	
Clockwise	Counterclockwise	Clockwise	Counterclockwise
(6097.57)	(6251.34)	7102.91	6881.70
(4182.31)	(5545.43)	7213.47	6519.77
3682.96	(6281.37)	6166.58	---
3780.43	(5585.21)	7907.33	---
Avg 3731.70		7097.57	6700.74

Combined Avg 6899.16

Ratio = .54
Savings = 46% (3167.46 pounds)

Section 20 - Tangent

Lube Data (Pounds)		Dry Data (Pounds)	
Clockwise	Counterclockwise	Clockwise	Counterclockwise
5489.28	606.73	6940.26	3192.02
5464.14	588.14	6819.25	2895.44
5433.30	655.40	5755.70	---
5447.08	616.69	6203.08	---
Avg 5458.45	616.74	6429.51	3043.73
Combined Avg 3037.60		Combined Avg 4736.62	

Ratio = .64
Savings = 36% (1699.02 pounds)

Section 22 - Tangent

	Lube Data (Pounds)		Dry Data (Pounds)	
	Clockwise	Counterclockwise	Clockwise	Counterclockwise
	8440.01	-2890.42	10269.77	- 934.99
	8093.16	-2161.53	9953.08	-1249.76
Avg	8266.59	-2525.98	10111.43	-1092.38
	Combined Avg 2870.31		Combined Avg 4508.53	

Ratio = .6365
Savings = 36.4% (1638.22 pounds)

Section 10 - Tangent

	Lube Data (Pounds)		Dry Data (Pounds)	
	Clockwise	Counterclockwise	Clockwise	Counterclockwise
	8153.49	-2760.22	8605.90	-2816.77
	7836.80	-2813.25	8475.20	-2786.86
Avg	7995.14	-2786.74	8540.55	-2801.82
	Combined Avg 2604.20		Combined Avg 2869.37	

Ratio = .9076
Savings = 9.24% (265.17 pounds)

Total FAST

Lube Data (Pounds)		Dry Data (Pounds)	
Clockwise	Counterclockwise	Clockwise	Counterclockwise
3438.16	3383.14	5279.61	
Combined Avg 3410.65		Combined Avg 5279.61	

Ratio = .6509
Savings = 34.9% (1828.96 pounds)

APPENDIX E

TRAIN RESISTANCE TABLES, COMPARISON, RADIAL TRUCKS ON DRY TRACK AND CONVENTIONAL TRUCKS ON LUBRICATED AND DRY TRACK

Table E-1 presents train resistance data for test consists with radial and conventional 3-piece trucks operating at 40 mph over curved and tangent sections of lubricated and unlubricated track. Running took place on the Facility for Accelerated Service Testing (FAST) track at the Transportation Test Center (TTC) in Pueblo, Colorado.

Train resistance values were determined using a diesel-electric locomotive on which the traction motor characteristics had previously been established. This resulted in the ability to determine the amount of train resistance (the energy required to operate the train) simply by measuring the input current and voltage to the armatures of the locomotive traction motors.

The aforementioned runs were, in fact, made to (1) establish the durability of data-gathering systems placed onboard the locomotive and (2) demonstrate the ease with which train-operating variables could be evaluated for their effect on train resistance.

Radial trucks and rail gage face lubrication have already been recognized as two means for achieving greater economy of operation by reducing energy requirements. Reaffirming these established facts, the information presented in Table D-1 shows how any variable which will significantly affect train resistance can be detected and quantified through use of the 'calibrated locomotive' train resistance measuring techniques. Averaged resistance data are provided for radial trucks on dry track and conventional 3-piece trucks on dry and lubricated track.

From these data, ratios were calculated as presented, allowing percent-savings to be identified by comparing various operating modes with alternative modes.

TABLE E-1. TOTAL TRAIN RESISTANCE (LOCOMOTIVE + 6 CARS)--RADIAL TRUCKS ON DRY TRACK, CONVENTIONAL TRUCKS ON DRY AND LUBRICATED TRACK.

Section 03 - 5° Curve

	Radial Trucks (Dry Rail)		Conventional 3-Piece Trucks	
	CW* Runs	CCW* Runs	Lub Rail (CW+CCW/2)	Dry Rail (CW+CCW/2)
	10174.01	- 2854.54	Note: These data are given in Appendix D.	
	11119.30	- 2867.96		
	10802.62	- 2868.75		
3-Run Avg(s):	10698.64	- 2863.75		
	.....		.....	.....
Combined Avg:	3917.45		3761.39	7543.31

Resistance Ratio:

$$\frac{\text{Radial Truck}}{\text{Conventional Truck (Lub)}} = \frac{3917.45}{3761.39} = 1.041$$

$$\frac{\text{Radial Truck}}{\text{Conventional Truck (Dry)}} = \frac{3917.45}{7543.31} = 0.519$$

Savings: $(1.0 - 0.519) \times 100 = 48.1\%$, or 3625.86 lbs

Section 07 - 5° Reverse Curve

	Radial Trucks (Dry Rail)		Conventional 3-Piece Trucks	
	CW Runs	CCW Runs	Lub Rail (CW+CCW/2)	Dry Rail (CW+CCW/2)
	3742.85	6142.10	Note: These data are given in Appendix D.	
	3574.06	5819.55		
	2734.58	6328.75		
3-Run Avg(s):	3350.50	6096.80		
	.....		.....	.....
Combined Avg:	4723.65		3265.25	8704.60

Resistance Ratio:

$$\frac{\text{Radial Truck}}{\text{Conventional Truck (Lub)}} = \frac{4723.65}{3265.60} = 1.447$$

$$\frac{\text{Radial Truck}}{\text{Conventional Truck (Dry)}} = \frac{4723.65}{8704.60} = 0.590$$

Savings: $(1.0 - 0.590) \times 100 = 41\%$, or 3280.95 lbs

---

*CW, CCW = Clockwise, Counterclockwise

Section 17 - 3° Curve

	Radial Trucks (Dry Rail)		Conventional 3-Piece Trucks	
	CW Runs	CCW Runs	Lub Rail (CW+CCW/2)	Dry Rail (CW+CCW/2)
	5973.93	- 667.44	Note: These data are given in Appendix D.	
	6143.76	- 946.42		
	6766.09	- 100.39		
3-Run Avg(s):	6294.61	- 874.75		
	.....		.....	.....
Combined Avg:	2709.93		2720.79	5542.15

Resistance Ratio:

$$\frac{\text{Radial Truck}}{\text{Conventional Truck (Lub)}} = \frac{2709.93}{2720.79} = 0.996$$

$$\frac{\text{Radial Truck}}{\text{Conventional Truck (Dry)}} = \frac{2709.93}{5542.15} = 0.489$$

Savings: (1.0 - 0.489) x 100 = 51.1%, or 2832.22 lbs

Section 17 - 5° Curve

	Radial Trucks (Dry Rail)		Conventional 3-Piece Trucks	
	CW Runs	CCW Runs	Lub Rail (CW+CCW/2)	Dry Rail (CW+CCW/2)
	-24919.78	34529.44	Note: These data are given in Appendix D.	
	-25025.61	34962.29		
	-29235.93	34443.59		
3-Run Avg(s):	-26393.77	34638.44		
	.....		.....	.....
Combined Avg:	4122.33		3984.25	6615.91

Resistance Ratio:

$$\frac{\text{Radial Truck}}{\text{Conventional Truck (Lub)}} = \frac{4122.33}{3984.25} = 1.035$$

$$\frac{\text{Radial Truck}}{\text{Conventional Truck (Dry)}} = \frac{4122.33}{6615.91} = 0.623$$

Savings: (1.0 - 0.623) x 100 = 38%, or 2493.58 lbs

Section 13 - 4° Curve

Radial Trucks (Dry Rail)		Conventional 3-Piece Trucks	
CW Runs	CCW Runs	Lub Rail (CW+CCW/2)	Dry Rail (CW+CCW/2)
4250.92	3694.35	Note: These data are given in Appendix D.	
4302.95	3898.49		
4345.93	---		
3-Run Avg(s): 4345.93	3796.42		
Combined Avg: 4071.18		3731.70	6899.16

Resistance Ratio:

$$\frac{\text{Radial Truck}}{\text{Conventional Truck (Lub)}} = \frac{4071.18}{3731.70} = 1.017$$

$$\frac{\text{Radial Truck}}{\text{Conventional Truck (Dry)}} = \frac{4071.18}{6899.16} = 0.590$$

Savings: (1.0 - 0.590) x 100 = 41%, or 3280.95 lbs

Section 20 - Tangent

Radial Trucks (Dry Rail)		Conventional 3-Piece Trucks	
CW Runs	CCW Runs	Lub Rail (CW+CCW/2)	Dry Rail (CW+CCW/2)
6148.71	319.65	Note: These data are given in Appendix D.	
6572.83	553.08		
6213.14	371.98		
3-Run Avg(s): 6311.56	414.90		
Combined Avg: 3363.23		3037.60	4736.62

Resistance Ratio:

$$\frac{\text{Radial Truck}}{\text{Conventional Truck (Lub)}} = \frac{3363.23}{3037.60} = 1.107$$

$$\frac{\text{Radial Truck}}{\text{Conventional Truck (Dry)}} = \frac{3363.23}{4736.62} = 0.710$$

Savings: (1.0 - 0.710) x 100 = 29%, or 1699.02 lbs

Section 22 - Tangent

Radial Trucks (Dry Rail)		Conventional 3-Piece Trucks	
CW Runs	CCW Runs	Lub Rail (CW+CCW/2)	Dry Rail (CW+CCW/2)
11023.79	2578.75	Note: These data are given in Appendix D.	
9822.39	---		
2-Run Avg(s): 10423.09	2578.75		
Combined Avg: 3922.17		2870.31	4508.53

Resistance Ratio:

$$\frac{\text{Radial Truck}}{\text{Conventional Truck (Lub)}} = \frac{3922.17}{2870.31} = 1.366$$

$$\frac{\text{Radial Truck}}{\text{Conventional Truck (Dry)}} = \frac{3922.17}{4508.53} = 0.870$$

Savings: $(1.0 - 0.870) \times 100 =$ 31%, or 1638.22 lbs

Section 10 - Tangent

Radial Trucks (Dry Rail)		Conventional 3-Piece Trucks	
CW Runs	CCW Runs	Lub Rail (CW+CCW/2)	Dry Rail (CW+CCW/2)
9063.34	-2304.59	Note: These data are given in Appendix D.	
8419.91	-3077.31		
3-Run Avg(s): 8741.62	-2690.95		
Combined Avg: 3025.37		2604.20	2869.37

Resistance Ratio:

$$\frac{\text{Radial Truck}}{\text{Conventional Truck (Lub)}} = \frac{3025.37}{2604.20} = 1.162$$

$$\frac{\text{Radial Truck}}{\text{Conventional Truck (Dry)}} = \frac{3025.37}{2869.37} = 1.054$$

Savings: $(1.0 - 1.054) \times 100 =$ -5.4%, or -156 lbs

Total FAST

Radial Trucks (Dry Rail)		Conventional 3-Piece Trucks	
CW Runs	CCW Runs	Lub Rail (CW+CCW/2)	Dry Rail (CW+CCW/2)
3649.167	3421.026	Note: These data are given in Appendix D.	
Combined Avg: 3535.097		3410.65	5279.61

Resistance Ratio:

$$\frac{\text{Radial Truck}}{\text{Conventional Truck (Lub)}} = \frac{3535.097}{3410.65} = 1.036$$

$$\frac{\text{Radial Truck}}{\text{Conventional Truck (Dry)}} = \frac{3535.097}{5279.61} = 0.669$$

Savings: $(1.0 - 0.669) \times 100 = 33\%$